JOURNAL OF APPLIED PHYSICS

JOURNAL
OF
APPLIED PHYSICS

Vol. 15, No. 9 SEPTEMBER, 1944

In This Issue

Page

Physics in the Service of Southern Agriculture
MEMBERS OF THE STAFF, SOUTHERN REGIONAL RESEARCH LABORATORY, NEW ORLEANS, LOUISIANA 629

American Institute of Physics Building. II. An Architectural Study of the Building BLANCHETTE ARNAUD 642

Contributed Original Research

Forced Torsional Oscillations of an Elastic Half-Space. I
ERIC REISSNER AND H. F. SAGOCI 652

Forced Torsional Oscillations of an Elastic Half-Space. II
H. F. SAGOCI 655

Microanalysis by Means of Electrons
JAMES HILLIER AND R. F. BAKER 663

Torsional Vibration of Multi-Disk Systems EDWARD FISHER 676

Studies with the Electron Microscope Diffraction Adapter
ROBERT G. PICARD 678

Letters to the Editor

Comments on "Organization of Physics in America"
ALFRED N. GOLDSMITH 649

Reply to Comments
WALLACE WATERFALL AND ELMER HUTCHISSON 649

In Every Issue

Calendar of Meetings 648

Here and There 650

Index to Advertisers xxiv

BOARD OF EDITORS

ELMER HUTCHISSON, *Editor*

Associate Editors

R. B. BARNES
OTTO BEECK
W. F. BUSSE
S. H. CALDWELL
CLARK GOODMAN
SELIG HECHT
W. J. LYONS
MORRIS MUSKAT
THOMAS H. OSGOOD
PAUL E. SABINE
FREDERICK SEITZ
J. R TOWNSEND

Publication of the American Institute of Physics

ADMINISTRATIVE STAFF

HENRY A. BARTON, *Director*

MADELINE M. MITCHELL, *Publications Manager*

JOHN T. TATE, *Adviser on Publications*

GOVERNING BOARD

PAUL E. KLOPSTEG, *Chairman*

GEORGE B. PEGRAM, *Secretary*

T. D. COPE
R. B. DOW
L. A. DUBRIDGE
FLOYD A. FIRESTONE
HARVEY FLETCHER
R. C. GIBBS
K. S. GIBSON
HERMANN MARK
A. G. WORTHING
JOHN T. TATE
L. W. TAYLOR
N. W. TAYLOR
WALLACE WATERFALL

The JOURNAL OF APPLIED PHYSICS, published monthly at Prince and Lemon Sts., Lancaster, Pa., is devoted to physics in its role as the science basic to other natural sciences and to the arts and industries. Previous to 1937 this publication was known as PHYSICS. The JOURNAL OF APPLIED PHYSICS publishes editorials, news of physicists, and reviews, as well as technical papers of applied physics.

Manuscripts should be submitted to Elmer Hutchisson, Editor, 50th floor, 350 Fifth Avenue, New York 1, New York.

Subscriptions and orders for back numbers should be addressed to Prince and Lemon Streets, Lancaster, Pa. or to the American Institute of Physics, 57 East 55 Street, New York 22, N. Y.

Subscription Price

	U. S. AND CANADA	ELSEWHERE
To members of scientific societies	$5.00	$5.70
To all others	7.00	7.70

Back Number Prices

Complete set: Vol. 1, July, 1931–Vol. 14, 1943—**$87.50**
Yearly back number rate: **$7.70**
Single copies: **$0.70** each.

Changes of address and proofs should be addressed to the Publications Manager.

Advertising rates supplied on request. Orders, advertising copy, and cuts should be sent to the American Institute of Physics.

Entered as second class matter January 22, 1937, at the Post Office at Lancaster, Pennsylvania, under the Act of March 3, 1879
Accepted for mailing at the special rate of postage provided for in the Act of February 28, 1925, authorized May 2, 1932.

Copyright 1944, by the American Institute of Physics.

Journal
of
Applied Physics

Volume 15, Number 9 September, 1944

Physics in the Service of Southern Agriculture

BY MEMBERS OF THE STAFF*

*Southern Regional Research Laboratory, New Orleans, Louisiana***

RECOGNIZING the need for the more intensive application of scientific and technical study to the products of America's farms, Congress in 1938 established four research laboratories in different regions of the country. The purpose of these laboratories, in the words of the Congressional Act, is "to conduct researches into and to develop new scientific, chemical, and technical uses and new and extended markets and outlets for farm commodities and products and by-products thereof." The four laboratories are administered by the Bureau of Agricultural and Industrial Chemistry, Agricultural Research Administration, U.S. Department of Agriculture. The Southern Regional Research Laboratory, located about a half-mile across recently-reclaimed parkland from the shores of Lake Pontchartrain, in New Orleans, is one of these institutions.

At the Southern Laboratory principal attention has been focused on, and facilities provided for, research on three important, normally surplus, farm commodities grown in the southern region of the country: cotton (including cottonseed), sweetpotatoes, and peanuts. To this program has been later added the preparation and evaluation of rubber from the goldenrod plant. Since even before the laboratory building was occupied in the spring of 1941, the original peacetime research programs were revised and have been undergoing continuous modification to make more immediate contributions to national defense and our country's war effort.

The research work of the Southern Regional Laboratory is organized under seven divisions, three of which are devoted to problems related to cotton lint and cotton fabrics. Another division conducts investigations on cottonseed and peanut products, while a fifth division concentrates on only sweetpotato products. Neither of the remaining two divisions is concerned with specific commodities. One of these specializes in the more refined analytical laboratory techniques, both physical and chemical, having application to a wide variety of substances, while the other is concerned with the development of promising processes at the pilot-plant stage. In addition to these seven divisions of the regular research staff, there are now housed at the laboratory parts of two other divisions of the Bureau, one dealing with general problems in agricultural chemistry and the other with the chemical products derived

* Arranged and edited by W. James Lyons, Physicist on the Laboratory Staff and an Associate Editor of this journal.

** This is one of the laboratories of the Bureau of Agricultural and Industrial Chemistry, Agricultural Research Administration, U. S. Department of Agriculture.

FIG. 1. Textile-testing room. Here are made tensile strength, elongation, and other tests of physical properties of yarns, cords, and fabrics under closely-controlled, standard conditions.

from Southern pine trees and known collectively as naval stores.

While none of these divisions of the laboratory devotes its whole activity to the application of physics in the specialized sense, there are sections or groups in each one which concentrate on physical techniques. Most of the chemical processes under study and development, of course, involve the control of physical processes to a greater or less extent. It is, however, in the field of precise, objective measurement that the application of physical principles is most clearly discernible. Two types of physical measurement as practiced in industrial research are recognizable, and distinguishable by the significance of the quantities measured. One type covers measurements of what might be called the "scientifically-significant" properties of materials, such as structure, internal character, and atomic and molecular behavior toward various physical agents. Falling into this class also are the physical properties of the components of an industrial product, such as the cotton fibers in a yarn. A knowledge of these fundamental properties, while of little interest to the ultimate user of the product, is of importance to the research worker in understanding the material with which he is working, and in evaluating or controlling his experimental processes. The other type of physical measurement is concerned with "technically-significant" properties, the evaluation of which determines the suitability of a product for a particular application. While many of the required, technically-significant properties of industrial and household materials are chemical or biological in character, undoubtedly the large majority are physical. The Southern Regional Laboratory, in one or another division, has facilities and trained personnel for conducting measurements of, and investigations into, physical properties of both these types.

TEXTILE TESTING AND RESEARCH

The role of physics in the development of new and improved cotton-textile products is representative of its industrial applications. First, in order to set up specifications for a textile product so that it will satisfactorily meet the requirements of a particular use, it is necessary to correlate these requirements with measurable physical properties of the product, and if possible with those of the constituent fibers and yarns also. Secondly, during experimental manufacture, pertinent properties of the textile or its components must be measured to control quality. Finally, the finished product must be inspected and tested with reference to the specified properties. The Laboratory is well equipped to make physical measurements and tests in the textile field, the emphasis being placed on facilities for cotton-textile research. There are in current use two specially designed rooms in which all of the conventional, and many special tests can be made under the standard conditions for the testing of textiles. Completion of a third air-conditioned room, to be devoted primarily to fiber studies, has been delayed on account of the war, but is now going forward. Both of the testing rooms in current use are maintained at a relative humidity of 65 percent and a temperature of 70°F.

One of these testing rooms (Fig. 1) is maintained by the Cotton Processing Division, principally to secure the data on which the experimental products of the laboratory textile mill are evaluated in line with the above-mentioned objectives. The facilities, however, are available also to other divisions which from time to time require the testing of textiles. In use here are standard tensile-testing machines of both the pendulum and inclined-plane types, for measuring the breaking strength and elongation of textiles

over a range of from a few ounces to 800 pounds. One remarkably ingenious machine, an automatic yarn tester, will, without manipulation by the operator, secure and record fifty-two consecutive breaks on yarn from each of six bobbins, at the same time recording the elongation of each sample section of yarn at the instant of breaking. All of these machines measure the "breaking load," that is, the actual force in pounds which is being exerted on the particular specimen when it ruptures.

In most cases, more information than the breaking load is required to make adequate comparisons between samples. A yarn or tire cord, like any other industrial product, may be strong through mere bigness. To remove this factor and obtain a quantity which reflects the physical character of the yarn or cord independently of its size, it is customary in certain cotton-textile work to multiply the breaking load by the count of the yarn or cord. The "count-strength product" thus obtained is the analog in textile technology of the "ultimate tensile strength" used in physical research in other fields. Hence the count or number of a yarn or cord is nearly always determined when a breaking test is made, and for this purpose the testing laboratory uses a balance reading directly in yarn number when a standard length of yarn is placed on the beam. With some textiles the strength referred to actual linear dimensions, instead of count, has important technical significance. Unlike the diameter of a yarn, which is a rather indefinite quantity, the diameter or gauge of a tire cord or the thickness of a canvas duck can be measured readily. This is done on a dial micrometer gauge, the textile sample being subjected to a uniform pressure. Such gauge measurements, made as a regular part of every test of tire cord, are indispensable in the comparison of the strengths and other properties of different cords.

The elastic and plastic behaviors of textiles are, in many applications, highly important. In tire cord for ordinary uses, for instance, these properties may be regarded as more important than strength, once the latter has been brought up to an adequate level. As a measure of the extensibility of single yarns, yarn skeins, cords, and other textiles, the elongation of the specimen

FIG. 2. Fiber-microscopy laboratory, devoted to the study of cotton fibers and related products.

at selected loads is used. These data are obtained on autographic charts during application of the load on the specimen in a breaking test. All of the strength-testing machines in the testing room of the Cotton Processing Division are equipped to provide a record of the elongation, at either all loads up to and including that at break, or at only the breaking point.

It has long been known that moisture content has an important influence on the mechanical properties of fibers and textiles. Anomalies in experimental results on textiles have been traced to obscure differences in the moisture content of samples. In the light of these experiences, modern textile research requires not only that testing be conducted under carefully controlled, uniform conditions of humidity, but that the actual percentage of moisture in the textile under study be known. For this purpose the testing room has a large capacity, precision, temperature-controlled oven, having a range of from 75° to 500°F, and being equipped with forced-draft air circulation to insure thorough and uniform heating. While designed primarily to obtain the bone-dry weight or moisture regain of textiles, the oven is also used in research projects to condition samples for testing on a moisture-free basis, to age samples at various temperatures, etc.

The utility of a fabric for shelter or clothing often depends on its permeability to air. Satisfactory apparatus for measurements of this kind is of comparatively recent development. The design of the instrument in use at the Southern Regional Laboratory is based on the manometric

measurement of air flow through the fabric under a standard pressure drop across the fabric.

While the daily testing of yarns, cords, and fabrics is done according to standard procedures on standard equipment, a keen recognition of the physical principles involved in the various tests is required if their accuracy and reliability are to be maintained. Without constant technical vigilance, as regards both the physical factors involved and the statistical nature of the data, misinterpretation of the results can very easily follow. Though much attention has been given to standard tests in this testing laboratory, its facilities are being employed in the study and development of new tests. Prominent among recent developments is a machine for measuring the fatigue-life of yarns and cords under flexure, at either constant or varying tension, and at either room or elevated temperatures. The novel feature of the design is the character of the flexure to which the sample is subjected. An example of research of another type is afforded by the investigation on methods which will permit reduction in the number of tests and quantity of sample material required for representative results. Preliminary data in one phase of the project reveal that the conventional skein-strength test for yarn can be modified so as to reduce testing time considerably while increasing the amount of data obtainable from the sample. While the development itself is principally in the field of statistics rather than textile physics, it reflects the close relationship so often found between the two sciences in industrial research.

COTTON FIBER RESEARCH

The cotton research program of the Southern Laboratory is not limited to the physical properties of the spun or woven product. It has from the outset contemplated the detailed study of the properties of the ultimate cotton fiber as it occurs in nature in different varieties, and as modified by physical or chemical means. The setting up of specifications for a textile product includes the selection of the kind of fiber (variety, staple length, character, etc.) to be used. Evidently, the most rational selection is one based on known correlations between the mechanical properties of the fibers and those of the product, the obvious objective being the use of the most advantageous combination of properties, natural and endowed. The correlations, in turn, must be based on a broad and thorough knowledge of fiber properties.

The measurement of a strictly physical property of cotton fibers most frequently made is that of fiber strength. The Cotton Fiber Research Division has apparatus for making this measurement by three different methods. As in the case of yarn and fabric testing, measurements on fibers are conducted under standard conditions of humidity and temperature. One instrument gives directly a measurement of single-fiber strength. Individual fibers, suitably mounted beforehand, are placed in clamps on the machine and broken one at a time. In the remaining two methods the fibers are broken in bundles. The modified Chandler method employs uniformly-compressed, cylindrical bundles of known circumference, held in clamps designed to fit one of the vertical textile-testing machines. Conforming to general usage in physics and engineering, the tensile strength of the cotton sample as determined by this method is reported in pounds per square inch of bundle cross section. In most frequent current use, at the Southern Regional Laboratory, is the Pressley method, of comparatively recent origin. In this method a flat fiber-bundle of known length and weight is broken in an instrument especially designed for the purpose. The results are reported in pounds per milligram, a unit which in textile practice has the advantage of economic significance, traceable back to the fact that cotton and other textile fibers are sold on a weight basis. As is to be expected from the differences in experimental conditions, these methods of fiber testing do not give identical values when results are put on a common basis.

There are certain other measurements on cotton fibers which, though of a spatial or geometric rather than physical nature, are frequently made in conjunction with the strength-testing of fibers. These measurements, for which the methods and apparatus have become quite standardized, consist of "staple" length, or the distribution of fiber length, fineness in terms of weight per inch, and maturity. To these may be added as an alternative method the measurement of geometric fineness.

Facilities for the estimation of fiber maturity and the measurement of geometric fineness are available in the fiber-microscopy laboratory (Fig. 2). Here also are conducted special microscopic studies of the effects of various physical, chemical, and (sometimes) biological treatments or agents on fibers and fibrous botanical specimens. The work of this unit is rightly regarded as of a physical nature, for the properties studied may, in a general way, be regarded as physical, and are to a certain extent related to the physical properties of yarns and fabrics; the use of microscopic techniques, furthermore, is an application of optics.

The measurement of geometric fineness, mentioned above, involves the cross sectioning of a bundle of the sample fibers. The sectioning, done in a special device under a wide field, stereoscopic microscope, is somewhat "freehand" in character. However, because it has been found to yield cross sections of the highest quality, the technique has been applied extensively to other studies on yarns, cords, and fabrics. Combined with the use of suitable stains, the method has given conclusive information on the depth of penetration of modifying chemicals, protective coatings, adhesives, etc. Photomicrography, often with the use of the Kodachrome process for colored transparencies and prints, provides in connection with all the microscopic observations, permanent records to which subsequent analysis or measurement may be applied.

Included in the fiber research program are various studies for which no standard procedures have been developed; for these experiments the apparatus must be assembled from general physical laboratory equipment, or especially built. Such studies have included breaking tests on fibers which compete with cotton, or for which cotton might be a wartime substitute, and observations on the deformation characteristics of cotton fibers, yarns, and cords under various conditions. The latter observations have usually been made with a micrometer microscope or cathetometer, though a high power microscope has also been used with some success.

The investigation of these secondary physical properties of fibers has been undertaken with a view to broadening the basis for the correlation

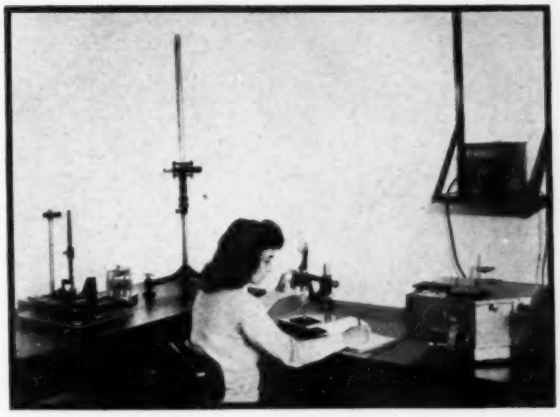

FIG. 3. Some instruments used in evaluating physical properties bestowed on textiles by various chemical finishes, showing compressometer in use, with reflectometer on the right.

of fiber and product properties. The more remote objective is the uncovering of the causal relationships between the two properties. It is true that by amassing a body of data on various fiber samples, on the one hand, and on yarns and fabrics on the other, certain fiber properties have been correlated with those of yarns or cords. As a general method, however, this one has disadvantages. A knowledge or working theory of the chain of physical phenomena relating fiber properties to product properties provides a much more efficient basis on which to predict product behavior. Unfortunately, with the large number of interacting fiber properties involved, the theoretical approach has remained in a rather undeveloped state. A beginning has been made however, and at the Southern Regional Laboratory the theoretical method has received attention and has been applied as a tentative guide in a few investigations. A physical theory of yarn properties, if and as it is fully developed, may be envisioned as the textile analog of the kinetic theory of gases.

In order to study empirically the influence of various fiber properties, certain types of experiments are conducted in the Cotton Fiber Research Division on yarn and tire-cord properties. These experiments are designed with emphasis on the establishment of relationships between fiber and product properties. Optical measurements on yarns and cords were mentioned above. Flexure endurance tests on tire cords of treated

FIG. 4. General spectroscopic laboratory, showing medium quartz, grating, and Littrow spectrographs.

and untreated cotton, rayon, experimental constructions, etc., are among the other tests of this sort going forward in the physical research field. For this purpose a second fatigue-life testing machine is in use. While designed and built at the Laboratory, it operates on a principle different from that of the tester previously referred to. Interesting preliminary results, confirming a theory that fatigue failure in tire cord is, in part at least, due to processes within the individual fibers, have been found.

For many months a research program on the factors influencing the adhesion of tire cord to carcass rubber stock has been under way. In the test in current use the specimen consists of a short length of the cord under test imbedded at each end in a strip of rubber. The molding of the test piece simulates the conditions under which a tire is molded. The test consists of the measurement on a standard rubber-testing machine of the force required to separate the cord from one of the end strips. While the test has been used in other laboratories for several years it has not been standardized, and is still in a developmental stage. The study of the various factors in the test itself which might influence the reliability of the results has been undertaken by the Southern Regional Laboratory. This study has required the application of a variety of moderately precise, though simple, physical measurements. Results obtained by means of this test indicate that the adhesion of cord and rubber is influenced by fiber characteristics as well as by such product characteristics as gauge and construction.

TESTING OF TEXTILE FINISHES

The evaluation of the properties of grey and finished textiles in terms of performance, durability, and appearance is an important phase in the development of new chemical finishes or finishing techniques for cotton products. This necessitates first analyzing the requirements of a textile material for a particular purpose, and then selecting appropriate tests for these requirements. Standard apparatus and procedures are usually available, but in some instances adaptations or special methods must be developed.

The Cotton Chemical Finishing Division is well equipped with most of the conventional testing equipment, including one of the special air-conditioned rooms previously mentioned. Here are conducted all tests affected by the moisture content of the fibers. The scope of the testing is wide and varied, to meet the requirements of the end-use of the product. In the organization of the Testing Section no distinction is made between tests as to whether they are physical, chemical, or of service nature. There are, however, several testing techniques which display in their design the application of physical principles.

One of the first requisites of a finishing treatment is that it must not weaken the fiber or fabric appreciably. On the other hand, many treatments increase the strength of the material. Determinations of breaking strength are therefore routine procedures. They are often conducted after the material has been subjected to accelerated aging conditions selected to simulate the effects of heat, light, and weather, separately or in combination. Weather effects are obtained either by outdoor exposure or by a special weathering machine in which the fabric is subjected to a spray of water and the radiation from a carbon-arc lamp. For fabrics that are subjected to strains in service, the determination of stress-strain relations and of elongation at break are important. All breaking-strength machines are equipped with attachments for recording, or for reading directly the elongation of the material during test.

It is recognized, however, that breaking strength is not necessarily a measure of the serviceability to be expected from a material. For example, in upholstery and some clothing fabrics, resistance to abrasion may be the most relevant property. It is largely dependent on the finish of the material as well as on the construction, and it may have no relation to the breaking strength. The machine used for measuring resistance to rubbing abrasion operates on the continuous rotary principle so that wear can be observed at all angles to the weave. It is provided with a vacuum attachment which removes lint and abrasive particles during the course of the test.

The consumer depends largely on the appearance and feel of a fabric when making a selection. While these composite properties do not lend themselves to direct measurement, it is possible to isolate the component factors. These factors are readily recognizable as familiar physical properties on which it is possible to obtain quantitative laboratory measurements. (See Fig. 3.) Among the factors determining the appearance of a fabric are its weave, color, and luster, while thickness, weight, softness (compressibility), and stiffness or flexibility affect the tactile characteristics. The *weave* and *construction* of fabrics can be readily analyzed directly; the *color* can be identified by reference to standard color cards or by spectrophotometry; and *luster* and *gloss* are measured on a reflectometer or glossmeter. The tactile properties such as *thickness* and *compressibility* are measured on a thickness gauge and a compressometer. The latter measures the change of thickness with pressure increasing and then decreasing. The *flexural* characteristics are obtained with a flexometer which measures the amount of work done in folding a piece of fabric through a given angle and the amount of work recovered when the fabric unfolds. These values provide a measure of the *stiffness* and *crease-resistance* of the fabric. Resistance to crushing, creasing, and wrinkling are especially important characteristics for cotton dress fabrics. The *weight* of a fabric can be determined by weighing a small sample on an analytical balance and calculating the weight per unit area, which is usually expressed in ounces per square yard.

The tests mentioned in the preceding paragraph are generally applied to the newly finished fabric, and again after it has been subjected to the effects of various agents that may affect it in service. The weathering machine already mentioned, a Fade-Ometer for measuring the effects of light alone, washing machines for simulating laundering and dry-cleaning processes, ovens for heat treatment, etc., all assist in producing test conditions for comparing the efficiency of different finishes, and for determining their durability in service.

The chemical-finishing research program embraces the improvement of cotton fabrics used for special purposes, or their adaptation to such purposes. Among the tests of a physical nature conducted on water-resistant fabrics, for example, may be mentioned resistance to the penetration of water under pressure, wettability, and air permeability (porosity). The last test is important on fabrics which have been "proofed" by chemical finishing, as a measure of the ability of the fabric to "breathe." Tests on fabrics for other special purposes, such as resistance to mildew and to fire, are also conducted, but these are largely chemical or biochemical, rather than physical, in nature.

PHYSICAL METHODS OF ANALYSIS

In the Physics Section, which serves all divisions of the Laboratory, are conducted those measurements and observations involving the more highly specialized and costly applications of physical techniques. Included in this unit is a laboratory for spectroscopy and spectrophotometry, equipment for x-ray diffraction, and facilities for electrical and optical measurements. (See Fig. 4.)

The use of the spectroscope as an analytical tool has been so well developed that the analytical department of a truly modern chemical research institution can no longer be considered as rendering adequate assistance to the research staff without the services of this instrument in at least one or more of its many modifications. Spectrographic equipment for analytical purposes can be listed more or less loosely in four classifications depending upon the manner in which the spectral radiations are employed.

Thus there is emission spectroscopy, or spectrochemical analysis; absorption spectroscopy, or spectrophotometry; scattering spectroscopy, or the Raman effect; and finally fluorescence spectroscopy, or fluorophotometry. Each is capable of making considerable or important contributions to analytical chemistry and hence to chemical research. Equipment is available at the Southern Regional Laboratory for rendering at least some services in each of these four fields of spectroscopy.

For emission analysis a large quartz Littrow-type spectrograph and a small grating spectrograph are available. The radiation source, either the conventional low voltage d.c. arc or the high voltage a.c. arc, is aligned to the large instrument and then the smaller instrument is aligned to the fixed source. With this arrangement spectrograms can be obtained simultaneously in the ultraviolet region with the quartz spectrograph and in the visible region with the grating spectrograph, thus affording qualitative identification and, if required, quantitative determination of some forty-five of the chemical elements with a single exposure and a sample as small as a few milligrams. The arrangement affords also a maximum saving of the operator's time and a minimum consumption of the specially purified chemicals used as buffers and carriers, and of the expensive rods used to hold the samples. The spectrograms are then projected by means of a Balopticon to juxtapose them with charts of the most persistent lines of each element, previously prepared with the same two spectrographs by the use of very pure chemicals. Matching of the most persistent lines provides a reliable and rapid identification of the elements present in the unknown sample.

If a quantitative determination of any of the elements shown to be present in the sample is required, the spectrograms are placed in a Leeds and Northrup recording densitometer and the optical densities of selected lines are measured. From these measurements the quantity of any constituent may be readily estimated from previously obtained plate-calibration and analytical curves. In this Laboratory spectrochemical analyses are proving particularly useful in providing rapid qualitative surveys of the inorganic constituents of ashed samples, often preliminary to complete chemical analyses. They also assist in the control of those elements which are present only in extremely small quantities, yet are of great importance because of their functions as, for example, catalytic agents in problems of stability and storage, or in biochemical studies.

The forms of apparatus available for absorption studies are conveniently divided into two types, photoelectric and photographic. A Beckman quartz prism photoelectric spectrophotometer covers the range from 200 to 2000 millimicrons and is thus capable of measuring absorption throughout the ultraviolet, the visible, and the near infra-red regions of the spectrum. A grating photoelectric spectrophotometer, limited to absorption measurements in the visible region, is available for studies of colored compounds and a medium quartz spectrograph, used in conjunction with a Spekker photometer, provides a spectrophotometer capable of photographing absorption spectra through the ultraviolet region. These instruments permit qualitative identification of organic compounds, as well as quantitative determinations of organic groups and of inorganic cations and anions.

In this Laboratory the quartz spectrophotometer has proved useful in the identification of compounds isolated from various commodities and by-products in experimental processes. Examples are the identification of alpha-tocopherol (vitamin E) concentrated from oils by use of a molecular still, or quercitrin (related to vitamin P) isolated from the pigment residue after extraction of rubber from goldenrod. Quantitative measurements on compounds that show characteristic absorption also have been made with this instrument. Examples of such applications include the direct determination of eleostearic acid in tung oil, and the relative composition of oil mixtures by measurements of triene conjugation produced by alkali saponification.

The visual photoelectric spectrophotometer is finding advantageous use in studies directed toward the adoption of certain colorimetric methods of analysis. From the spectrophotometric curves obtained by use of the instrument, the wave-length position of the maximum absorption band of colored solutions, and the spectral characteristics of suitable, colored-glass filters

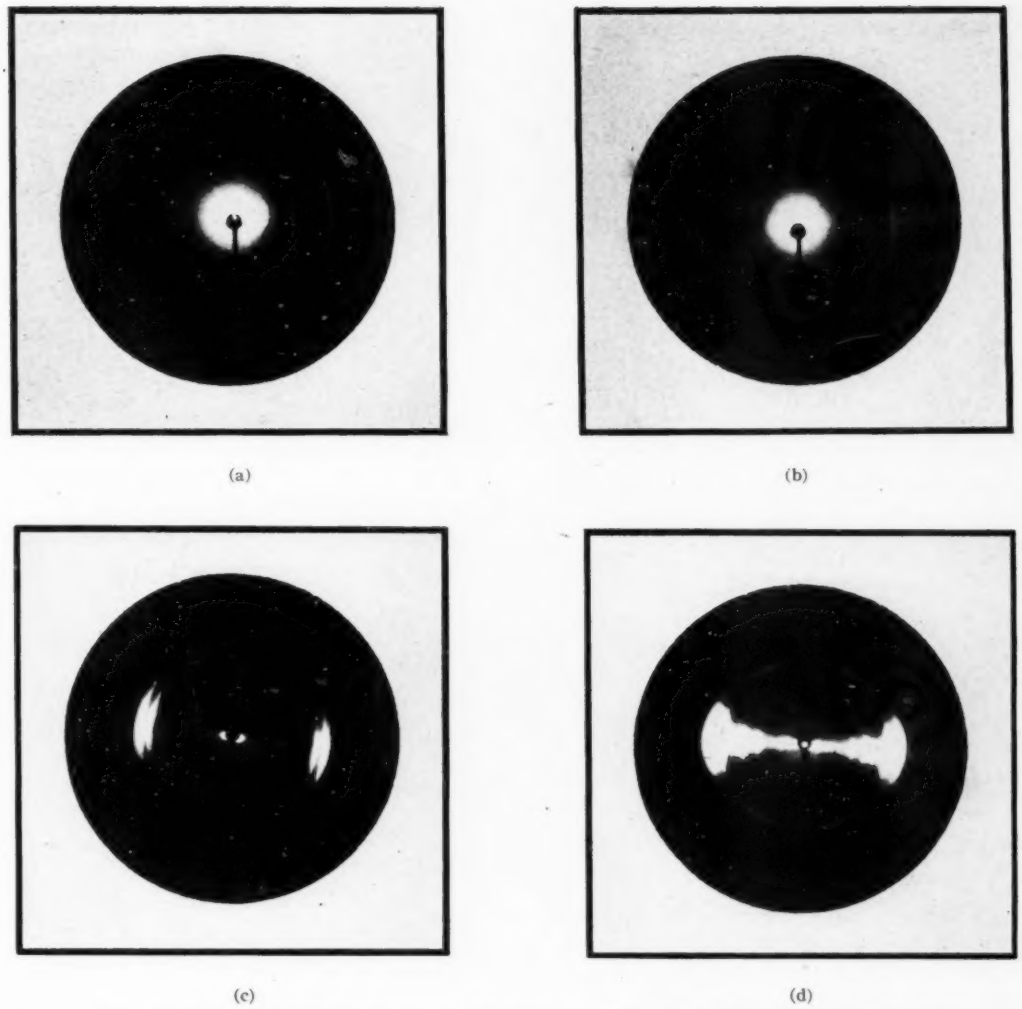

FIG. 5. X-ray diffraction patterns obtained on cotton variously treated: (a) native cellulose; (b) wet-stretched fibers (note contraction of arcs, indicating increased orientation); (c) complete mercerization; and (d) degree of mercerization limited by cord twist (note superposition of native and hydrate pattern).

are established. Employing the visible absorption of colored solutions, the instrument is being extensively used for such measurements as the estimation of carotene extracted from sweet-potatoes, or of copper content in cotton fabrics treated with copper salts for mildew prevention.

The photographic spectrophotometer is most useful for quickly ascertaining the purity of liquids, such as those purified for use as solvents for test substances in absorption spectroscopy, or for the determination of the presence of extremely minute traces of aromatic and certain aliphatic impurities in a solution.

A large aperture, glass prism Gaertner spectrograph, with Raman-tube and mercury-arc accessories is available for measurements of Raman shifts. This equipment is particularly useful in the detection and determination of the relative amounts of various tautomeric isomers of an organic substance.

Fluorescence spectroscopy is employed for the quantitative evaluation of either organic substances or inorganic ions where fluorescence radiation is one of the most characteristic properties, or where simple derivatives possessing fluorescent properties can be prepared. An electronic photofluorometer is used for fluorescent quantitative determinations of vitamin B_1 (thi-

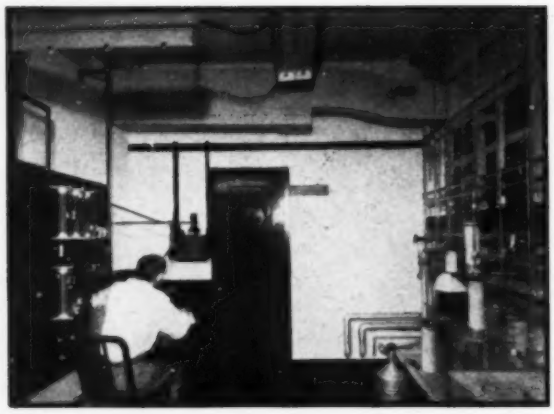

FIG. 6. Calorimetric apparatus for the precision measurement of absolute specific heats of oils and solutions.

amine chloride), vitamin B_2 (riboflavin), chlorophyll, coproporphyrin, etc.

By thus providing rapid and accurate methods for the qualitative detection and quantitative determination of most of the chemical elements, for the identification and determination of the numerous compounds (both organic and inorganic) which possess either characteristic absorption or fluorescent properties, and for the detection of the relative amounts of isomeric forms, spectroscopy makes a major contribution to modern methods of chemical analysis, and therefore a noteworthy contribution to chemical research.

The important physical properties of materials may be regarded as being largely the result of their ultimate internal structures. The effects upon the basic, fine structure of different chemical or physical processes (or of variations in the conditions under which specific processes are carried out) can be closely followed by x-ray diffraction studies. At the Southern Regional Laboratory the x-ray diffraction method is being liberally employed on cotton textiles. Typical of the data obtained in a comparative study are the patterns shown in Fig. 5. The patterns clearly disclose the effectiveness of different mercerization methods as concerns modification of the basic structure of cotton cellulose. Diffraction data have proved to be the most crucial evidence available at this Laboratory, for evaluating the effects of certain experimental treatments on cotton fibers.

By providing for the determination of lattice spacings, diffraction data contribute information on the composition of agricultural derivatives. Thus they have been used for the identification of solid phases, and the analysis of long chain hydrocarbons, such as those isolated from cottonseed and peanut oils. Spacing measurements as applied to hydrocarbons are an important part of the criteria of purity in products from natural sources.

The optical properties of crystalline materials naturally occurring in, or derived from, agricultural commodities provide a means for following experimental processes applied to these commodities. The Physics Section has facilities for investigating these properties by petrographic methods. Included in the optical laboratory is equipment for photomicrography and precision refractometry and polarimetry. Another optical research technique, which has proved useful in the analysis of high speed cyclic motions in processing and testing machines, is the stroboscope.

THERMAL AND THERMODYNAMIC PROPERTIES

The possible economic success of a proposed industrial process may very often be appraised from thermal and thermodynamic properties. Such data are also essential to the design and construction of pilot-plant and industrial equipment such as, for example: (1) fractionating and stripping stills for the separation of fatty acids, esters, and glycerides and for solvent recovery; (2) oil hydrogenation equipment; and (3) oil winterizing equipment.

The physical and physico-chemical data to be obtained depend upon the immediate problems of the laboratory. They might include specific heats, entropies, free energies, heats of fusion, heats of solution, heats of vaporization, heats of reaction, solubilities, partition coefficients, vapor pressures, freezing points, various temperature coefficients, and other physical constants of either pure compounds or mixtures.

The first consideration in planning the measurement of such physical properties is the degree of accuracy required. For some purposes highly precise and accurate data are necessary. Frequently, however, especially when dealing with

impure substances, or more or less indefinite mixtures, moderate precision is adequate. The time required to obtain the data is usually an important factor and must be considered, as, for instance, when a pilot-plant operation waits upon the results of laboratory measurements on material involved in the process. In such cases it may sometimes be necessary to sacrifice high precision for speed.

Some experiments are of the long term variety and require a more or less permanent set-up of equipment. A great many times, however, only a few measurements on a substance, with a temporary assembly of equipment, are necessary. Facilities are thus required for a wide variety of experiments and measurements. In some types of investigations, observations made with simple standard equipment, such as constant-temperature baths and cryostats, are quite adequate. For those tests or experiments of which high precision is an essential feature, recourse is necessarily taken to means of more refined measurement. For example, for the measurement of temperature, the fundamental dimension of thermodynamics, carefully calibrated, mercury thermometers, platinum-resistance thermometers, and thermocouples are available. Auxiliary precision equipment, such as cathetometers, potentiometers, bridges, standard resistances, and galvanometers, are used in conjunction with the temperature-measuring devices in the thermodynamic studies. In general, the precision instruments are continually being adapted to various uses as they are, from time to time, moved from one assembly to another.

The following are typical of the determinations which have been made recently: the thermal conductivity and hysteresis of tire carcass sections; the heat of mixing of cottonseed oil and petroleum ether; the heat of wetting of cotton; temperature coefficients of viscosity, density, and other physical properties; and the specific heat and "heat of fusion" of cottonseed oil alone and mixed with petroleum ether.

The last determinations mentioned above were made on calorimetric equipment especially set up for thermal studies on vegetable oils. The apparatus, a view of which is shown in Fig. 6, was designed to employ the adiabatic method. As adapted at the Southern Regional Laboratory, the method is in the high-precision class, and is applicable to solutions, and liquids generally. Measurements in the cottonseed-oil study were made over the range −193° to +65°C. The heat absorbed by the specimen, which was sealed in an aneroid calorimeter, was supplied and accurately measured electrically, temperature differences down to 0.001°C being read.

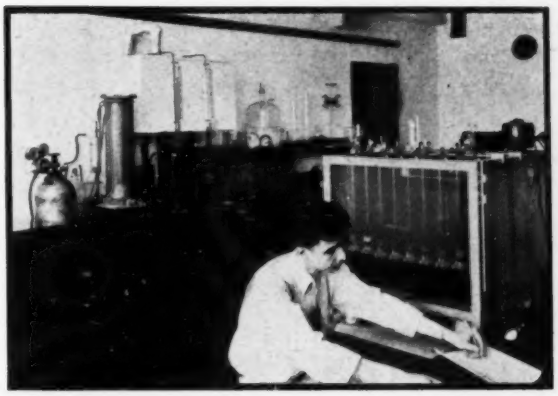

FIG. 7. Viscometric laboratory, showing refrigerating unit, cuprammonium generator, low temperature storage box, and constant temperature bath.

APPLICATIONS OF VISCOMETRY

The measurement of viscosity is widely used throughout the Southern Regional Laboratory both as a tool in fundamental research and as a means of grading or evaluating a material for technical applications. Viscometers of the rolling-ball, rotating-cylinder, and capillary types are in use, several variations of the second and third types being available. The choice of viscometer type is, of course, dictated by the character of the liquid under study.

Chemical methods have been found to be inadequate for following the changes which take place in processing or modifying vegetable proteins separated from cottonseed and peanut meals. The measurement of the viscosities of protein solutions has been found to be of major importance among the physical methods to which recourse has been taken for process studies. Such measurements have also been indispensable for evaluating the usefulness of the proteins in the production of adhesives, fibers, sizes, etc. Viscometers of the Hoeppler rolling-ball type, such as are used in the Oil, Fat, and Protein Division, have proved to be best suited to the

viscometry of vegetable protein solutions. A feature which is of advantage in this work is the wide range of viscosities to which the instrument is adaptable. The viscosity of these solutions is influenced greatly by changes in *p*H. Accordingly, *p*H determinations are made in connection with the viscosity measurements; the latter measurements are of little or no value unless they are individually referred to the *p*H of the corresponding solution.

Viscometry constitutes an important part of the studies on colloidal properties in the Cotton Fiber Research Division. The fluidity (commonly used in textile practice instead of viscosity) of a cuprammonium solution serves as a measure not only of the average molecular-chain length in a sample of cotton, but also of the strength of the fibers. As a means of evaluating the degradation of cellulose caused by certain treatments of cotton, the fluidity is often more sensitive than actual strength measurements on the samples.

The cuprammonium solvent being used in the regular fluidity determinations on cotton and other cellulosic fibers has the standard American Chemical Society composition. To maintain its composition by excluding light and oxygen, the cuprammonium is stored in the dark, at between 10° and 15°C, under an atmosphere of nitrogen. The viscometers employed consist of burets, to the lower ends of which are affixed specially constructed and accurately calibrated capillary tubes. For use with solutions having widely different fluidities, capillaries in a range of diameters are available. Fluidity measurements are made in a large water bath held close to 25°C. (See Fig. 7.)

Because undeteriorated cotton cellulose dispersed in cuprammonium reagent exhibits anomalous viscous behavior, provision is made in the procedure to obtain a measure of the velocity gradients at several points during the discharge. The sizes of sample and capillary are so selected that, with small adjustments, the fluidity results can be referred to a velocity gradient of 500 $sec.^{-1}$ and concentration of 0.5 percent as the standard conditions for cotton cellulose.

In the Sweetpotato Products Division, viscosity determinations are conducted as a means of grading the starches and pastes prepared in experimental and pilot-plant processes. Starches for various technical applications are specified according to viscosity. Here a Stormer, rotating-cylinder viscometer is used, the readings being taken at 90°C.

In the Physical Chemical Section an investigation is under way relating the viscosity of cottonseed and peanut oils to their iodine numbers and degree of hydrogenation. These measurements are being made in modified Ostwald viscometers at various temperatures ranging from 25° to above 200°C. The data obtained are to be used in the development of pilot-plant processes and the design of appropriate equipment for the treatment of oils.

This section has also conducted viscometric work on benzene solutions of the goldenrod rubber produced in pilot-plant experiments. The results, expressed finally as intrinsic viscosity, were used on a comparative basis to evaluate the quality of the various batches of rubber. Here again the modified Ostwald viscometer was used, in this case in a constant temperature bath which maintains a temperature of 25°C. Care had to be taken to protect the rubber solutions from light, and they were therefore handled in a partially darkened laboratory. This precaution is necessary because light has a marked effect on rubber solutions, especially in the presence of chlorophyll.

TESTING OF RUBBER AND PROTEIN ADHESIVES

In addition to the mechanical testing which is conducted on textile materials at the Southern Regional Laboratory, some testing of this type is also being conducted on other materials. The Engineering and Development Division has employed a Scott vertical rubber-testing machine, equipped with an autographic recording mechanism, to obtain strength and elongation data on goldenrod rubber. The production of this rubber on pilot-plant scale has been under investigation as part of the Emergency Rubber Project of the Department of Agriculture. With the wide variety of standard dies available, samples in many shapes and sizes may be tested in this machine. The machine is also being used in the previously mentioned study of the adhesion between rubber and tire cords of various types, treated and untreated.

Research directed toward the development of adhesives from cottonseed and peanut oil meals and from proteins derived from the meals is almost entirely dependent on physical measurements. The first step in the development of adhesives or glues is to prepare products having flow characteristics which permit their effective use in commercial glue spreaders. A viscometer which operates on the torsion principle is suitable for a rough evaluation of the flow properties of such products. In the case of plywood glues, another step is necessary, namely, to determine how well the gluing can be done with any given experimental product. This can be accomplished not by simply examining the glue mixture but only by actually making glued joints and measuring the force required to shear the joints. Two types of joint tests are made. One is the block shear test which uses a special shearing tool in conjunction with a universal testing machine; the other is the plywood shear test which is made with an ordinary cement-briquette testing machine that has been equipped with special jaws. The plywood test is especially useful in estimating the strength of a glued joint after the test pieces have been soaked in water.

CONCLUSION

In the Regional Research Laboratories, as in other laboratories and institutes of applied science and engineering, the problems which present themselves for solution generally involve the interaction of a wide variety of natural phenomena. They do not arise neatly classified as to the single scientific discipline to which each is amenable. In the development of an adequate experimental attack on a specific problem the theories and techniques of two or three sciences may become intertwined. In the present survey the aim has been to include, with an effort at thoroughness, those methods of *observation* and *measurement* to which physics has contributed in a well-defined and prominent role. There are at the Southern Regional Laboratory many semiplant processes in operation, such as those in the textile mill, and many applications of electronic and electromagnetic control devices, all of which are of a physical nature. However, because a necessarily brief discussion of the former cannot be informative, while the latter are well-known to technical people generally, it has not appeared feasible to include them in the present survey.

"Sound management rests upon the development of new opportunities, new uses, new products, new services, new desires which in themselves can be considered from a social point of view, purely constructive. Research is the department of a business which gives to the management the substance on which it grows. Research is the department of a business which carries the responsibility of giving to management new facts of nature and the interpretation of those facts into utility so that the management can provide improved products, more economically priced products and, above all, new products to meet the unexpressed human desires."

Quoted by Henry P. Kendall, President, The Kendall Company

The American Institute of Physics Building

IN the October, 1943 issue of this Journal, an early history of the new American Institute of Physics building was published which created widespread interest and favorable comment. Further articles were promised so that physicists could become better acquainted with their new headquarters. A second article of this series, one devoted to the architectural features of the house is presented below.—THE EDITOR.

II. An Architectural Study of the Building

BY BLANCHETTE ARNAUD

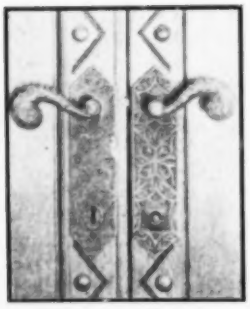

IN describing the house of the American Institute of Physics, one might apply the words used by Francis Bacon in his "Essay on Building" to describe his new house in the then modern style which we now call Tudor, *viz:* A house composed of "delicate and rich cabinets, daintily paved, richly hanged, glazed with crystalline glass; and all other elegancy that can be thought upon."

There are certain comparisons that can be made between the times when the two houses were built. The day of the Tudors was, in England, a period of extraordinary expansion, social change, and new wealth. Feudalism was outworn; the Wars of the Roses had brought death and economic ruin to the old aristocracy; the well-known procedures of Henry VIII, the establishment of new industries, and the discoveries in the New World had brought into existence new wealth which bought aristocracy for a group of individuals who could not claim their titles by heredity; the "New Learning" and new styles were being imported from the Continent; the old fortress-castle, so picturesque to look at and so dreary to live in, was forever useless and outmoded. There was a frenzy of building, for the people wanted light, comfort, gaiety, and the latest fashion in art and decoration, which last, paradoxically, was at once a new manner and an attempt to reproduce the old motifs of classical antiquity. It was a revival of the past, but not the recent past; for it is a curious fact that in every age, the style of one's father's day is "old fashioned" and undesirable, whereas that which is older is antique, desirable, and fit material for emulation and re-creation.

In the fifteenth and sixteenth centuries, builders and craftsmen were avidly studying handbooks of classic ornament, but most of them lacked the opportunity of becoming familiar with the original monuments which this ornament adorned. They used the motifs according to their needs and understanding, producing a lavish, vigorous, indigenous style that was inevitably creative, expressing the vitality of the people who called it into being.

The early twentieth century, continuing the mood and tempo of the late nineteenth century, was also a period of expansion, new wealth, social change, and revivalism in art. As in the sixteenth century, designs of a preceding period were being carefully studied in books. But in the twentieth century, the choice was not confined to classical antiquity: One might select the style of any period and any place from Egypt to Versailles.

Mr. Erdmann, who built the Institute's house, was a bachelor; he wanted something rich but masculine. The robust style of the Tudors was his final choice, the process of elimination having been a matter of some labor and concern to the architects. But whereas the sixteenth-century house might have been somewhat naive and unrestrained, each craftsman taking full liberty in the exercise of his skill,

the twentieth century house is luxurious but restrained, showing the practised eye and active supervision of the professional architect.

It is with considerable accuracy that the Institute's house can be called Tudor, in spite of some variation of style in the decoration of the several parts of the house; for the Tudor period may be said to extend from the time of Henry VII through the reign of James I, or from about 1450 to 1640 and even after, so that it includes such minor divisions as Elizabethan and Jacobean. The style was an enduring one because it expressed so adequately the needs and temper of the society that gave it being. It was unmistakably English in spite of Classic, Italian, and Flemish influences; it was virile and exuberant; it was consciously and superficially Classic, while remaining subconsciously and basically Mediaeval—characteristics equally true of the social culture of the period.

After the long popularity of the broken curves and florid detail of the Tudor style, a reaction was bound to follow. It came quite suddenly in the middle of the seventeenth century, a complete change in style having been brought about almost entirely by the taste and ability of a single individual—Inigo Jones (1573–1652). Deeply impressed by the austere classicism of Palladio, Jones developed a style characterized by pure line, refinement of proportion, and restraint in the use of decoration. This manner is also represented in the Institute's building.

The façade of the house, while adapted to twentieth-century building regulations, expresses the Mediaeval-Renaissance transition. The round arches, the engaged Doric columns, the consols, the Corinthian pilasters are all Renaissance. But the expansive, square-headed, stone-mullioned windows above the first floor are typically Gothic. Mediaeval builders designed their windows to conform to the structure, and when the interior void was made up of vertical members supporting horizontal ceilings, the wall penetration was made to correspond to the inner void. In other words, pointed windows were used only with vaulted interiors. The stone mullions are reminiscent of Gothic stone tracery, as are also the mouldings over the third-floor windows—in modified form here, but originally designed to lead the rain water away from the windows. The heavy stone mullions have the double function

The English Renaissance façade. This is an early photograph; the lower stone railing and doorway were modified when the street was widened.

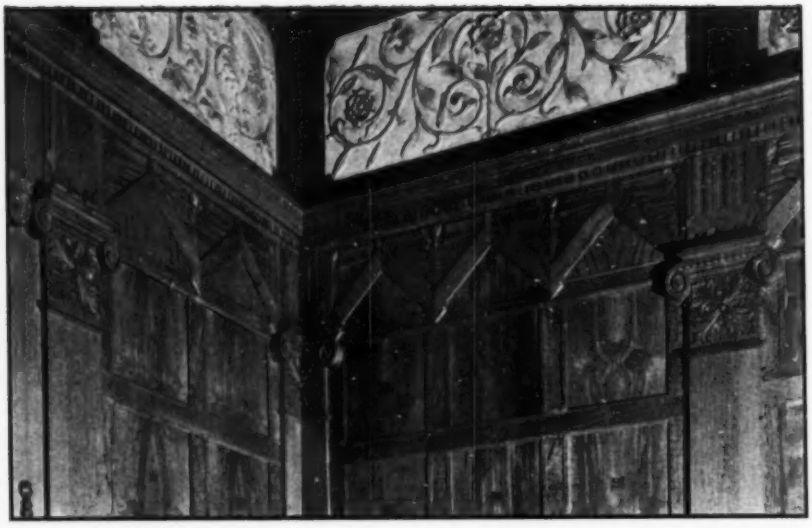

Detail of wall panelling and plaster frieze.

of providing strong glass frames and of breaking up the window space, counterbalancing the disproportion of void in the mass of the wall. The leadings that hold the small panes together have also an aesthetic as well as a functional value, for they give texture to the openings which would otherwise look blank. The cresting of the fourth- and fifth-floor windows in flattened stone appliqué is typically Tudor, but is derived from the applied tracery of the late Gothic period.

Gothic, too, are the gable and the finial at its peak. In fact, the English never have given up their special liking for gabled roofs, which they have used in a manner that is highly picturesque if not always logical or well balanced. The flat stone façade without projections is as characteristic of the Tudor town house as it is of the brownstone front.

Throughout the interior each room presents variations of Tudor decoration.

The entrance hall is sheathed in a handsome yellow stone marble with black veining. The rest of the house is panelled in wood. The design of each wall is beautifully proportioned to the dimensions of the room, and the workmanship is excellent.

Wood wainscoting is especially suitable where the weather is likely to be inclement, for the wood sheathing is a good insulation against cold and dampness, and the texture and rich color lend an atmosphere of greater warmth than stone or plaster. It was very popular in Tudor England, replacing the Mediaeval use of stone walls hung with tapestries. The early Tudor method, current in the fifteenth century, was to sheathe the walls with small panels, the size of a single plank, which system is used in the stair halls, and in the East office on the third floor. Each panel was a decorative unit in the wall design, being framed

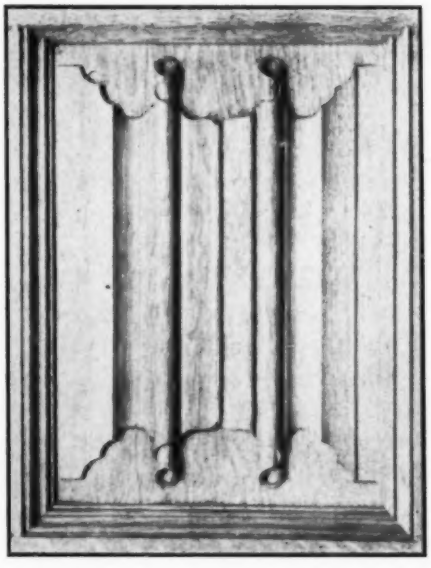

A panel from the wall sheathing in the East office on the third floor showing the highly intricate and delicately carved linen-fold motif.

in a moulding, and sometimes carved into a pattern.

The linen-fold was a very popular motif which came into fashion at this time, and was extensively used for many decades because of its highly decorative quality and the possibilities of inexhaustible variation. It is a basic form, made up of a strong vertical line relieved by a flowing horizontal, the treatment of the fabric-end motif providing means for endless variety in curvilinear patterning. But this theme is not limited to the linen-fold or to the Tudor period, for it is the treatment of end-draperies that lend much beauty to the figure compositions of the Greek, the Chinese, and the Romanesque artists. There are two examples of the linen-fold here: one in the East office on the third floor, and the other in the top panelling of the North office on the second floor.

It was in the fifteenth century in England that the Classic orders found their way to the interior of the houses and were there used as decorative motifs. The pilaster was found to be highly useful to frame doors, windows, and fireplaces, and to divide the wall spaces into bays, providing a rhythmic treatment that relieved the monotony of an unbroken repetition of pattern. One can see how much diversity of design was made possible by this device in most of the rooms of this house, as, for example, in the first floor conference room, where the wainscoting is made up of long panels with applied mouldings of rather complex profile—a manner that followed the earlier method of square panelling. The surmounting shell frieze here is especially beautiful.

In true Tudor style, all the ceilings are decorated. The story of how the English developed their predilection for ornamented ceilings is an interesting one, and is also an excellent example of how a tradition develops. Like other Tudor characteristics, the decorated ceiling is Mediaeval in origin.

In building a Gothic vault, the French so constructed the masonry fill that it spanned the areas between the main arches without secondary ribs either for appearance or support. Consequently the French, excelling in the craft of masonry, continued to construct vaults that were undecorated, pure in line, and structurally perfect. But the English laid up their stones in a different way, so that secondary ribs were required, sometimes to cover the zig-zag intersection of the stone courses, sometimes as additional supports. While less ingenious than the French method from an engineering point of view, it was nevertheless good structure, and the extra ribs or tiercerons, radiating from the capitals, evolved into the fan vaults, which were so decorative that they continued to be used even when there was no longer any structural need for them. In the last phase of the Gothic

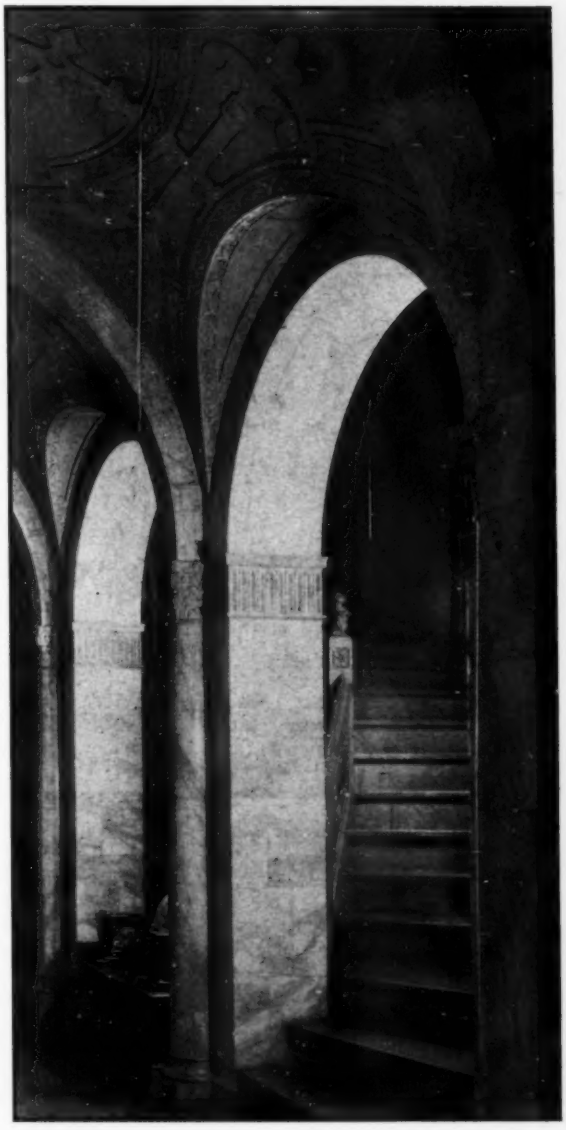

Detail of handsome marble work in the entrance hall.

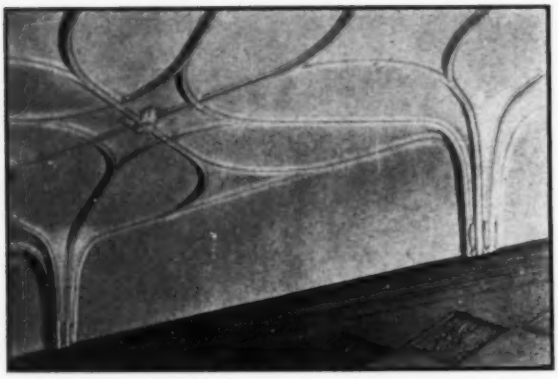

Detail of interlaced ribs on one of the fine plaster ceilings.

style, the arch was flattened, and was finally superseded in the early Renaissance by a hung ceiling. But ceilings decorated with ribs and pendants were still in high favor; so the practice developed of applying mouldings in complicated patterns to horizontal surfaces.

For this purpose plaster was found to be a most suitable material, being economical, light, durable, and easily worked, lending itself to innumerable variations of treatment—panels, geometric forms, interlaced mouldings, all-over patterns, or rosettes, fruits, and flowers in high relief. It was first introduced to England by Italian craftsmen working on Henry VIII's palace of Nonesuch, and thereafter gained continuously in popularity. In the sixteenth and seventeenth centuries, plaster work was a craft in which the English excelled.

The Institute's house presents an interesting variety of ceiling decorations. The intertwining curvilinear mouldings in the East office on the third floor are obviously reminiscent of the Gothic vault ribs. The overlapping geometric forms of the North office on the second floor exemplify a later development; while the entrance hall and the Societies' Room are decorated in flattened appliqué or "strap work" that bespeaks Flemish influence which was strong throughout the Tudor period.

The Renaissance style was first imported directly from Italy, and Italian artists and craftsmen were in great demand. But meanwhile the Low Countries also had accepted the new fashion, and fostered a host of able artisans who adapted the Classic patterns according to their own taste and understanding. These craftsmen found their way to England in increasing number, for the two countries were all but neighbors. There were active trade relations and close religious ties between them, and many Flemish workmen established themselves in England as refugees, finding asylum as well as occupation in that country. The English used Flemish handbooks as well as labor, but conformed the product to their own needs, traditions, and predilections. So it is quite inevitable that the Tudor style is a Renaissance variant that is neither Roman, nor Italian, nor Continental.

In both rooms on the second floor, the walls and ceilings are united by a plaster frieze moulded in delicate vine patterns, that of the Societies' Room being picked out in color, harmonizing with the colored field of the ceiling.

The rooms above the second floor are finished in a later manner introduced by Inigo Jones. In the West office on the third floor, the ceiling

Detail of highly carved stair rail.

decoration is restricted to border mouldings that frame a great oval garland of fruits and flowers.

Whatever the richness of window, wall, or ceiling, the fireplace is the focal point of any room. In this house each one is treated differently. In the North office on the second floor the wall panelling carries along over the mantle, continuing the pattern without change, two pilasters marking off a bay, and thus accentuating the fireplace. In the conference room on the first floor a section is similarly encased by pilasters, while the panels over the mantle are designed in geometric patterns proportioned to the shorter wall space between mantle and frieze, further accent being given by the turned split spindles, and the flat cresting applied against the plaster.

In several of the chimney pieces the opening is in the form of a flat arch (a typically late Gothic or Tudor form). Its inner mouldings follow the opening, but the outer mouldings carry up straight to form a square frame, so that the space between forms a tapering spandrel enriched by carving.

The fireplace in the Societies' Room is a monumental piece in two contrasting marbles, one of yellow with brown veining, the other of grey with rose veining. (This practice of combining marbles was originally a Flemish influence.) It is constructed in two stages with superimposed orders, Ionic below and Corinthian above, the cornice of the lower order being also the mantle and the base for the upper stage. The small Corinthian columns flank a decorative frame which encloses a large sculptured coat-of-arms with heraldic supports—a design to please the fancy rather than to provide information about the Erdmann ancestry. The stone cresting of the upper stage is complemented by the cresting of the woodwork above.

The metal work throughout the house offers an exhibition of fine workmanship and a rich variety of design. The lighting fixtures, wall brackets, locks, and hinges are worthy of examination.

The upper rooms are reached by handsome staircases, which in this house offered no mean problem to the architect who, in spite of high ceilings and limited ground space, constructed the stair in a single curved flight. The decorated

Monumental fireplace in the Societies' Room. Decorations shown are those used when the house was owned by Mr. Erdmann.

stair of Tudor days is highly significant for it illustrates the story of the times. In the Middle Ages the life of the household centered about one great room. In a manor or castle it was called the "hall," a word which has fixed itself inextricably in our vocabulary and now carries a variety of meanings. The hall was handsome, impressive, and certainly there were some advantages in the communal life that went on there: The master and mistress were above, but not segregated from their servants and retainers.

There is a recall, at the Institute, of the life of the great hall in the inscription executed in stained glass and incorporated in the window of the North office on the second floor: *His table*

*dormant in his halle alway stood redy covered al the longe day.** For be it remembered that the great hall was an all-purpose room that was occupied day and night; so the dining table was not a fixed piece of furniture, but was a board laid on wooden horses or trestles, which was set up for the meal and removed when the repast was over. The "board" as furniture is obsolete, but as language it is living vocabulary; and when we talk of "board meetings" or of "board and lodgings," we can think upon the respectable antiquity of the term.

But the evolution of the staircase was the subject under consideration. Whatever the romance and allure of the great hall, it was a place of many discomforts: draft, dirt, confusion, and lack of privacy. As has been explained, times were changing during the reign of Henry VIII, and feudal ways were being abandoned. The great hall was forsaken, its place being taken in the new houses by the "gallery"—a long room with many windows occupying the southern side of the house on the second floor. In the extensive Mediaeval houses, access from floor to floor was usually provided by a spiral stair built into a tower which was contiguous with, but exterior to, the main plan. In the new houses of the sixteenth century, the stair was brought within doors, as it were, and the raising of the main room to the second floor lent additional importance to the stair leading to it. Henceforth, in every important house, the stair was to be one of the principle architectural features, and the finest craftsmanship was expended upon balustrades and newel posts.

The first- and second-stair flights in the Institute's house exhibit some fine carving and ingenious designing, the same pattern filling equally well the rectangular frame on the landing and the lozenge-shaped quadrilateral forms where the banister follows the stair.

It would seem that the building of the American Institute of Physics should fill all the needs of its new occupants, providing not merely comfort and convenience, but also stimulation for imagination and aesthetic sensibilities. It is a beautiful building that will be used and enjoyed for many years.

* Chaucer's *Canterbury Tales, Prologue;* "The Franklin," lines 23 and 24.

Calendar of Meetings

September

11–16	American Association for the Advancement of Science, Cleveland, Ohio
13–15	Society of Automotive Engineers, Milwaukee, Wisconsin

October

5– 6	American Institute of Mining and Metallurgical Engineers, Pittsburgh, Pennsylvania
5– 7	National Electronics Conference, Chicago, Illinois
5– 7	Society of Automotive Engineers, Los Angeles, California
6– 9	Electronic Parts and Equipment Industry Conference, Chicago, Illinois
9–14	American Society of Civil Engineers, Cleveland, Ohio
10	Physics Club of Chicago, Chicago, Illinois
16–18	American Institute of Mining and Metallurgical Engineers, Cleveland, Ohio
16–20	American Society for Metals, Cleveland, Ohio
16–21	American Welding Society, Cleveland, Ohio
20–21	Optical Society of America, Hotel Pennsylvania, New York, New York
28	American Mathematical Society, New York, New York

November

2– 3	Society of Automotive Engineers, Tulsa, Oklahoma
14	Physics Club of Chicago, Chicago, Illinois
16–18	Electron Microscope Society, Chicago, Illinois
17–18	Society of Rheology, New York, New York

December

12	Physics Club of Chicago, Chicago, Illinois

January

9	Physics Club of Chicago, Chicago, Illinois

February

13	Physics Club of Chicago, Chicago, Illinois

March

13	Physics Club of Chicago, Chicago, Illinois

April

10	Physics Club of Chicago, Chicago, Illinois

May

8	Physics Club of Chicago, Chicago, Illinois

Letters to the Editor

Comments on "Organization of Physics in America"

ALFRED N. GOLDSMITH
The Institute of Radio Engineers, New York, New York
July 5, 1944

IN the *Journal of Applied Physics* for May, 1944, there appears a paper entitled "Organization of Physics in America" by Messrs. Wallace Waterfall and Elmer Hutchisson which, from its position as a leading article, its mode of presentation, and the eminent standing of its authors, carries at least an implication that it represents an expression of policy of the American Institute of Physics and that the data which it presents are authoritative and expressive of the views of that Institute.

It is noted that only the field of "application" in the electronic domain is admittedly that of The Institute of Radio Engineers, judging from the diagram in the cited article. It would appear to have been a scientific approach to the subject if the authors, prior to the issuance of their specific statements, had elected to check the accuracy of such statements. This could readily have been accomplished by asking the engineering societies to state their own concepts of the nature and limits of their activities. In the case of The Institute of Radio Engineers, at least, no such inquiry has been received. In the interest of dependability of statement and as a matter of inter-society courtesy, such an inquiry would have been both timely and appreciated.

It is not unusual for a society or institute to define or delimit its own activities and to determine, in its own best judgment, the field of its activities. However, it is perhaps unique to find one learned society gratuitously defining the scope of other scientific organizations. So far as is known, the engineering societies have never ventured to define the scope and to circumscribe the activities of the American Institute of Physics, nor would it be proper for them so to do.

The chart or diagram on page 408 of the article is inaccurate historically and otherwise. In the case of The Institute of Radio Engineers, the actual activities over the last thirty-one years include a far wider range than that indicated. The Institute has been active in the field of electronics and also to a certain extent in other fields. Thus, in "chemical physics," such topics as fluorescence, vacuum-tube materials, insulating materials, and other products have been discussed. In the field of "electricity and magnetism," a wide range of papers covering theory in the alternating-current field and in the domain of wave generation and research has been presented. Of necessity, problems of mechanical construction, optical theory and design (as required in facsimile and television), and acoustical theory (as needed in the development of microphones, loudspeakers, studio designs, and the like) have been exhaustively treated in the *Proceedings of the I. R. E.*

The diagram is similarly inaccurate, as regards the Institute, in other classifications. Considering educational matters, the Institute has frequently published important tutorial papers having as their aim the advancement of instruction in the communications and electronic fields. It has committees actively engaged in the study of engineering education.

Similarly, as regards the classification "fundamental and research," few periodicals have contained a larger proportion of research papers during the last decade than the *Proceedings of the I. R. E.*

Similar comment applies to the classification "instrumentation"—a field wherein instruments, measurements, and tests have been a subject of major interest to the Institute not only through publications and standardization work but in the work of its various committees.

The Institute of Radio Engineers therefore regards itself as active in all aspects of the communication and electronics field, as a matter of primary interest. As allied matters in which it must serve its membership and the corresponding arts and sciences, the Institute will properly consider such matters as have been illustratively given in a preceding portion of this communication. It will continue in the future, as in the past, to serve not only teachers in this field but also research investigators, instrument designers, and development and production engineers in these fields.

It is to be hoped that the viewpoint expressed in the article on "Organization of Physics in America" does not represent a permanent policy of the American Institute of Physics. In that case it would have been preferable if it had been preceded by a cautionary notice to that effect. Certainly its subject matter and contentions cannot be accepted by the other organizations that are mentioned in the article and its accompanying diagram, nor is the underlying philosophy and mode of presentation of the paper conducive to that hearty cooperation between scientific organizations of standing for which all may hope.

It is believed proper, in the interests of accuracy and full presentation of all viewpoints, to suggest that this communication be published in the *Journal of Applied Physics* with equal prominence and placement to that to which it responds.

Reply to Comments

WALLACE WATERFALL AND ELMER HUTCHISSON

As our article states, the suggestions made in it were intended to be provocative and replies such as made by our distinguished critic are indeed welcome. Contrary, however, to Dr. Goldsmith's assumption, the *Journal of Applied Physics* has never been so presumptuous as to attempt to speak for the American Institute of Physics as a whole. The fact that our paper was signed indicates that for this paper, as well as for other papers in the Journal, the responsibility is that of the authors only. The position of the article in the Journal is the one which has been reserved for articles dealing with subjects of this kind since the Journal was initiated.

Unfortunately, Dr. Goldsmith has misinterpreted the purpose of the article as well as its specific statements. No attempt was made on the chart to define or circum-

scribe the activities of the engineering societies mentioned but rather to indicate their general position in the field of applied physics. We had no thought whatever of saying that the Institute of Radio Engineers was not concerned with teaching, research, or the development of instruments in the field of radio engineering. We were concerned exclusively with the organization of the various fields of physics.

The references to earlier discussions make it clear our article was inspired by criticism which has been directed by physicists at the whole field of physics for its failure to organize in a way which would minimize overlapping of societies and journals. Even within the field of physics, we believe that some overlapping is not only inevitable but desirable. If this is true in the field of physics considered in the somewhat narrow sense in which one usually speaks, it is even more so in the broader technical field which includes all branches of engineering.

It is hoped that this additional note will clear up any misunderstanding such as that of Dr. Goldsmith.

Here and There

New Appointments

Dr. Elmer Hutchisson has been appointed Dean of the Faculty of Case School of Applied Science according to a recent announcement of President William E. Wickenden. He will succeed in this position Dr. Theodore M. Foche who retires on August 31. Dr. Hutchisson was formerly Head of the Physics Department, University of Pittsburgh, and is now engaged in war research in New York City. He is expected to take up his new duties as soon as he can be released from his present position and will give especial attention to Case School's rapidly growing program of organized research and advanced study. He will continue as Editor of the *Journal of Applied Physics*.

Dee Breen was recently appointed Western Division Sales Manager of Littelfuse, Incorporated, with territory covering the western states, and headquarters at the company's plant, El Monte, California. Before the war Mr. Breen was expediter for the Chrysler Corporation. From this position he was called to Washington to serve as expediter of materials for the U. S. Signal Corps, and after this work was completed, he was brought to Littelfuse, Chicago where he was promoted to his present position.

Division of High-Polymer Physics

The Council of the American Physical Society on June 24, 1944 appointed the following men to the Executive Committee of the new Division of High-Polymer Physics: R. B. Barnes, W. F. Busse, P. Debye, J. H. Dillon, J. P. Elting, W. J. Lyons, and L. A. Wood. From among these men the following officers of the Division were elected: Chairman, Dr. Dillon; Vice Chairman, Professor Debye; Secretary, Dr. Lyons; and Treasurer, Dr. Wood.

National Electronics Conference

A National Electronics Conference covering television, ultra-high frequency, and radio developments in the communications field and industrial measurements, electronic controls, induction heating, and power and medical applications of electronics will be held at the Medinah Club, Chicago, October 5–7.

A comprehensive program, embracing all important fields of electronics, has been prepared by Professor Arthur B. Bronwell, Northwestern University, Evanston, Illinois, who is Chairman of the Program Committee. An opening address will be given by Mr. Ralph R. Beal, entitled, "Electronic research opens new frontiers." Mr. W. C. White, Director of the Electronics Laboratory, General Electric Company, will speak on "Electronics in industry" at one of the Conference luncheons.

The tentative program of technical topics for the Conference includes the following papers grouped according to main topic divisions:

(1) Television

"Color and Ultra-High Frequency Television" by Dr. P. C. Goldmark, *Columbia Broadcasting System.*

"Reflective Optics in Television" by I. G. Maloff and D. W. Epstein, *RCA Manufacturing Company.*

"Radio Relay Systems" by C. W. Hansell, *RCA Laboratories.*

(2) Ultra-High Frequencies

"A Lighthouse Tube; a Pioneer U. H. F. Development" by E. F. Peterson and E. D. McArthur, *General Electric Company.*

"Principles of Klystron Amplifiers" by Dr. Robert Haxby, *Sperry Gyroscope Company.*

"Developments of Electronic Tubes" by I. E. Mouromtseff, *Westinghouse Electric and Manufacturing Company.*

"Wire-Frequency-Range Tuned Circuits for High Frequencies" by Dr. D. B. Sinclair, *General Radio Company.*

"Ultra-High Frequency Converters and Conversion Diagrams" by Dr. Harry Stockman, *Cruft Laboratory, Harvard University.*

(3) Radio

"Generation of Quasi-Continuous Frequency Spectra for Use with Secondary Frequency Standards" by Dr. Harold Goldberg and Richard G. Talpey, *Stromberg-Carlson Telephone Manufacturing Company.*

"A Frequency Dividing Lock-In Oscillator F-M Receiver" by G. L. Beers, *RCA Manufacturing Company.*

"Incremental Permeability Tuning" by W. J. Polydoroff, *Consulting Engineer.*

"Audible Audio Distortion" by H. H. Scott, *General Radio Company.*

"Broadband Carrier and Coaxial Cable Networks" by F. A. Cowan *American Telephone and Telegraph Company.*

(4) Industrial Measurements and Special Devices

"The Supersonic Reflectoscope; An Instrument for Inspecting the Interior of Metal Parts by Means of Sound Waves" by Dr. F. A. Firestone, *University of Michigan.*

"Dynamic Strain Gauges" by C. A. Dohrenwend, *Armour Research Foundation.*

"The Mass Spectrometer and its Practical Applications" by J. A. Hipple, *Research Laboratories, Westinghouse Electric and Manufacturing Company.*

"Two-Million Volt X-Ray Unit" by Dr. E. E. Charlton and W. F. Westendorp, *General Electric Company.*

"Industrial Fluoroscopy of Light Materials" by Dr. Scott W. Smith, *Kelley-Koett Manufacturing Company.*

"Application of Amplifier Theory to Mechanical Stability Problems" by John M. Cage, *Allis-Chalmers Manufacturing Company.*

(5) Industrial Electronic Controls

"Electronic Mechanisms in Process Plant and Industrial Laboratory" by T. A. COHEN, *Wheelco Instrument Company.*

"Electronic Measurements of Non-Electrical Quantities in Industrial Processes" by H. D. MIDDELL, *General Electric Company.*

"Cathode Ray Tubes and Their Application" by Dr. P. S. CHRISTALDI, *Allen B. DuMont Laboratories.*

"Electronics in Industrial Instrumentation" by WALTER P. WILLS, *Brown Instrument Company.*

"Design Factors in the Application of Relays to Electronic Circuits" by R. H. HERRICK, *Automatic Electric Company.*

(6) Induction Heating

"High Frequency Induction Heating" by C. J. MADSEN AND R. M. BAKER, *Westinghouse Electric and Manufacturing Company.*

"New Methods and Techniques in High Frequency Heating" by DR. EUGENE MITTELMANN, *Illinois Tool Works.*

"The Use of High Frequency Electronic Generators to Obtain Controlled Power Concentrations for Industrial Heating Applications" by DR. WESLEY ROBERTS, *RCA Manufacturing Company.*

(7) Electronic Applications in the Power Field

"A Survey of Power Applications of Electronics" by A. C. MONTIETH, *Westinghouse Electric and Manufacturing Company.*

"Power Rectifiers and Inverters" by J. A. COX AND G. F. JONES, *Westinghouse Electric and Manufacturing Company.*

"Electronic Power Converters" by DR. E. F. W. ALEXANDERSON, *General Electric Company.*

(8) Medical Applications of Electronics

"Electronic Equipment in the Medical Profession" by DR. A. H. CARTER, *American Medical Association.*

"Electroencephalography" by DR. RALPH GIRARD, *University of Chicago.*

(9) Recent Theoretical Developments in Electronics

"Theory of Microwave Oscillation Generators Using Velocity Modulated Electron Beams" by DR. E. U. CONDON, *Westinghouse Electric and Manufacturing Company.*

"Theorem of Lorentz and Its Importance for All Problems of Electrons in Magnetic Fields" by DR. LEON BRILLOUIN, *Columbia University.*

"Transient Response of Wide-Band Amplifiers" by DR. W. W. HANSEN, *Sperry Gyroscope Company.*

The Medinah Club of Chicago, 505 North Michigan Avenue, Chicago 11, Illinois, will be headquarters for the National Electronics Conference.

A.S.T.M. Officers 1944–1945

Nominations for officers of the American Society for Testing Materials for 1944–1945 are announced as follows:

President: P. H. BATES, *National Bureau of Standards*
Vice President: ARTHUR W. CARPENTER, *The B. F. Goodrich Company*

Members of Executive Committee: W. C. HANNA, *California Portland Cement Company;* L. B. JONES, *The Pennsylvania Railroad Company;* J. T. MACKENZIE, *American Cast Iron Pipe Company;* J. G. MORROW, *The Steel Company of Canada, Ltd.;* SAM TOUR, *Sam Tour and Company, Inc.*

Electronic Parts and Equipment Industry Conference

The radio and electronic parts industry and trade have now made definite their plans for a large conference this fall. The event: Electronic Parts and Equipment Industry Conference. The place: Stevens Hotel, Chicago. The time: Thursday, Friday, and Saturday, October 19–20–21, 1944. The sponsors: Association of Electronic Parts and Equipment Manufacturers (formerly Western Division, Sales Managers Club); Sales Managers Club (Eastern Division); and the National Electronics Distributors Association. All communications, excepting those regarding sleeping room reservations which should be addressed to the Stevens Hotel direct, should be addressed to P.O. Box 5070-A, Chicago 80, Illinois.

New Mathematical Tables

(June 12, 1944)

Four new mathematical tables, described below, can now be purchased at the prices shown from the National Bureau of Standards, Washington 25, D. C. A complete list of the tables obtainable from the Bureau will be sent on request.

MT25. Seven-Point Lagrangian Integration Formulas. BY G. BLANCH AND I. RHODES.

Formulas (not requiring differences) are given for the integral $f(x)$, when the latter has been approximated by polynomials of degree six, thus affording greater accuracy than by Simpson's rule; or for comparable accuracy, permitting the evaluation of integrand at fewer points in the region. Certain remainder terms are also considered.

(Reprinted from *Journal of Mathematics and Physics,* December, 1943.) 4 pages, with cover, 25 cents.

MT26. A Short Table of the First Five Zeros of the Transcendental Equation $J_0(x)Y_0(kx)-J_0(kx)Y_0(x)=0$. BY A. N. LOWAN AND A. HILLMAN.

The first five zeros of the above equation were computed for $k=1\frac{1}{2}$, 2, $2\frac{1}{2}$, 3, $3\frac{1}{2}$, 4. Zeros are given in Table I. The products of these zeros by $(k-1)$ are given in Table II.

(Reprinted from *Journal of Mathematics and Physics,* December, 1943.) 2 pages, with cover, 25 cents.

MT27. Table of Coefficients for Inverse Interpolation with Central Differences. BY HERBERT E. SALZER.

Contains tables giving the five fourth-order coefficients for $m=0(.001)1.000$; to 10 decimals (good to about a unit in the last decimal), and also the ten sixth-order coefficients for $m=0(.1)1.0$; exact values. A condensed one-page table of fourth-order coefficients at intervals of 0.1 is also given for convenience in cases where a larger table is unnecessary.

(Reprinted from *Journal of Mathematics and Physics,* December, 1943.) 15 pages, with cover, 25 cents.

MT28. Table of $f_n(x)=\dfrac{n!}{(x/2)^n}J_n(x)$. BY THE MATHEMATICAL TABLES PROJECT.

Values are given for $x\leq 10$, and $n\leq 20$, in the following ranges: f_2 and f_3, 0(.01)10; 9D; f_4 and f_5, 0(.01)6.50, 6.5(.1)10; 9D; f_6 to f_8, 0(.01)1.50, 1.5(.1)10; 9D; f_9 to f_{20}, 0(.1)10; 9D.

Modified second central differences are tabulated alongside the entries.

(Reprinted from *Journal of Mathematics and Physics,* February, 1944.) 16 pages, with cover, 25 cents.

Contributed Original Research

Forced Torsional Oscillations of an Elastic Half-Space. I

ERIC REISSNER AND H. F. SAGOCI
Massachusetts Institute of Technology, Cambridge, Massachusetts
(Received June 13, 1944)

1. INTRODUCTION

THE subject of this and a subsequent note is the investigation of the torsional oscillations in a homogeneous, isotropic elastic half-space under the influence of periodic shear stresses applied in rotationally symmetric manner to a circular portion of the surface of the half-space. This same problem was studied some time ago[1] under the supposition that the law of variation of shear stresses over the surface is given. Under these circumstances it is possible to obtain an explicit solution of the problem by means of Fourier-Bessel integral methods and this solution was evaluated for the case of shear stresses increasing linearly from the center of the stressed surface region to the edge of the stressed surface region. Of greater practical interest, as was previously pointed out,[1] is the case that the law of variation of displacements over the loaded portion of the surface is prescribed. Specifically, the question arises for the distribution of surface shear if the load is applied by means of a rigid disk which means that the torsional displacement varies linearly from the center of the disk to the edge of the disk. Mathematically this is a mixed boundary problem and Fourier-Bessel methods only reduce the problem to an integral equation problem which in turn may be reduced to the problem of solving an infinite number of linear equations for an infinite number of unknowns.[1]

In this and the following paper it is shown that an explicit solution of the mixed boundary problem can be obtained by introducing in a suitable manner a system of oblate spheroidal coordinates. In the present paper the formulation of the problem is given and a solution in closed form is obtained for the static case of torsional deformation. In the subsequent paper the characteristics of the vibration problem are determined by means of spheroidal wave functions.

Results of interest of the present calculations are expressions for the angle of rotation of the loaded surface in terms of the applied torque, for phase difference between angle of rotation and applied torque, and for the shear stress distribution under the rigid disk.

2. FORMULATION OF THE PROBLEM

To be obtained are the stresses and displacements in a homogeneous isotropic elastic half-space ($z \geq 0$), a circular portion of whose surface ($r \leq r_0$) is forced to rotate an angle Φ, the axis of rotation being perpendicular to the surface of the half-space. The remaining portion of the surface ($r_0 < r$) is assumed to be free of stress (Fig. 1).

On the basis of the general equations of the theory of elasticity[2] it had been shown previously[1] that in the solution of this problem only the circumferential displacement component v occurred and that all components of stress are zero except the following two components of shear stress

$$\tau_{z\theta} = \mu \frac{\partial v}{\partial z}, \quad \tau_{r\theta} = \mu \left(\frac{\partial v}{\partial r} - \frac{v}{r} \right). \tag{1}$$

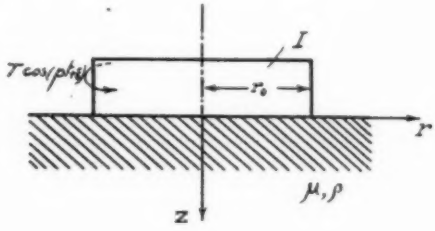

FIG. 1.

[1] E. Reissner, Ing. Arch. **8**, 229–245 (1937).

[2] See, for instance, A. E. H. Love, *A Treatise on the Mathematical Theory of Elasticity* (Cambridge University Press, London, 1927), pp. 144–145.

The differential equation for v is, if internal damping is neglected,

$$\mu\left(\frac{\partial^2 v}{\partial r^2}+\frac{1}{r}\frac{\partial v}{\partial r}-\frac{v}{r^2}+\frac{\partial^2 v}{\partial z^2}\right)=\rho\frac{\partial^2 v}{\partial t^2}. \quad (2)$$

The boundary conditions of the problem are

$$z=0, \quad r\leq r_0, \quad v=\Phi r, \quad (3)^*$$

$$z=0, \quad r_0\leq r, \quad \tau_{z\theta}=\mu\frac{\partial v}{\partial z}=0. \quad (4)$$

The applied torque T is given by

$$T=2\pi\int_0^{r_0}\tau_{z\theta}(r,0)r^2dr. \quad (5)$$

It is of importance to notice that the solution of Eq. (2) can be reduced to the solution of the wave equation. Introducing a function W defined as

$$W=v(r,z,t)\cos\theta, \quad (6)$$

there follows that the equation for W is

$$\mu\nabla^2 W=\mu\left(\frac{\partial^2 W}{\partial r^2}+\frac{1}{r}\frac{\partial W}{\partial r}+\frac{1}{r^2}\frac{\partial^2 W}{\partial\theta^2}+\frac{\partial^2 W}{\partial z^2}\right)=\rho\frac{\partial^2 W}{\partial t^2}. \quad (7)$$

3. INTRODUCTION OF OBLATE SPHEROIDAL COORDINATES

Looking upon the infinitely thin circular disk as the limiting case of an ellipsoid of revolution suggests introduction of the system of curvilinear coordinates in which the disk becomes one of the coordinate surfaces. Such coordinates ξ, η are[3] the following

$$\frac{r}{r_0}=[(1+\xi^2)(1-\eta^2)]^{\frac{1}{2}}, \quad \frac{z}{r_0}=\xi\eta. \quad (8)$$

The surfaces $\xi=$const. represent ellipsoids of revolution, the surfaces $\eta=$const. represent hyperboloids of one sheet (Fig. 2). The half-space $z\geq 0$ is defined in the new coordinates by $\eta\geq 0$ while the portion $r\leq r_0$ of the surface of the half-space is characterized by $\xi=0$.

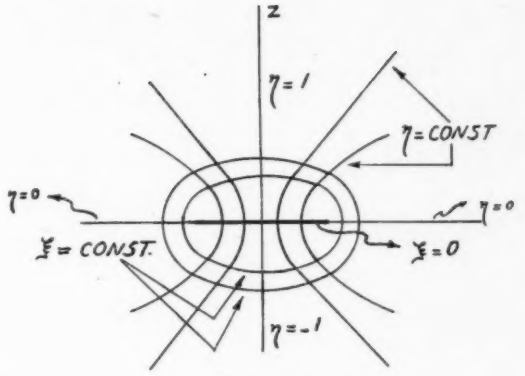

FIG. 2.

In terms of the coordinates ξ, η the boundary conditions (3) and (4) become

$$\xi=0, \quad v=\Phi r_0(1-\eta^2)^{\frac{1}{2}}, \quad (9)$$

$$\eta=0, \quad \partial v/\partial\eta=0. \quad (10)$$

Equation (10) indicates that the solution for the half-space $\eta\geq 0$ may be thought of as contained in the solution for the space exterior to the limiting ellipsoid $\xi=0$, the additional requirement being that this solution is an even function of η.

4. SOLUTION FOR THE STATIC CASE ($\partial\Phi/\partial t=0$)

The equation of motion (7) is solved by separation of variables

$$W=\cos\theta f(\xi)g(\eta). \quad (11)$$

The equations for f and g are

$$[(1+\xi^2)f'(\xi)]'+\left(d_l-\frac{1}{1+\xi^2}\right)f(\xi)=0, \quad (12)$$

$$[(1-\eta^2)g'(\eta)]'+\left(d_l-\frac{1}{1-\eta^2}\right)g(\eta)=0. \quad (13)$$

The values of the separation constants d_l insuring periodicity in η are[4]

$$d_l=(l+1)(l+2), \quad l=0,1,2,\cdots. \quad (14)$$

Solutions of Eqs. (12) and (13) are the associated Legendre polynomials

$$g_l(\eta)=A_l P_{l+1}^1(\eta)+B_l Q_{l+1}^1(\eta), \quad (15)$$

$$f_l(\xi)=C_l P_{l+1}^1(i\xi)+D_l Q_{l+1}^1(i\xi). \quad (16)$$

---

* In what follows it would be possible to obtain the solution of the more general problem in which Φr is replaced by $f(r)$.

[3] See, for instance, Stratton, Morse, Chu, and Huttner, *Elliptic Cylinder and Spheroidal Wave Functions* (John Wiley & Sons, Inc., New York, 1941).

[4] Whittaker and Watson, *Modern Analysis* (Cambridge University Press, London, 1940), pp. 323–326.

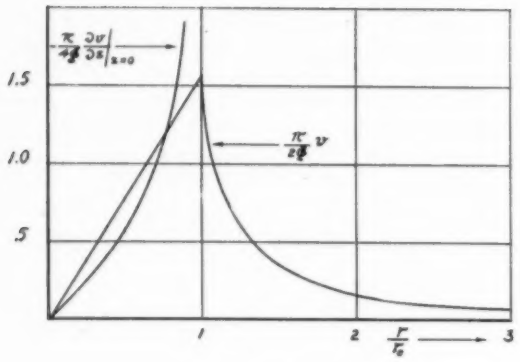

FIG. 3.

As $P_{l+1}^1(i\xi)$ becomes infinite as ξ approaches infinity and $Q_{l+1}^1(\eta)$ becomes singular for $\eta=1$, it must be required

$$B_l=C_l=0. \tag{17}$$

The condition that v and W are even functions of η requires that only even values of the subscript l occur. A series solution for v possessing appropriate behavior is then

$$v=\sum_{l=0,\,2,\,\cdots} A_l P_{l1}^1(\eta)Q_{l1}^1(i\xi). \tag{18}$$

We note that the first terms of this series are the functions[5]

$$P_1^1(\eta)=(1-\eta^2)^{\frac{1}{2}}, \tag{19}$$

$$Q_1^1(i\xi)=(1+\xi^2)^{\frac{1}{2}}\frac{d}{d\xi}\left[\frac{i}{2}\log\frac{i\xi+1}{i\xi-1}-1\right]$$

$$=(1+\xi^2)^{\frac{1}{2}}\left[\frac{\xi}{\xi^2+1}+\tan^{-1}\xi-\frac{\pi}{2}\right]. \tag{20}$$

It can be seen, according to Eq. (9), that the first term of the series (18) is sufficient to satisfy the boundary conditions of the problem. There follows

$$A_0=-\frac{\Phi r_0}{\pi/2};\quad A_l=0,\quad l=2,\,4,\,\cdots \tag{21}$$

and the expression for the displacement v becomes in terms of the curvilinear coordinates and

$$v=\frac{2}{\pi}\Phi r_0(1-\eta^2)^{\frac{1}{2}}\left[\frac{\pi}{2}-\frac{\xi}{\xi^2+1}-\tan^{-1}\xi\right]. \tag{22}$$

From Eq. (22) there follows that in cylindrical coordinates the surface displacements are given by

$$v(r,0)=\begin{cases}\Phi r, & r\leqslant r_0\\ \Phi r_0\left\{\dfrac{r}{r_0}\left(1-\dfrac{2}{\pi}\tan^{-1}\left[\left(\dfrac{r}{r_0}\right)^2-1\right]^{\frac{1}{2}}\right)\right.\\ \qquad\left.-\dfrac{\pi}{2}\left[1-\left(\dfrac{r_0}{r}\right)^2\right]^{\frac{1}{2}}\right\}, & r_0\leqslant r.\end{cases} \tag{23}$$

The shear stress distribution under the plate is given by

$$r\leq r_0,\quad \tau_{z\theta}(r,0)=\mu\left(\frac{\partial v}{\partial z}\right)_{z=0}=\frac{\mu}{r_0\eta}\left(\frac{\partial v}{\partial \xi}\right)_{\xi=0}$$

$$=-\frac{4\Phi\mu}{\pi}\frac{(1-\eta^2)^{\frac{1}{2}}}{\eta} \tag{24}$$

and in cylindrical coordinates

$$r\leq r_0,\quad \tau_{z\theta}(r,0)=-\mu\frac{4}{\pi}\frac{\Phi}{[(r_0/r)^2-1]^{\frac{1}{2}}}. \tag{25}$$

At the edge of the disk ($r=r_0$) the shear stress becomes infinite. Surface displacements and shear according to Eqs. (23) and (25) are plotted in Fig. 3.

The relation between torque and rotation is obtained by substituting Eq. (25) in Eq. (5). The result is

$$T=\frac{16}{3}\mu r_0^3\Phi. \tag{26}$$

This formula may be compared with the expression for the angle of rotation at the center of the disk under the assumption of a linear shear stress distribution.[1] In that case Eq. (26) holds when the factor 16/3 is replaced by a factor π. This indicates that when the results of the theory are to be applied to the interpretation of soil-mechanical data, no quantitative agreement can be reached unless rather accurate information regarding the distribution of the stresses acting between the actuating disk and the foundation is known. This fact must also be taken into consideration for the solution of the problem of the vibrations of an elastic half-space due to stresses applied normal to the surface of the half-space. It suggests itself that earlier work[6] on this problem should be extended with this observation in mind.

[5] Hobson, *Spherical and Ellipsoidal Harmonics* (Cambridge University Press, London, 1931).

[6] E. Reissner, Ing. Arch. **7**, 381–396 (1936).

Forced Torsional Oscillations of an Elastic Half-Space. II

H. F. SAGOCI
Massachusetts Institute of Technology, Cambridge, Massachusetts
(Received June 13, 1944)

In this paper a study is made of the forced torsional oscillations of an elastic half-space, the physical constants of which are assumed to be known, under the action of a rigid circular disk oscillating periodically about an axis through its center. A method is also given for the determination of the shear modulus of the half-space through a study of its torsional oscillations.

INTRODUCTION

THE problem to be discussed in what follows and the solution of a special case were formulated in a previous paper.[1] They are:

A system of traveling waves, dying out at infinity, is set up in an isotropic homogeneous elastic half-space by means of a rigid oscillator, shaped as a circular disk, which oscillates periodically about an axis through its center. At the surface of the half-space the displacement, represented by v, is proportional to the distance r from the center for all points under the plate; every point on the surface outside the disk is free from shear stresses.

Assuming the physical constants of the half-space known it is proposed to find expressions for the displacement and for shear stresses at any point of the surface and to derive the relation between the angle of rotation Φ and the resultant moment M of surface shear stresses.

1. EQUATIONS OF MOTION AND BOUNDARY CONDITIONS

In an isotropic elastic system having cylindrical symmetry the equations of motion of a particle, expressed in cylindrical coordinates r, θ, z, can be separated into two independent groups.[2] The differential equation which represents torsional oscillations is

$$\mu\left(\frac{\partial^2 v}{\partial r^2}+\frac{1}{r}\frac{\partial v}{\partial r}-\frac{v}{r^2}+\frac{\partial^2 v}{\partial z^2}\right)=\rho\frac{\partial^2 v}{\partial t^2}, \tag{1}$$

where μ is the shear modulus and ρ the density. It is of importance that through the substitution

$$W=v(r, z, t)\cos\theta, \tag{2}$$

Eq. (1) reduces to the wave equation

$$\mu\nabla^2 W=\mu\left(\frac{\partial^2}{\partial r^2}+\frac{1}{r}\frac{\partial}{\partial r}+\frac{1}{r^2}\frac{\partial^2}{\partial\theta^2}+\frac{\partial^2}{\partial z^2}\right)W=\rho\frac{\partial^2 W}{\partial t^2}. \tag{3}$$

Furthermore, it was shown in the earlier paper that, since a circular disk can be looked upon as the limiting case of a spheroid of revolution, the introduction of spheroidal coordinates ξ, η, related to cylindrical coordinates through

$$r=r_0[(1-\eta^2)(1+\xi^2)]^{\frac{1}{2}}, \quad z=r_0\xi\eta, \tag{4}$$

where r_0 represents the radius of the disk, transforms the boundary conditions into

$$\begin{aligned} &v=Cr_0(1-\eta^2)^{\frac{1}{2}}e^{ipt}=\Phi r, \quad \xi=0,\\ &\tau_{z\theta}=\mu\frac{\partial v}{\partial z}\Big|_{z=0}=0, \quad \eta=0, \end{aligned} \tag{5}$$

$\Phi=Ce^{ipt}$ being the angle of rotation and p the frequency of oscillations.

2. SOLUTION OF THE WAVE EQUATION IN SPHEROIDAL COORDINATES

As will be shown, the solution of the problem can be expressed in terms of spheroidal wave functions. A detailed account of the solutions of the wave equation is given by Stratton and Chu.[3] In their notation the solution of Eq. (3) for oblate spheroidal coordinates can be written as

$$W=S_{ml}(-ic, \eta)R_{ml}(-ic, i\xi)\Phi(\theta)e^{ipt}, \tag{6}$$

where the angular and radial wave functions are

[1] E. Reissner and H. F. Sagoci, J. App. Phys. **15**, 652 (1944).
[2] E. Reissner, Ing. Arch. **8**, 229–245 (1937).
[3] L. J. Chu and J. A. Stratton, J. Math. Phys. **20**, 259–309 (1941).

given, respectively, by

$$S_{ml}(-ic,\eta)=(1-\eta^2)^{\frac{1}{2}}V_{ml}(-ic,\eta),$$
$$R_{ml}(-ic,i\xi)=(\xi^2+1)^{\frac{1}{2}}U_{ml}(-ic,i\xi), \quad (7)$$

and where

$$c=r_0p(\rho/\mu)^{\frac{1}{2}}. \quad (8)$$

The functions Φ, U, and V satisfy the following differential equations:

$$\Phi''(\theta)+m^2\Phi(\theta)=0,$$
$$(\xi^2+1)U''_{ml}(-ic,i\xi)+2(m+1)\xi U'_{ml}(-ic,i\xi)$$
$$-(b_l-c^2\xi^2)U_{ml}(-ic,i\xi)=0, \quad (9)$$
$$(1-\eta^2)V''_{ml}(-ic,\eta)-2(m+1)\eta V'_{ml}(-ic,\eta)$$
$$-(b_l+c^2\eta^2)V_{ml}(-ic,\eta)=0.$$

In Eq. (9) the subscripts refer to the separation constants m and b_l, m being an integer and b_l being given by[3]

$$b_l=l(l+2m+1)+\epsilon_l(c), \quad l=0,1,2\cdots, \quad (10)$$

where $\epsilon_l(c)$ represents a function vanishing with c.

Equation (2) indicates that one has to take $m=1$. By summing over all values of l, with appropriate amplitude factors A_l, one then obtains

$$v=e^{ipt}\sum_l A_lS_{1l}(-ic,\eta)R_{1l}(-ic,i\xi). \quad (11)$$

3. CHOICE OF THE PROPER OBLATE SPHEROIDAL FUNCTIONS

Among the solutions given by the general expression (11) one must choose those which will satisfy the conditions of the particular problem in question.

The first of conditions (5), which assigns to v the value zero at the origin, excludes the use of any function with singularities at $\eta=1$, for $S_{1l}(-ic,\eta)$. Therefore one is restricted to choose angular functions of the first kind[4] which have no singularities at $\eta=1$. They are represented by $S^{(1)}_{1l}(-ic,\eta)$.

As to the choice of radial functions $R_{1l}(-ic,i\xi)$, it is well known that in a system of traveling spherical waves, where there is an outward energy propagation, hence attenuation of the wave motion as $R\to\infty$, the asymptotic behavior of the radial functions can be expressed by $(1/KR)e^{-iKR}$, where $K^2=p^2(\rho/\mu)=(c^2/r_0^2)$. By analogy, in a set of spheroidal waves the asymptotic behavior of the radial functions can be represented by $(1/c\xi)e^{-ic\xi}$. As $c\xi\to\infty$, the behavior of the functions $R^{(1)}_{1l}(-ic,i\xi)$ of the first kind and $R^{(2)}_{1l}(-ic,i\xi)$ of the second kind is given by[4]

$$R^{(1)}_{1l}(-ic,i\xi)\to\frac{1}{c\xi}\sin\left(c\xi-\frac{l+1}{2}\pi\right),$$
$$R^{(2)}_{1l}(-ic,i\xi)\to-\frac{1}{c\xi}\cos\left(c\xi-\frac{l+1}{2}\pi\right). \quad (12)$$

Therefore one is led to use functions of the fourth kind

$$R^{(4)}_{1l}(-ic,i\xi)=R^{(1)}_{1l}(-ic,i\xi)-iR^{(2)}_{1l}(-ic,i\xi). \quad (13)$$

4. EVENNESS OF THE ANGULAR SOLUTIONS

The prime signs in the expressions for spheroidal wave functions, given in the appendix, indicate that summations are to go over alternate values of n. To determine whether n is even or odd use is made of the second of Eqs. (5). This condition implies that $(\partial v/\partial\eta)|_{\eta=0}=0$; thus from (11)

$$\frac{\partial}{\partial\eta}S^{(1)}_{1l}(-ic,\eta)\bigg|_{\eta=0}=0. \quad (14)$$

Equation (14) is satisfied when $S^{(1)}_{1l}(-ic,\eta)$ is an even function of η. Now as $c\to0$ the lth term in the summation

$$S^{(1)}_{1l}(-ic,\eta)=\sum_n{}'f_n{}^lP^1_{n+1}(\eta)$$

becomes dominant, that is,

$$S^{(1)}_{1l}(-ic,\eta)\approx f_l{}^lP^1_{l+1}(\eta).$$

Keeping this in mind and making use of Rodrigue's formula[5]

$$P_n{}^m(\eta)=\frac{(1-\eta^2)^{m/2}}{2^nn!}\frac{d^{n+m}}{d\eta^{(n+m)}}(\eta^2-1)^n, \quad (15)$$

it is seen that $S^{(1)}_{1l}(-ic,\eta)$ is even when l is even and odd when l is odd. Equation (11) can then

[4] For a discussion of the properties of spheroidal functions of various kinds see Stratton, Morse, Chu, and Hutner, *Elliptic Cylinder and Spheroidal Wave Functions* (John Wiley & Sons, Inc., New York, 1941). Explicit expressions for some functions and for some of their special values taken from that work have been listed in the appendix.

[5] See, for instance, Whittaker and Watson, *Modern Analysis* (Cambridge University Press, London, 1940), p. 324.

be rewritten as

$$v=e^{ipt}\sum_{l=0,2,4\cdots}^{\infty}A_l S_{1l}^{(1)}(-ic,\eta)R_{1l}^{(4)}(-ic,i\xi). \quad (11a)$$

5. DETERMINATION OF THE AMPLITUDE FACTORS A_l

The coefficients A_l are determined by the application of the first of the Eqs. (5). Taking v from the boundary conditions, (11a) can be rewritten in the form

$$\sum_{l=0,2\cdots}^{\infty}A_l S_{1l}^{(1)}(-ic,\eta)R_{1l}^{(4)}(-ic,io)=Cr_0(1-\eta^2)^{\frac{1}{2}}. \quad (5a)$$

To determine A_l observe the orthogonality relations[4]

$$\int_{-1}^{+1}S_{1l}^{(1)}(-ic,\eta)S_{1m}^{(1)}(-ic,\eta)d\eta=\delta_{lm} \quad (16)$$

with

$$\delta_{lm}=\begin{cases}0 & \text{if } l\neq m,\\ 2\sum_{n=0}^{\infty}{}'(f_n^l)^2\dfrac{(n+2)!}{(2n+3)n!} & \text{if } l=m.\end{cases} \quad (17)$$

Multiplying both sides of (5a) by $S_{1l}^{(1)}(-ic,\eta)$ and integrating, there follows

$$A_l=\frac{2}{\delta_{ll}R_{1l}^{(4)}(-ic,io)}\int_0^1 Cr_0(1-\eta^2)^{\frac{1}{2}}\times S_{1l}^{(1)}(-ic,\eta)d\eta=\frac{4Cr_0f_0^l}{3\delta_{ll}R_{1l}^{(4)}(-ic,io)}. \quad (18)$$

In Eq. (18) use has been made of the fact that $(1-\eta^2)^{\frac{1}{2}}=P_1^1(\eta)$, that

$$S_{1l}^{(1)}(-ic,\eta)=\sum_{n=0}^{\infty}{}'f_n^l P_{n+1}^1(\eta),$$

and that the associated Legendre polynomials form an orthogonal set. Combining (18) and (11a) there results as final expression for the torsional displacement

$$v=\frac{4}{3}Cr_0e^{ipt}\sum_{l=0,2\cdots}^{\infty}\frac{f_0^l}{\delta_{ll}R_{1l}^{(4)}(-ic,io)}\times S_{1l}^{(1)}(-ic,\eta)R_{1l}^{(4)}(-ic,i\xi). \quad (11b)$$

6. STRESS DISTRIBUTION UNDER THE PLATE

v as given by (11b) satisfies the condition that at the surface of the half-space shear stresses are zero when $r>r_0$. When $r<r_0$, that is, under the plate, the stress distribution is given by

$$\tau_{z\theta}|_{\xi=0}=\mu\frac{\partial v}{\partial z}\Big|_{\xi=0}=\frac{-i\mu}{r_0\eta}e^{ipt}\times\sum_{l=0,2\cdots}^{\infty}A_lK_lS_{1l}^{(1)}(-ic,\eta). \quad (19)$$

$-iK_l$ in this expression is an abbreviation for $(d/d\xi)R_{1l}^{(4)}(-ic,i\xi)|_{\xi=0}$ and $R_{1l}^{(4)}(-ic,i\xi)$ is given by (13).

For a numerical discussion take the real part of the expression (19); there results

$$R_e\{\tau_{z\theta}\}=\tfrac{2}{3}C\mu(-F_2\cos pt+F_1\sin pt), \quad (20)$$

where

$$F_1=\sum_{l=0,2\cdots}^{\infty}\frac{2f_0^l}{\delta_{ll}}\frac{K_lR_{1l}^{(1)}}{[R_{1l}^{(1)}]^2+[R_{1l}^{(2)}]^2}\frac{S_{1l}^{(1)}(-ic,\eta)}{\eta},$$

$$F_2=\sum_{l=0,2\cdots}^{\infty}\frac{2f_0^l}{\delta_{ll}}\frac{K_lR_{1l}^{(2)}}{[R_{1l}^{(1)}]^2+[R_{1l}^{(2)}]^2}\frac{S_{1l}^{(1)}(-ic,\eta)}{\eta}. \quad (21)$$

In these expressions $R_{1l}^{(1)}$ and $R_{1l}^{(2)}$ have been used for $R_{1l}^{(1)}(-ic,io)$ and $R_{1l}^{(2)}(-ic,io)$, respectively.

In (20) F_2 represents the component of stress in phase with the displacement of the ground, whereas F_1 is the component in quadrature with it. The functions F_1 and F_2 have been evaluated for different values of c and r/r_0, using only two terms[6] of the series. As will be discussed in a later section, for the range of parameters under consideration, that is, $0\leqslant c\leqslant 2.0$ and $0\leqslant r/r_0\leqslant 1.0$, two terms determine F_1 and F_2 with sufficient accuracy. Figures 1 and 2 represent families of curves F_1 and F_2, respectively, as functions of r/r_0.

The two sets of curves are not plotted to the same scale. In the range of the present calculations the values of F_2 are several times larger than the corresponding values of F_1, so that the component of stress in phase with the reaction of the ground is of major importance. In the limiting

[6] The reason for this is that tables for coefficients of spheroidal wave functions which were available, namely, tables by Stratton, Morse, Chu, and Hutner, give these coefficients only for values of l up to 2.

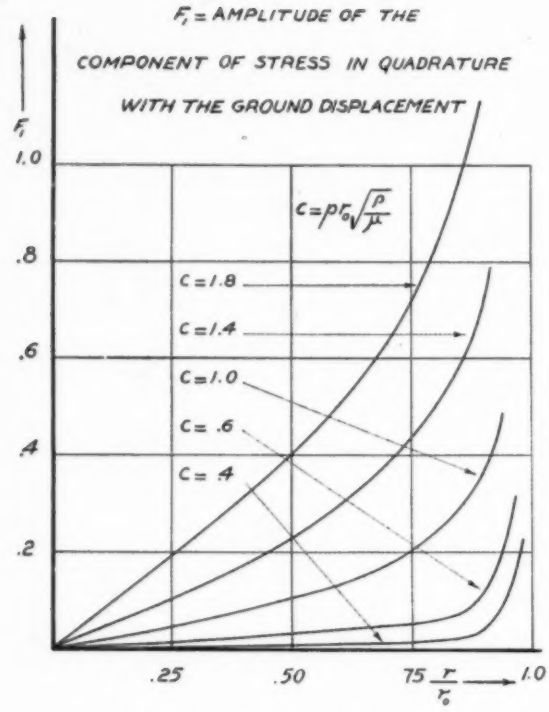

FIG. 1. Stress distribution under the plate: component of stress in quadrature with the ground displacement.

case $c=0$—that is, the static case—F_1 vanishes completely and only F_2 remains. The fact may be emphasized that as the frequency increases, F_2 decreases while F_1 increases. Therefore for large enough values of the frequency the term ninety degrees out of phase with the ground reaction is expected to become the major component of stress.

It may be noted that at the center of the disk the stress vanishes, while at the edge of this it becomes infinite of the order of $1/\eta = 1/[1-(r^2/r_0^2)]^{\frac{1}{2}}$.

7. RELATION BETWEEN THE ANGLE OF ROTATION Φ AND THE RESULTANT MOMENT M OF SURFACE SHEAR STRESSES

In the discussion of the motion of the vibrator it will be found necessary to express the angle of rotation in terms of the torque of the shear stresses. For a circular ring of radius r and width dr, the element of torque is

$$dM = \tau_{z\theta} 2\pi r^2 dr. \tag{22}$$

Substituting from (19) into (22), integrating, and interchanging summation and integration, there follows

$$M = \frac{-2\pi i\mu}{r_0} e^{ipt} \sum_{l=0,2\cdots}^{\infty} A_l K_l \int_0^{r_0} \frac{S_{1l}^{(1)}(-ic,\eta)}{\eta} r^2 dr. \tag{23}$$

With the help of the relations (4) between cylindrical and oblate spheroidal coordinates and the expression $P_1^1(\eta) = (1-\eta^2)^{\frac{1}{2}}$ (23) becomes

$$M = -2\pi i\mu r_0^2 e^{ipt} \times \sum_{l=0,2\cdots}^{\infty} A_l K_l \sum_{n=0}^{\infty}{}' f_n^l \int_0^1 P_1^1(\eta) P_{n+1}^1(\eta) d\eta. \tag{23a}$$

The integral in (23a) is the same as the one encountered in Eq. (18) for the determination of the coefficients A_l and it is evaluated in the same manner. Owing to the orthogonal properties of the associated Legendre polynomials, (23a) reduces to

$$M = -\frac{4\pi i}{3} \mu r_0^2 e^{ipt} \sum_{l=0,2\cdots}^{\infty} A_l K_l f_0^l. \tag{24}$$

Writing A_l explicitly, as in (18), one sees that (24) is the desired relation between the angle of rotation Φ and the moment M. Rearranging so as to isolate Φ and clearing the denominator of the resulting expression from complex quantities, (24) can be written in the form

$$\Phi = \frac{\beta - i\gamma}{\beta^2+\gamma^2} \frac{9i\bar{M}e^{ipt}}{16\pi\mu r_0^3}, \quad M = \bar{M}e^{ipt}, \tag{25}$$

where

$$\beta = \sum_{l=0,2\cdots}^{\infty} \frac{(f_0^l)^2}{\delta_{ll}} \frac{K_l R_{1l}^{(1)}}{[R_{1l}^{(1)}]^2+[R_{1l}^{(2)}]^2}, \qquad \gamma = \sum_{l=0,2\cdots}^{\infty} \frac{(f_0^l)^2}{\delta_{ll}} \frac{K_l R_{1l}^{(2)}}{[R_{1l}^{(1)}]^2+[R_{1l}^{(2)}]^2}. \tag{26}$$

Taking real parts Φ can be written in either one of the two forms

$$Re\{\Phi\} = \frac{9\bar{M}}{16\pi\mu r_0^3} (\beta^2+\gamma^2)^{-\frac{1}{2}} \cos(pt-\Delta), \qquad \Delta = \tan^{-1}\frac{\beta}{\gamma}, \tag{27}$$

$$Re\{\Phi\} = \frac{9\bar{M}}{16\pi\mu r_0^3} \left(\frac{\gamma}{\beta^2+\gamma^2} \cos pt - \frac{\beta}{\beta^2+\gamma^2} \sin pt \right). \tag{28}$$

The quantities β/γ, $\gamma/\beta^2+\gamma^2$, and $\beta/\beta^2+\gamma^2$ have been computed for several values of c, using two terms of the series. In Fig. 3 the curves πg_1 and πg_2 are plots of (9/16) $(\gamma/\beta^2+\gamma^2)$ and (9/16) $(\beta/\beta^2+\gamma^2)$, respectively. πf_1 and πf_2 are curves corresponding to πg_1, πg_2, respectively, given by Reissner,[2] under the assumption of a prescribed linear stress distribution when $r<r_0$ and a zero stress when $r>r_0$.

It is evident in Fig. 3 that for small frequencies the component of the angle of rotation in phase with the ground reaction is dominant. Here, as in the discussion of stress distribution, attention will be called to the behavior of the curves πg_1 and πg_2; they show that for larger frequencies the out of phase component of C becomes of increasing importance.

Figure 4 represents the tangent of the phase angle between Φ and M. It is noticed that the phase angle increases with the frequency. Both Fig. 3 and Fig. 4 are of interest for the determination of the shear modulus.

8. THE CASE OF A POINT SOURCE

It is evident from (8) that $c=0$ when either $p=0$ or $r_0=0$. The former case corresponds to the static problem and has been studied in a previous paper,[1] the latter to a point source. As in the discussion of the static problem, only the first terms of all series to be dealt with remain. When taking the limit of v as $r_0\to 0$ it is assumed that $\xi\to\infty$ in such a way as to leave $r_0\xi$ finite and equal to the radius of the limiting sphere.

If expressions for oblate spheroidal functions, taken from the appendix, are substituted in Eq. (11a) it follows that

$$v=\lim_{r_0\to 0}\left\{A_0e^{ipt}\frac{[(1-\eta^2)(1+\xi^2)]^{\frac{1}{2}}}{\xi}\left(\frac{\pi}{2c\xi}\right)^{\frac{1}{2}}\times[J_{3/2}(c\xi)-iJ_{-3/2}(c\xi)]\right\}. \quad (29)$$

Using the relations

$$J_{3/2}(c\xi)=\left(\frac{2}{\pi c\xi}\right)^{\frac{1}{2}}\left(\frac{\sin c\xi}{c\xi}-\cos c\xi\right),$$
$$J_{-3/2}(c\xi)=\left(\frac{2}{\pi c\xi}\right)^{\frac{1}{2}}\left(\sin c\xi+\frac{\cos c\xi}{c\xi}\right), \quad (30)$$

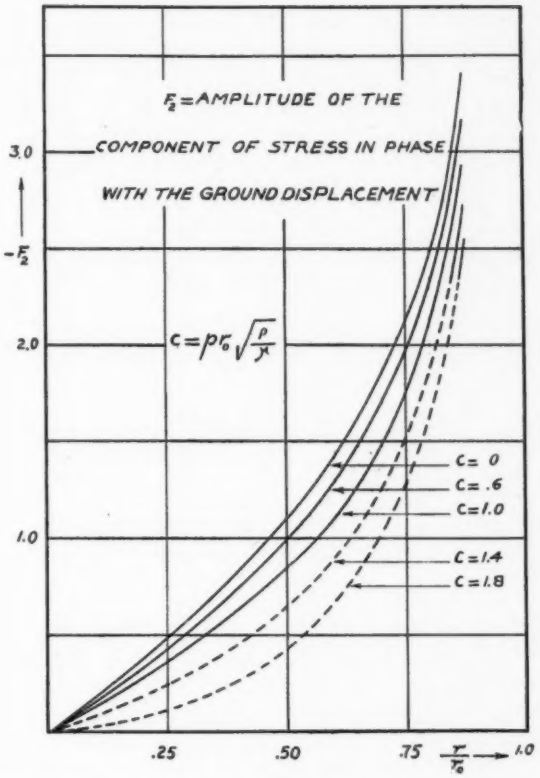

FIG. 2. Stress distribution under the plate: component of stress in phase with the ground displacement.

(29) can be written as

$$v=\lim_{r_0\to 0}\left\{A_0\frac{r}{r_0c\xi^3}\left(\frac{1}{c\xi}+i\right)ie^{i(pt-c\xi)}, \quad (29a)\right.$$

which is equivalent to

$$v=\lim_{r_0\to 0}\left(\frac{iA_0}{K^2}\right)\frac{r}{R}\left(\frac{1}{R}+iK\right)e^{i(pt-KR)},$$
$$R^2=r^2+z^2, \quad (29b)$$

where $K^2=c^2/r_0^2=p^2(\rho/\mu)$. With the help of Eq. (18) the constant factor in (29b) becomes

$$\lim_{r_0\to 0}\frac{iA_0}{K^2}=\lim_{r_0\to 0}\frac{iCr_0}{K^2R_{10}^{(4)}}. \quad (31)$$

It will be recalled that the expression (18) was obtained by using the boundary condition (5), when $z=\xi=0$, over the circular plate. If, as $r_0\to 0$, the limit of the right-hand side of expression (31) is taken before letting $\xi=0$, it is found that $\lim_{r_0\to 0}(iA_0/K^2)\to-\lim_{r_0\to 0}Cr_0^3$ and that a comparison of this last factor with the constant factor in the expression for v given by Reissner,[2] in the

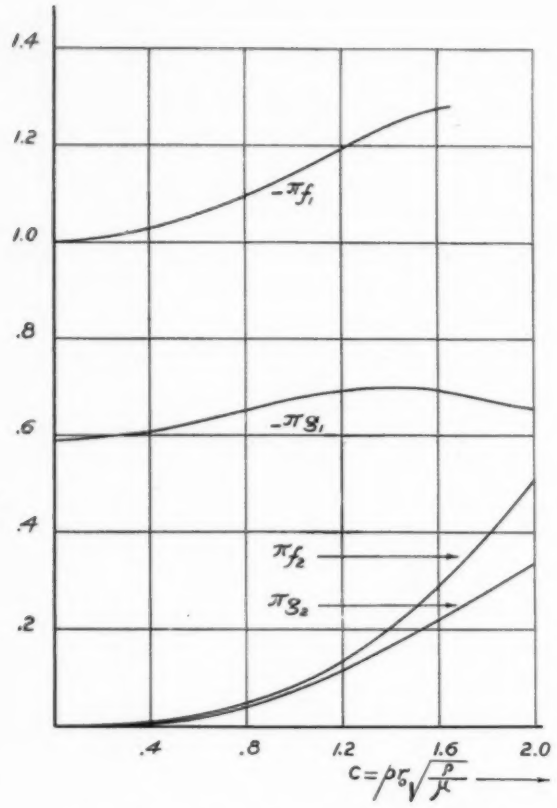

FIG. 3. The ratio of the angle of rotation Φ to the moment M.

case of a point source, identifies $\lim_{r_0\to 0} -Cr_0^3$ with $-M/4\pi\mu$, where M is defined as the resultant moment of shear stresses as $r_0\to 0$. Therefore the solution for a point source is given by

$$v=-\frac{M}{4\pi\mu}\frac{r}{R}\left(\frac{1}{R}+iK\right)e^{i(pt-KR)}. \qquad (31a)$$

9. NUMERICAL RESULTS

A detailed account on numerical results including tables for F_1, F_2, β/γ, $\beta/\beta^2+\gamma^2$, $\gamma/\beta^2+\gamma^2$ and auxiliary tables for oblate spheroidal functions

$$S_{1l}^{(1)}(-ic,\eta),\quad R_{1l}^{(1)}(-ic,i\xi),\quad R_{1l}^{(2)}(-ic,i\xi),$$

$$(d/d\xi)R_{1l}^{(2)}(-ic,i\xi)\,|_{\xi=0},$$

can be found in a thesis* on which this paper is based. Here a brief discussion is given as to the range of computations and the accuracy with which various quantities have been determined.

It is appropriate to start the discussion by giving the reasons why all computations have been restricted to the range of frequencies $0\leqslant c\leqslant 2.0$. The tables by Stratton, Morse, Chu, and Hutner, used in evaluating oblate spheroidal wave functions, are for $m=0, 1, 2$, $l=0, 1, 2$, and $0\leqslant c\leqslant 5.0$. However, beyond $c=2.0$ it was found that the convergence of most of the series dealt with became so slow that using two terms to evaluate them became unsatisfactory.

Through a comparison of the first two terms it was found that the convergence of F_1 is quite fast, the smaller the frequency the faster the convergence, and that up to frequencies $c=1.8$ the second term is less than 0.1 percent of the first term. The convergence of F_2 is slower. For instance, for $r/r_0=0.8660$ it is found that the second term is only 0.06 percent of F_2 when $c=0.2$, while when $c=1.8$ it is about 3 percent of F_2. The fact may be emphasized that as r/r_0 becomes smaller the accuracy with which F_2 is given becomes less and less satisfactory. For $r/r_0=0.2588$ the second term is still less than 0.8 percent of the first when $c=0.2$, but when $c=1.8$ the second term is about 72 percent of the first. In other words, if more terms were used in the series, in Fig. 2 the curves F_2 for higher frequencies would be expected to be closer to the uppermost curve $c=0$, which is known exactly. It may be added that in Fig. 2 all points known within 4 or 5 percent have been joined by solid lines while those that are more doubtful have been joined by dotted lines.

The difference in behavior between F_1 and F_2 is due to the presence of a factor $R_{1l}^{(2)}/K_l$ in the lth term of the latter and a factor $1/K_l$ in the lth term of the former. It was found that for small frequencies K_l is exceedingly large and that it decreases with increasing frequency. Therefore, the convergence of F_1 is quite fast for small frequencies, but it becomes slower as the frequency increases. On the other hand, it was found that $R_{1l}^{(2)}$ and K_l have the same general behavior; hence the presence of $R_{1l}^{(2)}$ in F_2 counteracts the effect of $1/K_l$.

As far as the series connected with the angle of rotation is concerned, it was found that when

* "Forced torsional oscillations of an elastic half-space," by H. F. Sagoci, submitted in partial fulfillment of the requirements for the degree of Doctor of Science from the Massachusetts Institute of Technology (1944).

$c=0.2$, the second term of β is only 3×10^{-11} percent of β, while the second term of γ is about 2×10^{-4} percent of γ. For $c=2.0$ the corresponding figures are 8.8×10^{-3} percent and 3.2 percent. Therefore for small frequencies the curves πg_1, πg_2, and $\tan\Delta$ are known quite accurately; even in the worst case—that is, when $c=2.0$—they are known within a few percent.

10. DETERMINATION OF THE SHEAR MODULUS OF AN ISOTROPIC HOMOGENEOUS ELASTIC HALF-SPACE THROUGH A STUDY OF THE MOTION OF THE OSCILLATOR

If the externally applied torque be represented by $T\cos(pt+\epsilon)$, the reaction of the ground by $\bar{M}\cos pt$ and the moment of inertia of the oscillator by I, the equation of motion of the latter is[2]

$$IR_e\{\ddot{\Phi}\}+\bar{M}\cos pt=T\cos(pt+\epsilon). \quad (32)$$

The phase angle ϵ between T and M is to be determined in such a way that in Eq. (32) the use of the real part of $\ddot{\Phi}$ is permissible. With the help of (28) Eq. (32) becomes

$$-\frac{9I\bar{M}p^2}{16\pi\mu r_0^3}\left(\frac{\gamma}{\beta^2+\gamma^2}\cos pt-\frac{\beta}{\beta^2+\gamma^2}\sin pt\right)+\bar{M}\cos pt=T\cos(pt+\epsilon); \quad (33)$$

expanding $\cos(pt+\epsilon)$ one finds

$$\tan\epsilon=\frac{\dfrac{9Ip^2}{16\pi\mu r_0^3}\dfrac{\beta}{\beta^2+\gamma^2}}{1-\dfrac{9Ip^2}{16\pi\mu r_0^3}\dfrac{\gamma}{\beta^2+\gamma^2}} \quad (34)$$

and

$$\bar{M}=T\left[\left(1-\frac{9Ip^2}{16\pi\mu r_0^3}\frac{\gamma}{\beta^2+\gamma^2}\right)^2+\left(\frac{9Ip^2}{16\pi\mu r_0^3}\frac{\beta}{\beta^2+\gamma^2}\right)^2\right]^{-\frac{1}{2}}. \quad (35)$$

Substituting from (35) into (28)

$$\Phi=\frac{9T}{16\pi\mu r_0^3}\left[\left(1-\frac{9Ip^2}{16\pi\mu r_0^3}\frac{\gamma}{\beta^2+\gamma^2}\right)^2+\left(\frac{9Ip^2}{16\pi\mu r_0^3}\frac{\beta}{\beta^2+\gamma^2}\right)^2\right]^{-\frac{1}{2}}\times\left(\frac{\gamma}{\beta^2+\gamma^2}\cos pt-\frac{\beta}{\beta^2+\gamma^2}\sin pt\right). \quad (36)$$

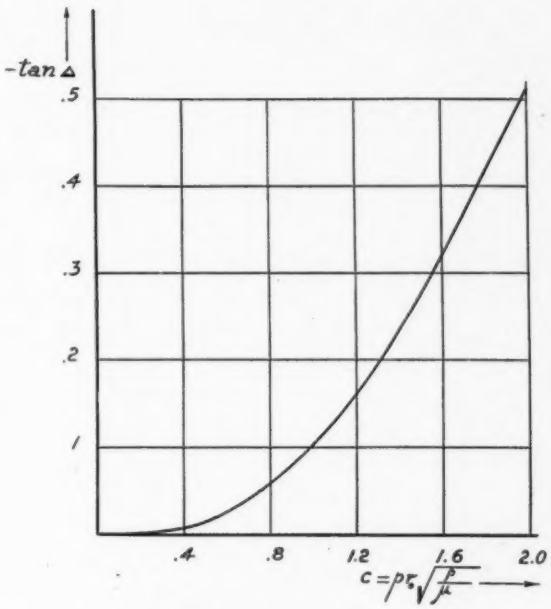

FIG. 4. The tangent of the phase angle between Φ and M.

Equation (36) will be used to determine the rigidity by measuring, for a given frequency, two values Φ_1 and Φ_2 of the angle of rotation at two different instants t_1 and t_2. Now taking the ratio of Φ_1 to Φ_2 one obtains

$$\frac{\Phi_1}{\Phi_2}=\frac{\gamma\cos pt_1-\beta\sin pt_1}{\gamma\cos pt_2-\beta\sin pt_2}, \quad (37)$$

from which it follows

$$\frac{\beta}{\gamma}=\frac{\Phi_2\cos pt_1-\Phi_1\cos pt_2}{\Phi_2\sin pt_1-\Phi_1\sin pt_2}. \quad (38)$$

Once the value of β/γ is known, using Fig. 4, which gives β/γ as a function of c, the corresponding value of c can be found. Then going back to Fig. 3 the corresponding values of $(9/16)(\gamma/\beta^2+\gamma^2)$ and $(9/16)(\beta/\beta^2+\gamma^2)$ can be read off from the curves πg_1 and πg_2. Thus in Eq. (36), rewritten for Φ_1, the rigidity μ remains the only unknown, since the applied torque T is given. Letting

$$\frac{9}{16\pi r_0^3}\frac{\gamma}{\beta^2+\gamma^2}=\alpha_1, \quad \frac{9}{16\pi r_0^3}\frac{\beta}{\beta^2+\gamma^2}=\alpha_2, \quad (39)$$

$$\Phi_1=\frac{T}{\mu}\left[\left(1-\frac{Ip^2}{\mu}\alpha_1\right)^2+\left(\frac{Ip^2}{\mu}\alpha_2\right)^2\right]^{-\frac{1}{2}}\times(\alpha_1\cos pt_1-\alpha_2\sin pt_1), \quad (40)$$

which finally yields the following quadratic equation for μ:

$$\mu^2-2Ip^2\alpha_1\mu+I^2p^4(\alpha_1^2+\alpha_2^2)-\frac{T^2}{\Phi_1^2}(\alpha_1\cos pt_1-\alpha_2\sin pt_1)^2=0. \quad (41)$$

Note that the density ρ occurs nowhere in the preceding discussion so that this method determines μ entirely independently of ρ. The steps involved in the determination of μ can be summarized as follows: At a given frequency take two readings of the angle of rotation, at times t_1 and t_2. With these determine $\tan\Delta=\beta/\gamma$ according to (38). Use Fig. 4 to find the value of c which corresponds to the value of β/γ just computed. Use Fig. 3 to determine corresponding values of $(9/16)\,(\beta/\beta^2+\gamma^2)$, $(9/16)\,(\gamma/\beta^2+\gamma^2)$ and hence α_1 and α_2 in (41). Solve the quadratic equation (41) to determine μ.

APPENDIX

To facilitate the use of the following list, arranged from expressions given by Stratton, Morse, Chu, and Hutner,[4] it may be pointed out that $P_n^m(\eta)$ and $Q_n^m(\eta)$ stand for associated Legendre polynomials of the first and second kind, respectively. $J_n(c\xi)$ represents a Bessel function. f_n^l and f_{-n}^l/ρ are numerical coefficients[5] for oblate spheroidal wave functions.

I. Angular Solutions of the First Kind

$$S_{1l}^{(1)}(-ic,\eta)=\sum_{n=0}^{\infty}{}'f_n^l P_{n+1}^1(\eta); \quad (1)$$

$$S_{1l}^{(1)}(-ic,0)=\frac{2i^l\left(\frac{l+1}{2}\right)!}{(\pi)^{\frac{1}{2}}\left(\frac{l}{2}\right)!}, \quad l=\text{even}; \quad (2)$$

$$S_{1l}^{(1)}(-ic,1)=0, \quad l=\text{even}. \quad (3)$$

II. Radial Solutions

a. Functions of the First Kind

$$R_{1l}^{(1)}(-ic,i\xi)=\frac{(\xi^2+1)^{\frac{1}{2}}}{\xi\sum_{n=0}^{\infty}{}'f_n^l\frac{(n+2)!}{n!}}\sum_{n=0}^{\infty}{}'i^{l-n}f_n^l\times\frac{(n+2)!}{n!}\left(\frac{\pi}{2c\xi}\right)^{\frac{1}{2}}J_{n+3/2}(c\xi); \quad (4)$$

$$R_{1l}^{(1)}(-ic,i0)=\frac{i^l(\pi)^{\frac{1}{2}}cf_0^l}{2(\frac{3}{2})!\sum_{n=0}^{\infty}{}'f_n^l\frac{(n+2)!}{n!}}, \quad l=\text{even}; \quad (5)$$

$$\frac{d}{d\xi}R_{1l}^{(1)}(-ic,i\xi)|_{\xi=0}=0, \quad l=\text{even}. \quad (6)$$

b. Functions of the Second Kind

$$R_{1l}^{(2)}(-ic,i\xi)=\frac{(\xi^2+1)^{\frac{1}{2}}}{\xi\sum_{n=0}^{\infty}{}'f_n^l\frac{(n+2)!}{n!}}\sum_{n=0}^{\infty}{}'i^{l-n}f_n^l\times\frac{(n+2)!}{n!}\left(\frac{\pi}{2c\xi}\right)^{\frac{1}{2}}N_{n+3/2}(c\xi); \quad (7)$$

$$R_{1l}^{(2)}(-ic,i\xi)=\frac{2\left(\frac{l+1}{2}\right)!}{\left(\frac{l}{2}\right)!\left(-\frac{1}{2}\right)!f_{-2}^l\sum_{n=0}^{\infty}{}'f_n^l\frac{(n+2)!}{n!}}\times\sum_{n=0}^{\infty}{}'f_n^l Q_{n+1}^1(i\xi), \quad l=\text{even}, \quad (8)$$

$$R_{1l}^{(2)}(-ic,i0)=\frac{2i^l}{f_{-2}^l\sum_{n=0}^{\infty}{}'f_n^l\frac{(n+2)!}{n!}}\times\left[\frac{\left(\frac{l+1}{2}\right)!}{\left(\frac{l}{2}\right)!}\right]^2, \quad l=\text{even}; \quad (9)$$

$$\frac{d}{d\xi}R_{1l}^{(2)}(-ic,i\xi)|_{\xi=0}=\frac{-4\left(\frac{l+1}{2}\right)!}{(\pi)^{\frac{1}{2}}\left(\frac{l}{2}\right)!\left(-\frac{1}{2}\right)!f_{-2}^l\sum_{n=0}^{\infty}{}'f_n^l\frac{(n+2)!}{n!}}\times\left[\pi\sum_{n=0}^{\infty}{}'i^n f_n^l\frac{\left(\frac{n+2}{2}\right)!}{\left(\frac{n-1}{2}\right)!}+\left(\frac{1}{2}\right)!f_{-2}^l+2\sum_{n=4}^{\infty}{}'i^n\frac{f_{-n}^l}{\rho}\frac{\left(\frac{n-1}{2}\right)!}{\left(\frac{n-4}{2}\right)!}\right], \quad l=\text{even}. \quad (10)$$

c. Functions of the Fourth Kind

$$R_{1l}^{(4)}(-ic,i\xi)=R_{1l}^{(1)}(-ic,i\xi)-iR_{1l}^{(2)}(-ic,i\xi), \quad (11)$$

$$\frac{d}{d\xi}R_{1l}^{(4)}(-ic,i\xi)|_{\xi=0}=-i\frac{d}{d\xi}R_{1l}^{(2)}(-ic,i\xi)|_{\xi=0}=-iK_l. \quad (12)$$

In all these equations prime signs indicate summation over only even values of n. The expression (8) for $R_{1l}^{(2)}(-ic,i\xi)$ can be used when the series (7) converges slowly or when it does not converge at all, that is, when $i\xi=1$. Attention should be called to the fact that throughout $n!$ has been used for $\Gamma(n+1)$.

Microanalysis by Means of Electrons

JAMES HILLIER AND R. F. BAKER
RCA Laboratories, Princeton, New Jersey
(Received June 26, 1944)

THE past decade has seen an exceedingly rapid growth of the development and use of electronic tools in all sciences. Among these is the electron microscope which is already achieving spectacular results in the investigation of the structure of matter in the size range 20 to 10,000A. This instrument is used, at the present time, almost exclusively as a means of extending our vision into the submicroscopic world; that is, it supplies information regarding the existence, size, shape, and structure of small particles and organisms. Such information is sufficient for the solution of innumerable research problems but it does not represent in any way a complete exploitation of the electron microscope or of the electron optical method. It has become increasingly apparent to those in close contact with the applications of electron microscopy that one of the most important advances which could be made at the present time would be the development of means for determining the composition of individual particles in a mixed specimen. A number of methods of attacking this problem have already been suggested.

The first of these is the correlation of the intensities of image points with the mass densities of corresponding object points.[1] Unfortunately, in this method there is an ambiguity between the thickness of a given object point and its composition requiring the simultaneous use of some auxiliary method of determining one or the other of these quantities. Moreover, there are—more often than not—intensity anomalies in the image arising from electron interferences which occur whenever the particles under investigation are crystalline.[2–5]

The second is the use of electron diffraction in a system* where the irradiating beam is confined to only that part of the specimen which is being investigated.[6–7] This method can be applied only in the case of crystalline particles and even in this its usefulness is limited by the fact that individual particles in electron microscope specimens are almost invariably single crystals requiring that they have the proper orientation in the specimen before a pattern can be obtained. Moreover, the pattern produced seldom consists of more than one or two spots which by themselves are not usually sufficient for the identification of a compound.

A third possible method for making a point chemical analysis on electron microscope specimens is by the use of specific reagents which change the mass density of the areas in question. Except for some exploratory work with the selective staining of bacteria for the electron microscope[8] very little has been published on this subject. The method appears to be tedious and not too certain of success in any given case.

In a recent short paper[9] one of us has described a fourth and more direct electronic method of attacking the problem outlined above. In the present paper a more detailed description will be given of the instrument developed for this purpose as well as a discussion of the theoretical implications of the results obtained.

The radiation excited by inelastic collisions between free electrons and atomic electrons has been investigated quite thoroughly over most of the electromagnetic spectrum. The associated problem regarding the energy loss suffered by the exciting electrons, on the other hand, has not been investigated nearly as thoroughly.

[1] L. Marton and L. I. Schiff, J. App. Phys. **12**, 759–765 (1941).
[2] B. von Borries and E. Ruska, Naturwiss. **28**, 366–367 (1940).
[3] M. von Ardenne, Zeits. f. Physik **116**, 736–738 (1940).
[4] H. Boersch, Zeits. f. Physik **118**, 706–713 (1942).
[5] J. Hillier and R. F. Baker, Phys. Rev. **61**, 722–723 (1942).

* This technique is not to be confused with the normal use of the electron diffraction where a relatively large area of the specimen including many particles is used for making an analysis.
[6] M. von Ardenne, E. Schiebold, and F. Gunther, Zeits. f. Physik **119**, 325–365 (1942).
[7] H. Boersch, Zeits. f. Physik **116**, 469–479 (1940).
[8] S. Mudd and T. F. Anderson, J. Exper. Med. **76**, 103–108 (1942).
[9] J. Hillier, Phys. Rev. **64**, 318–319 (1943).

While some work has been done on the excitation of the optical levels in gases at low pressure by relatively low velocity electrons, it is only recently, for instance, that Ruthemann[10] has extended it successfully to the case of the x-ray levels. Using electron velocities of 7000 ev, extremely thin targets of collodion and a focusing half-circle method of magnetically analyzing electron velocities, he was able to make an analysis of the velocity distribution in the transmitted electrons. In this distribution he observed sharp peaks indicating that a number of the transmitted electrons had suffered discrete energy losses. Moreover, the magnitude of these discrete losses corresponded quite accurately to the energy required for the removal of an electron from the K shells of carbon, nitrogen, and oxygen. Since, as will be shown below, the detection of this phenomenon can be extended to the K, L, M, etc., levels of heavier elements the possibility of using it as a method of making an elemental analysis of small particles appears extremely attractive.

A DISCUSSION OF THE DESIGN OF AN ELECTRON MICROANALYZER

In the above, it is proposed that the constituent elements of microscopic particles be identified by the specific retardation of velocity suffered by those transmitted electrons which have excited the x-ray levels of the atoms comprising the particle under investigation. In order to accomplish this aim, an instrument must be capable of performing a number of functions. It should include a means of measuring electron velocities which has sufficient range, sensitivity, and resolving power to permit the identification of any element in the periodic system. The experimental arrangement must also include some means for selecting for the analysis only those electrons which have been transmitted by a selected particle. Finally the design must include the flexibility and convenience required for the initial investigation of the fundamental phenomena involved.

Unfortunately, these fundamental requisites exclude the attractive possibility of applying some form of velocity analyzer to the image of a conventional electron microscope. This can be shown most simply by considering a specific case in which a specimen particle 100A in diameter is illuminated with 30,000-volt electrons and observed by an electron microscope system using an objective of 4-millimeter focal length and an angular aperture of 3×10^{-3} radius. From the familiar approximate formula for the chromatic aberration of the system, *viz.*,

$$r_{chr}=f_0\alpha_0(\Delta E/E), \tag{1}$$

where r_{chr} is the radius of the circle of confusion* due to electrons which have lost ΔE electron volts on passing through the specimen, f_0 is the focal length of the objective, and E the accelerating potential of the incident electrons. It can be seen that those electrons which are transmitted by the specimen particle with an energy loss of 2000 electron volts will illuminate an area of the image plane 1.7μ in diameter. Conversely, if electrons retarded by 2000 electron volts are detected at a point of the image their point of origin in the specimen can be specified only as lying within a corresponding circular area of the specimen 1.7μ in diameter. Considering this example still further it can be seen that the intensity in the image plane of the electrons which have been retarded by 2000 electron volts in the 100A particle will be almost *four orders of magnitude* less than it would be for an electron lens system free of chromatic aberration.

In addition to showing the impracticability of applying a velocity analyzer directly to a conventional electron microscope these considerations have pointed to the use of an electron probe since with it the effects of chromatic aberration can be completely eliminated. In fact, the use of an electron probe appears attractive in many ways. In its formation electrons having an extremely narrow velocity distribution can be used so that the chromatic aberration of the probe forming lens system is negligible. By proper choice of lens parameters, electron probes having a diameter of only 100A can be formed, thus making it possible to confine the irradiation of the specimen to the area or particle being

[10] G. Ruthemann, Naturwiss. **29**, 648 (1941); Naturwiss. **30**, 145 (1942).

* Throughout this paper measurements in the image are given in the scale of dimensions of the object plane.

analyzed. While the analysis would normally be carried out with the probe* point—i.e., the minimum cross section of the probe—coinciding with the specimen, a slight translation of the probe in a direction perpendicular to the plane of the specimen will set up the conditions which exist in the shadow type electron microscope[11] thus, very conveniently, enabling a high resolving power image of the same area of the specimen to be produced. Moreover, as the probe point is moved towards the plane of the specimen, the magnification of the shadow image will increase, appearing to the observer as an expansion of the image about its central point. The area of the image of the specimen which will have spread until it covers the entire field of view when the probe point coincides with the plane of the specimen and the magnification has gone to infinity, will correspond precisely with that area of the specimen from which transmitted electrons will be velocity analyzed.

Still another attractive feature of the use of the probe is the fact that electrons to be used in the analysis are in effect originating from a point source, thus permitting the elimination of the narrow collimating slits necessary in deflection methods of velocity analysis. The effective slit width obtained by the probe method is so small that it does not need to be considered in the calculations of the resolving power of the system.

A practical form of the instrument built around the use of an electron probe can now be seen to be a straightforward assembly of well-known electron optical components.

THE INSTRUMENT

Figure 1 is a photograph of the first experimental model of an electron microanalyzer. It can be seen that the instrument is similar in many respects to a conventional electron microscope; in fact, all the components except the analyzer chamber at the top were built originally for tests in connection with the electron microscope development. For this reason, and because the main purpose of this paper is the discussion of the electron optical and physical principles involved, the following description will be kept quite general and little reference will be made to specific design details. Figure 2 is a schematic representation of the instrument and its associated power supplies.

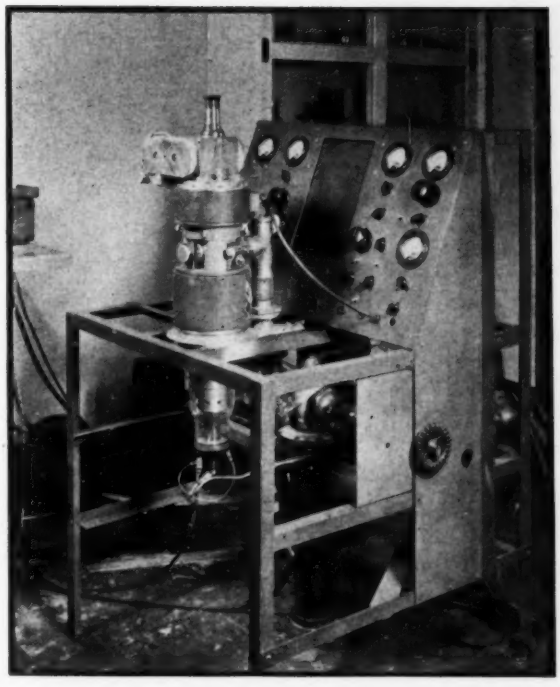

FIG. 1. A photograph of the electron microanalyzer in its first experimental form. The electron gun with high voltage shield removed is seen below the table. The first and second lenses, the object chamber, the third lens, the viewing screen, and analyzing magnet are seen above the table. The electrical control is to the rear. The main power supply is not shown.

In the previous section it has been indicated that the electron microanalyzer has two modes of operation, as a shadow type electron microscope and as an electron velocity analyzer of high resolving power. While in the first experimental model the two modes of operation were used alternately, recently some changes have been made which permit them to be used simultaneously.

For the mode of operation in which the instrument is used as a shadow microscope it consists

* It should be pointed out that the spherical aberration of the final lens of the probe forming system causes the minimum cross section of the electron beam to lie slightly closer to the final lens than the true probe point (i.e., the reduced image of the original electron source) which is effective in the production of the central regions of an electron shadow microscope image.

[11] H. Boersch, Zeits. f. tech. Physik **20**, 346–350 (1939); Naturwiss. **27**, 418 (1939).

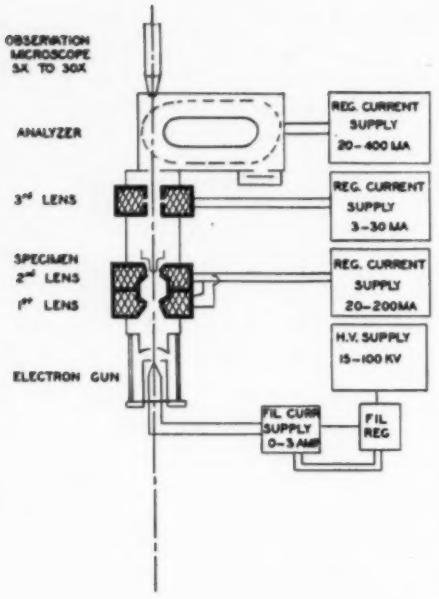

FIG. 2. A schematic cross section of the electron microanalyzer and block diagram representation of the associated power supplies.

of an electron gun, a two-stage probe-forming lens system, a movable specimen stage, a projection lens, a fluorescent screen, and a low power stage of optical magnification. When it is used for determining the electron retardation introduced by the specimen, it consists of the same electron gun, probe-forming lens system, specimen stage, and projection lens but has in addition a magnetic field velocity analyzer and a photographic chamber. The entire electron optical system is shown schematically in Fig. 3.

The electron probe which is common to both modes of operation is simply a greatly reduced image of the electron source. When used in the formation of the shadow images the probe is adjusted so that its axial position is either slightly above or below the plane of the specimen. No focusing is necessary, the definition in the image being determined by the size of the geometrical image of the source and effects of Fresnel diffraction. Thus, if d_1 is the distance from the probe point to the object, λ the wave-length of the electrons, $m_1m_2 \ll 1$ the magnification of the probe forming lens system, and d_s the diameter of the original electron source, the resolving power d_i may be written either as

$$d_i = (1/2)d_s m_1 m_2 \tag{2}$$

or as

$$d_i = (d_1\lambda)1/2, \tag{3}$$

according to which is the larger. Aberrations in the probe-forming lens system enter only as a distortion of the image. The magnification, on the other hand, is controlled by the position of the probe relative to the specimen and the screen and can be varied at will by adjustment of the strength of the probe-forming lenses.

It has been found convenient to observe the fluorescent image through a low power compound light microscope (30×) because the limiting apertures which are introduced to control the performance of the velocity analyzer limit the diameter of the image on the screen to about 2 millimeters. The use of auxiliary optical magnification is merely a means of artificially increasing the field of view at any given magnification of the observed image.

When the instrument is arranged to obtain the velocity distribution existing in the transmitted electron beam, the probe is adjusted to coincide with the plane of the specimen and the magnetic field of the velocity analyzer is turned on. It will be assumed that the specimen has been adjusted by observation of the shadow image so that the probe will pass through that part of the specimen for which an analysis is desired. The power of the third lens is adjusted so that an image of the illuminated area of the specimen is formed at the point at which the beam enters the homogeneous magnetic field of the velocity analyzer. Since the illuminated area of the specimen is exceedingly small and the arrangement of the third lens gives a reduced image of this area, the beam entering the analyzer can still be considered to be in the form of a probe, although the aberrations of the third lens cause the minimum diameter of this probe to be considerably larger than that of the true image. The velocity analysis is obtained by the well-known use of a homogeneous magnetic field and 180° focusing. An appropriately placed photographic plate is used for recording the velocity distribution.

Two limiting apertures are necessary when the instrument is used for analysis. The first is

situated in the second lens and influences the resolving power of the probe by limiting the spherical aberration of this lens. It should be pointed out that in this case "the resolving power of the probe" means the minimum diameter of the area of the specimen irradiated by the probe and must be distinguished from the resolving power in the shadow image produced by the probe which may be as much as an order of magnitude lower. It is given by the diffraction and aberration defects which must be added to the geometrical size of the image produced by final lens of the probe forming system. Thus, the resolving power d_p of the probe may be written either as

$$d_p = 2Cf_2\alpha_2^3 + d_s m_1 m_2, \tag{4}$$

or as

$$d_p = 2\lambda/\alpha_2 + d_s m_1 m_2, \tag{5}$$

according to which is the larger. In Eqs. (4) and (5), C is a dimensionless constant characteristic of the lens, f_2 is the focal length of the second lens, and α_2 is the angle subtended at the probe position by the radius of the limiting aperture of the second lens.

In the experimental system used the parameters in (2) and (5) were as follows:

$$d_s = 0.025 \text{ mm}$$

$$m_1 = 0.015$$

$$m_2 = 0.0375$$

$$\lambda = 0.05 \times 10^{-7} \text{ mm}$$

$$Cf_2 = 10 \text{ mm}$$

$$\alpha_2 = 0.0042 \text{ and } 0.021 \text{ rad.}$$

The parameter d_1 may have any value from 0 to 1 mm according to the magnification used in the shadow microscope image.

Substituting these values in (2) and (3) indicates that the limiting resolving power of the shadow microscope is about 70A providing d_1 is kept below 0.01 mm. In the present instrument this corresponds to an electronic magnification of 34,000 which is achieved only in the last stages of adjusting the probe for making analysis. For more normal magnifications of approximately 4000 which corresponds to $d_1 = 0.085$ mm the theoretical resolving limit is 200A. Using the above values for the parameters in (4) and (5) we find that the resolving power of the probe is 165A and 2000A for α_2 equal to 0.0042 and 0.021 radian, respectively. All of these values were found to agree very well with experiment. Some difficulty was encountered in measuring the minimum diameter of the probe until it was discovered that a darkening of the specimen occurred if the probe was allowed to remain in one position for a fairly long time. In this way it was found possible to determine the area irradiated by the probe and to measure it quite accurately by observation in the shadow image.

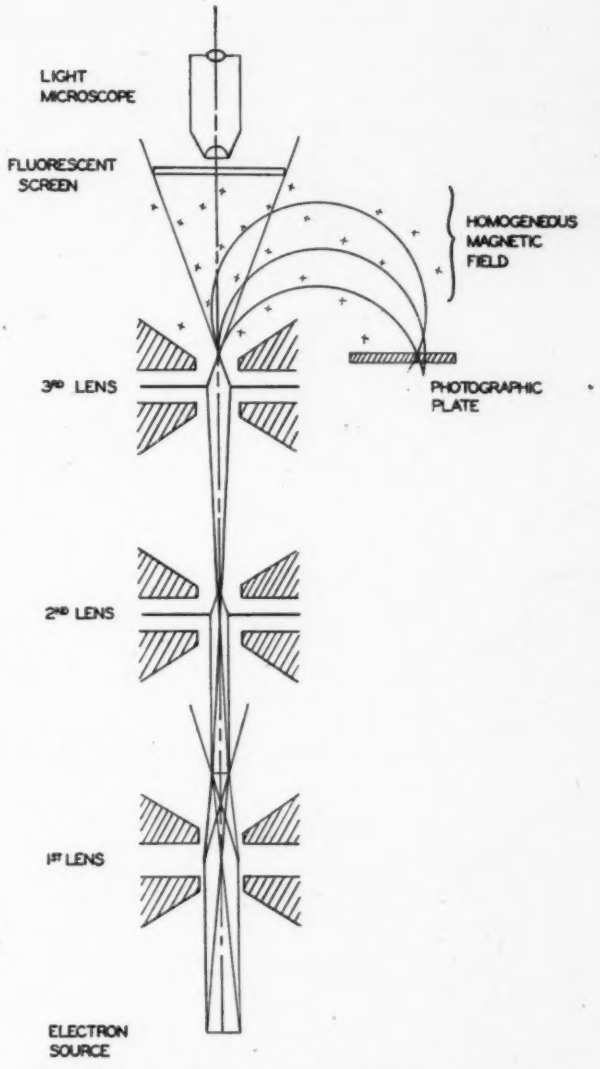

FIG. 3. A ray diagram of the electron microanalyzer. The specimen is placed immediately above the second lens near the position of minimum beam cross section.

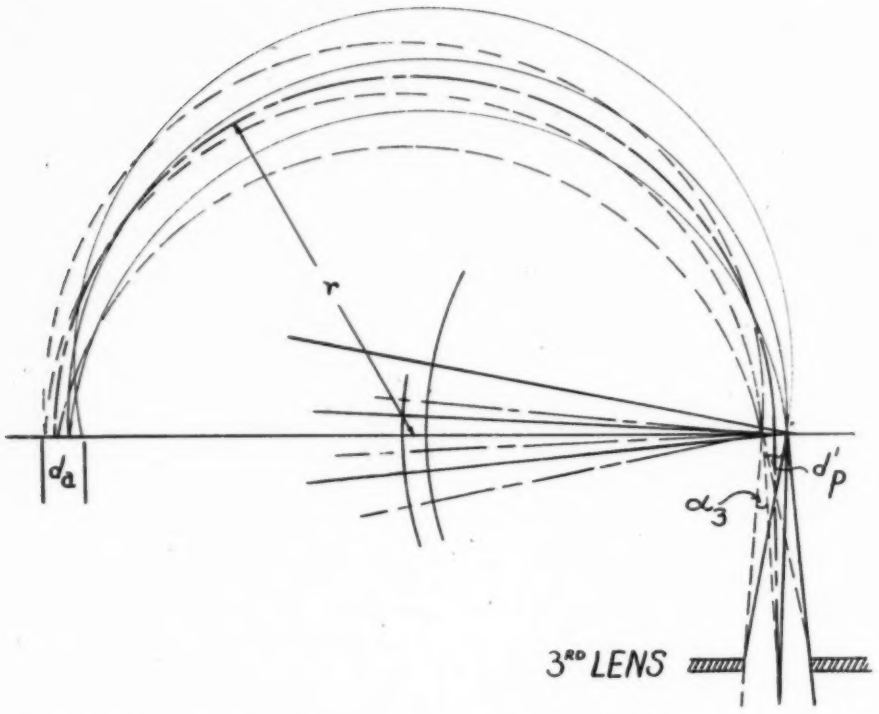

FIG. 4. A diagram showing the ray paths in the 180° magnetic deflection type of electron velocity analyzer incorporating a focusing lens.

The second limiting aperture is situated in the third lens and has as its primary purpose the control of the resolving power of the electron velocity analyzing system. Figure 4 is a ray diagram showing the trajectories of the electrons leaving the third lens and passing through the homogeneous magnetic field analyzer. It should be pointed out that this differs somewhat from the conventional velocity analyzing systems in that the beam entering the analyzer is in the form of a narrow cone instead of a collimated sheet. Thus, the diagram represents only those rays which are traveling in the plane of symmetry of the system. The maximum width of the image line produced in the analyzer is given by the expression

$$d_a = d_p' + 2r(1-\cos\alpha_3), \tag{6}$$

where d_p' is the diameter of the probe at the entrance position of the analyzer, r is radius of the circular paths of the electrons in the analyzer, and α_3 is the angular aperture of the beam entering the analyzer. In this expression, neglecting relativity effects,

$$r = 3.37E^{\frac{1}{2}}/H \tag{7}$$

and

$$\alpha_3 = d_3/2v_3, \tag{8}$$

where E is the velocity of the electron beam expressed in electron volts, H is the strength of the homogeneous magnetic field of the analyzer expressed in gauss, and d_3 is the diameter of the limiting aperture plane of the third lens and the entrance position of the analyzer.

If we express the resolving power of the system by the ratio $\Delta E/E$ we have the relations

$$\Delta E/E = 2\Delta r/r = (d_p'/r) + 2(1-\cos\alpha_3). \tag{9}$$

Since, in the practical case under consideration, d_p' is negligible and α_3 is small, we can write

$$\Delta E/E = \alpha_3^2. \tag{10}$$

For $d_3 = 1.0$ mm and $V_3 = 50$ mm. Equations (8) and (10) give 1/10,000 as the calculated resolving power of the system. The experimental resolving

power measured under the same conditions has been established at 1/5000. The discrepancy between the measured and calculated resolving powers of the instrument has not yet been investigated. The width of the line at the position of the photographic plate is given by the expression

$$2\Delta r = r\alpha_3^2. \tag{11}$$

For the practical case in which $r=80$ mm and $\alpha_3=10^{-2}$ radian the line width is immediately seen to be 8 microns. Such a line can be recorded satisfactorily on Eastman Medium Lantern Slide emulsion.

These simple expressions for the resolving power of the system can also be used to determine the degree of stability required in the magnetic analyzing field. From (7) we can write

$$\Delta E/E = 2\Delta H/H = 2\Delta i_a/i_a, \tag{12}$$

where i_a is the current in the coil windings producing the magnetic analyzing field. Thus, to achieve a resolving power of 1/10,000, the magnetic field and, hence, the exciting current, must not vary by more than 1/20,000, i.e., 0.005 percent during the exposure time.

It is obvious that the accelerating potential of the incident electrons must not vary by more than 1/10,000, i.e., 0.01 percent during the exposure time. The stability requirements of the first, second, and third lenses of the system are almost the same as those for the projection, objective, and condenser lenses, respectively, of a conventional electron microscope and hence will not be discussed here.

A discussion of the electron optics of the microanalyzer would not be complete without some mention of the effect of the chromatic aberration of the third lens. Figure 5 is a ray diagram demonstrating this effect and illustrating the symbols used below. It can be shown that it is necessary to place the photographic plate in the correct position if the entire velocity distribution is to be obtained in exact focus simultaneously. The proper position for the photographic plate can be determined from the

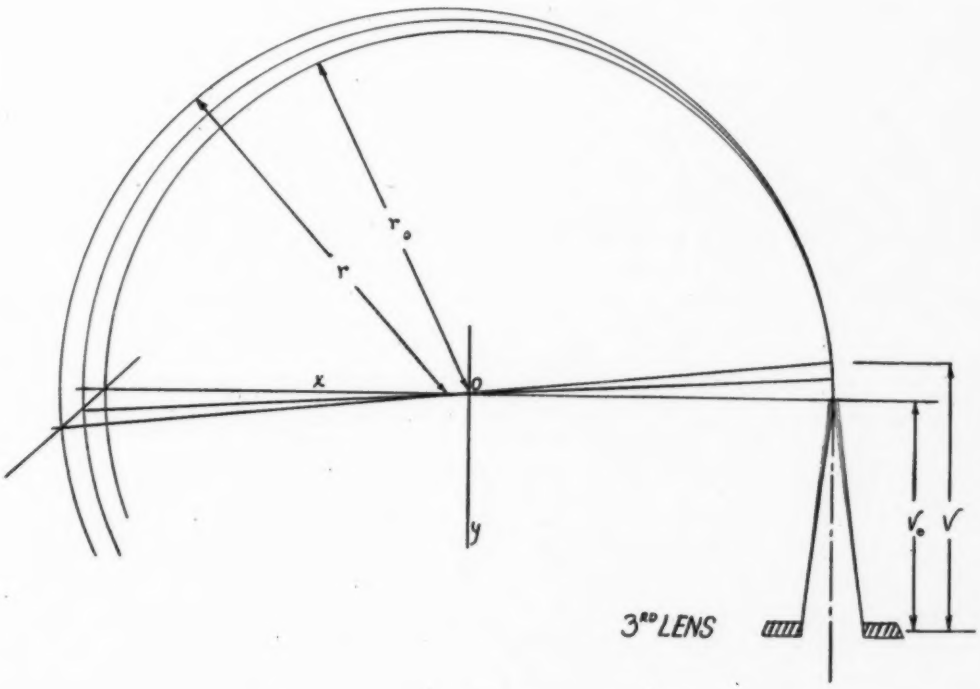

FIG. 5. A diagram illustrating the symbols used in the text to describe the effect of the chromatic aberration of the third lens.

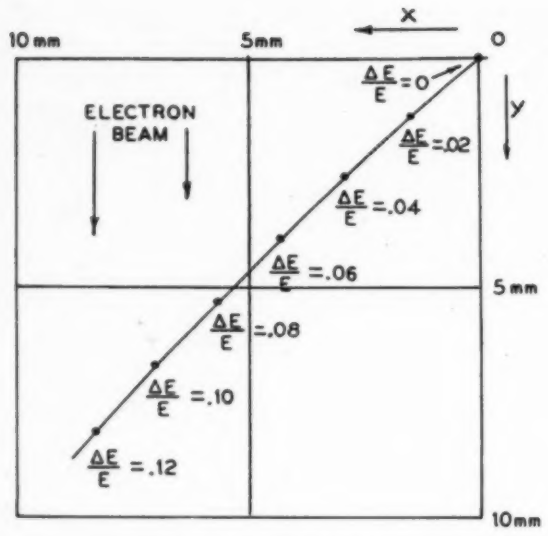

FIG. 6. Shows the position of the photographic plate for which all of the velocity distribution is in focus.

following expressions:

$$x = r\cos\left(\frac{v-v_0}{r}\right)+(r-r_0), \tag{13}$$

$$y = r\sin\left(\frac{v-v_0}{r}\right),$$

$$v = uE/(ku+E), \tag{14}$$

$$r = k_1E^{\frac{1}{2}}, \tag{15}$$

where x and y are the coordinates of the emulsion position at which electrons of velocity corresponding to E electron volts will be focused. The origin is taken at the center of the circular path corresponding to the minimum electron energy to be recorded. k and k_1 are constants, while u is the distance of the specimen from the third lens. In Fig. 6 the plate position has been plotted using the parameters of the experimental instrument. It can also be seen from (13), (14), and (15) that the optimum position of the plate does not depend on the velocity of the incident electrons for which the instrument is adjusted providing $r_0=$const. In the present experimental model the position of the plate defined by the above equations is not used, primarily because the extra construction necessary was not considered justified for preliminary tests. Instead, the plate is placed on the x axis. Two or three exposures with slightly different adjustments of the power of the third lens are usually sufficient to obtain focused records of all parts of the velocity distribution.

In the above calculations it has not been necessary to take into account the relativistic correction even though it is appreciable for electrons of the velocities used. However, in considering the calibration of the instrument this correction cannot be neglected. The fundamental formula (7) for the homogeneous magnetic field analyzer must now be written:

$$r=\left[\frac{2\times10^8}{e/mH^2}\right]^{\frac{1}{2}}\left[E+\frac{e}{2mc^2}E^2\times10^8\right]^{\frac{1}{2}}, \tag{16}$$

from which we can derive the working formula:

$$\frac{\Delta E}{E}=\frac{[1+(eE/2mc^2)\times10^8]}{[1+(eE/mc^2)\times10^8]}\times\left[2\left(\frac{\Delta r}{r}\right)+\left(\frac{\Delta r}{r}\right)^2\right]. \tag{17}$$

In Fig. 7 $\Delta E/E$ has been plotted against $\Delta r/r$ for accelerating potentials up to 90 kilovolts.

It can be seen from (17) that to determine ΔE with any given accuracy requires a knowledge of the value of E to the same accuracy. In the final calibration of the instrument an attempt was made to keep the errors below 2 percent, which involved the measurement of the accelerating potential to within at least 1 percent for each exposure. This constituted a major difficulty until it was determined that an absolute measurement of sufficiently high accuracy could be made by an internal calibration of the analyzer itself. The internal calibration involved a measurement of the magnetic field of the analyzer to within 2 percent and was accomplished by comparing the field with that of a standard solenoid. A conventional fluxmeter was used as the means of comparison.* Thus a calibration curve was plotted from which the value of the accelerating potential can be determined when the value of Hr is known. Both H and r can be determined accurately at the time of each exposure. Thus E can be determined from the curve in Fig. 8

* In absolute measurements three fluxmeters were found to give values differing by as much as 15 percent, while in the comparison method used the results obtained with all three meters agreed to within ½ percent.

enabling ΔE to be determined from the curve in Fig. 7.

RESULTS

Electron-optically the instrument performed in accordance with the theory discussed above. Probe diameters as small as 200A were obtainable though they were found to be unsuitable for use in the present system. When such a concentrated probe was used in the relatively poor vacuum of the present arrangement a deposit was formed with such rapidity on the specimen that it became opaque in a matter of seconds. This deposit appeared to be the same as that encountered in the electron microscope and to be due to the interaction of the electron beam with the grease and oil vapors which are present in the instrument. Since such extremely fine probes were not necessary for the initial fundamental investigations the difficulty caused by the deposit was avoided for the time being by using wider probes (2000A) of correspondingly lower intensity. Even for probes of this dimension only from 10^{-16} to 10^{-14} gram of material entered into the analyses described below.

The initial tests have been devoted almost entirely to the detection and measurement of the specific energy losses in thin targets of various materials. Ruthemann's work[10] on collodion membranes was extended by the use of high accelerating potentials (25 to 70 kilovolts). The lines due to the K levels of carbon and oxygen were almost invariably clear and strong (Fig. 9); that due to nitrogen, on the other hand, was

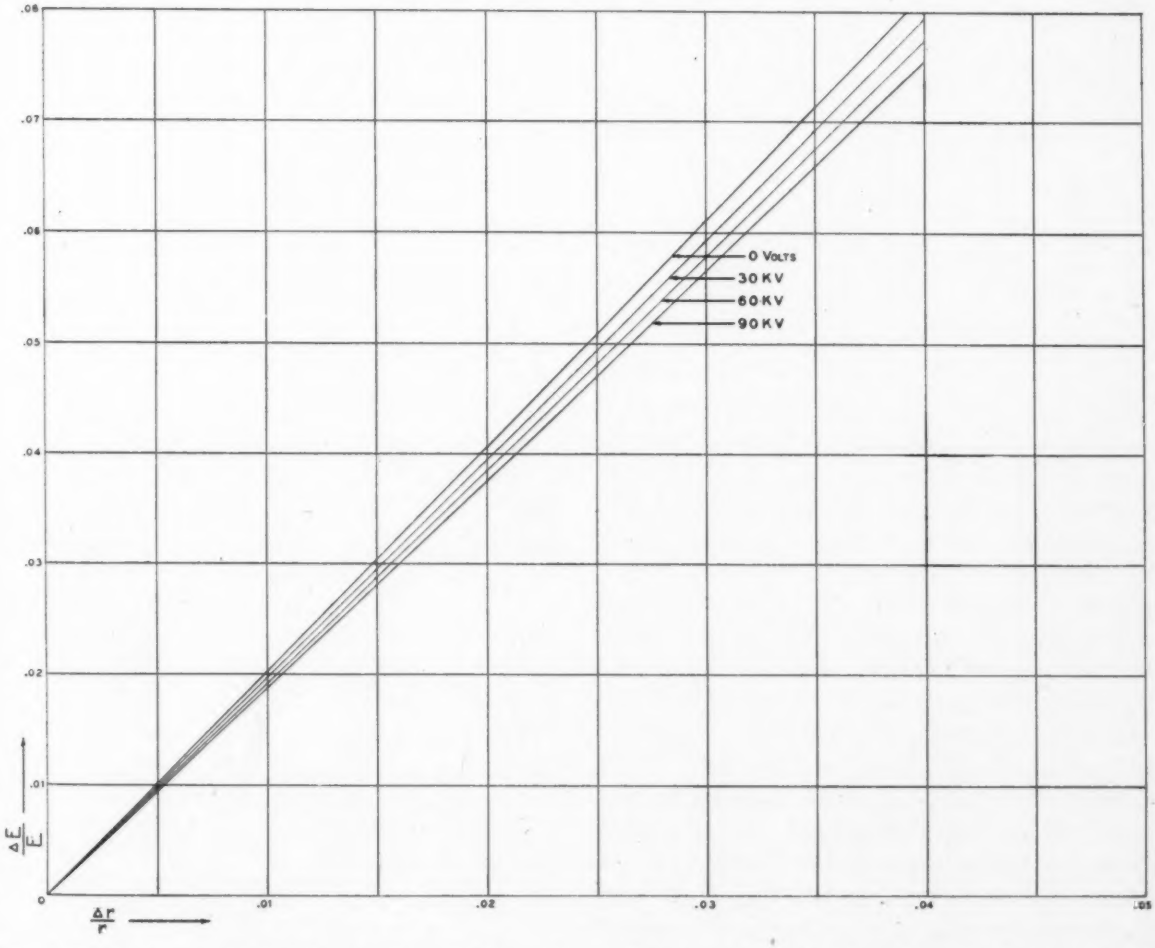

FIG. 7. Calibration curve for the magnetic velocity analyzer. The values of the incident electron velocities for which the relativity correction was calculated are indicated on the respective curves.

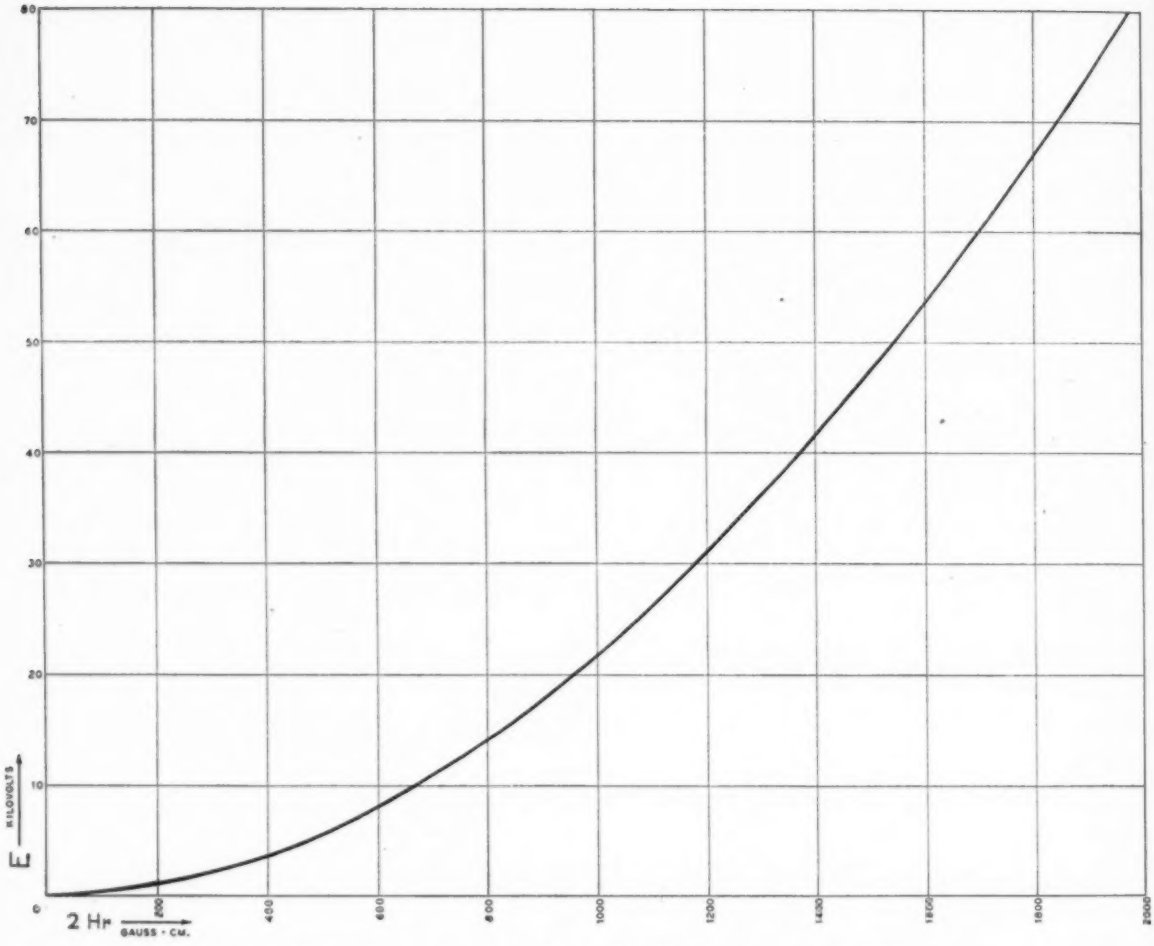

FIG. 8. Calibration of the magnetic field analyzer when used as a voltmeter.

observed in only a few cases. Tests were also made on thin evaporated films on collodion of beryllium, aluminum, silicon, iron, and zinc. The results of these tests are summarized in Table I. As photographic focusing was used throughout, all the lines observed were taken close to or at the best focus for the line. Furthermore, a series of exposures in which the time of exposure was varied were made in each case in order to obtain the optimum contrast for each line.

It was found that the discrete losses due to the K levels of Al and Si were the most difficult to record and required exposures two orders of magnitude longer than those necessary for the carbon K level. While the lines obtained from Al and Si were easily observed on the negatives they can be shown only with difficulty on a photometric curve or in a reproduction. However, since these lines consist of a jump in level of the general scattering (inelastic) of the background they become very evident if the graininess of the plate is averaged out. Figure 10 shows

TABLE I.

Element	Z	ΔE	Level	E kv	ΔE (ICT)*
Be	4	129.3	K	46.5	—
C	6	286.2	K	26.0	284.2
N	7	404	K	26.0	397.6
O	8	525.8	K	26.0	526.2
Al	13	1605	K	46.0	1553.7
Si	14	2033	K	47.8	—
Fe	26	703.9	L	26.0	709.8
					723.9
Fe	26	51.3	M	26.0	56.5
Zn	30	1160	L	46.0	1021.2
					1044.4

* Values obtained from the *International Critical Tables*.

the photometric curve obtained from a silica film (self-supporting) in which this has been done. It can be seen that the point at which the jump in level takes place can be determined quite accurately in even this extreme case. As yet no line due to a K level has been detected for elements beyond atomic number 14. However, at this point the L lines due to the L levels are

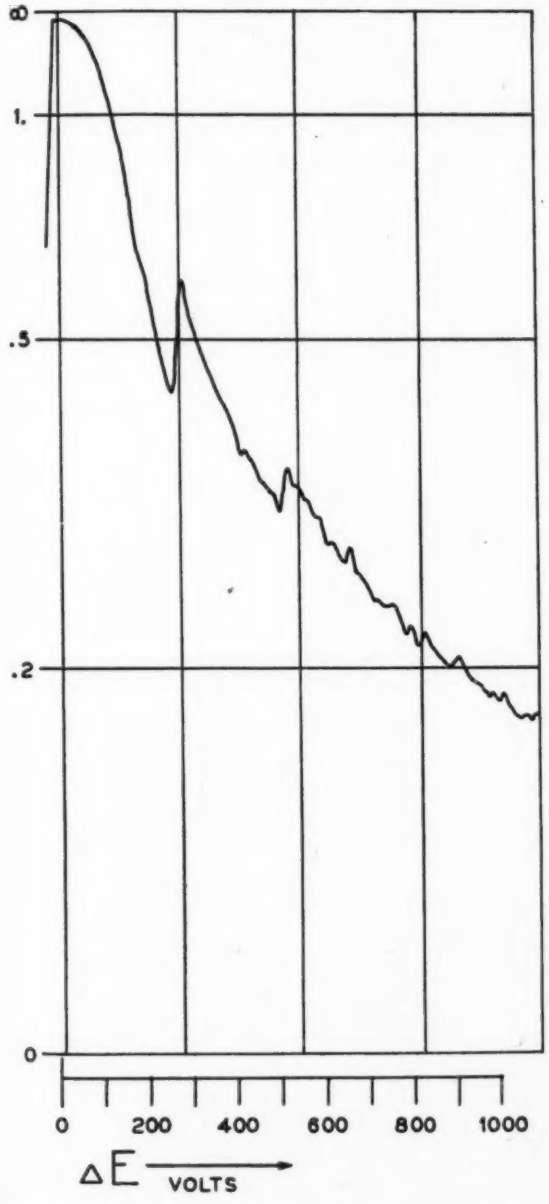

FIG. 9. A photometric curve obtained when collodion is used as a specimen in the microanalyzer. The peaks due to the K levels in C and O are present.

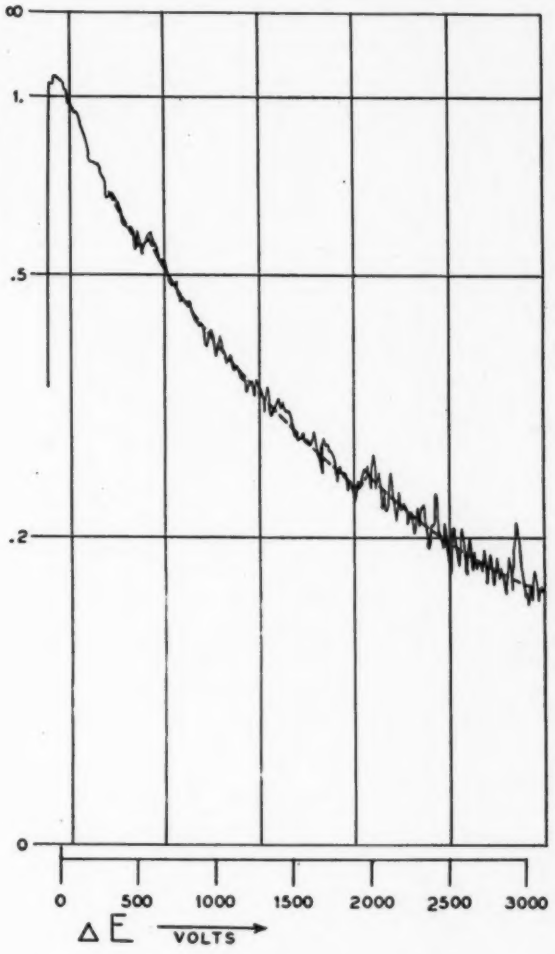

FIG. 10. A photometric curve obtained from a self-supporting film of silica. The peak due to the K level can be seen easily in this curve when the graininess of the plate is averaged out.

beginning to show up. For iron ($Z=26$) the L line is very strong (Fig. 11) and the M line is beginning to show up. At the time of writing zinc is the heaviest element for which a line (that due to the L level) has been detected.

In the course of the tests it was noted that the values of ΔE corresponding to the K levels of C and O increased with increasing accelerating potentials. This is illustrated for the case of carbon in Fig. 12. It should be noted that no formal experiment has been carried out as yet to investigate this phenomenon. The experimental points were obtained from the exposures made during the tests described in the above. Each point represents the mean value of all the results

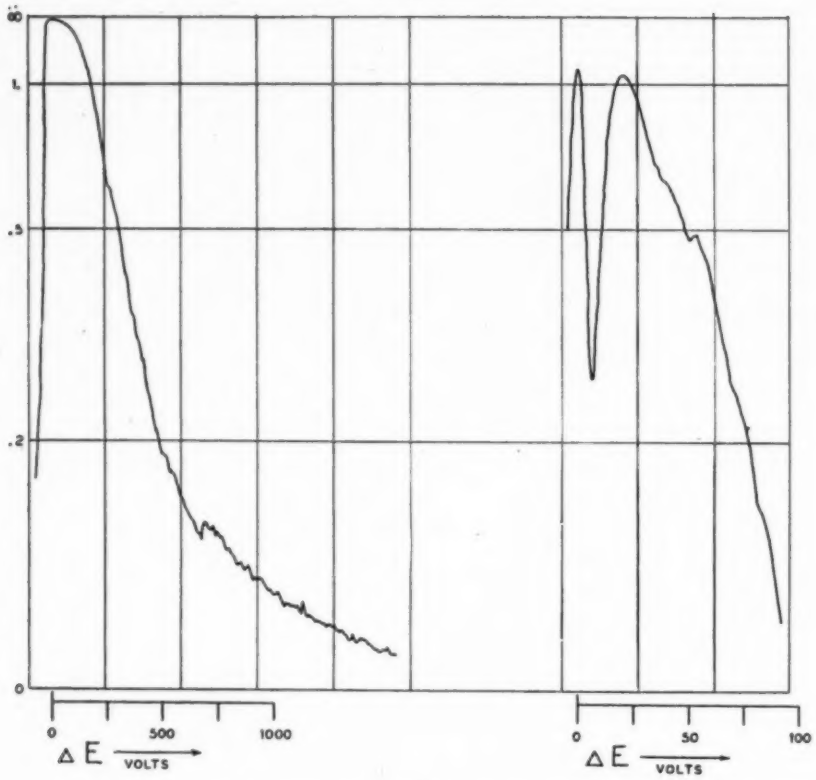

FIG. 11. (Left) A photometric trace of the velocity distribution obtained using evaporated film of iron on collodion. The L level of Fe is clearly visible. (Right) A lighter exposure on the same specimen is shown on an expanded scale. The M level shows up quite clearly and the resolving power of the instrument is quite apparent from the width of the line at $\Delta E=0$.

obtained at each designated voltage. The scattering of the points is due to the fact that the instrument had not been accurately calibrated for a large number of the exposures. Nevertheless, the magnitude of the effect is considerably greater than the errors involved.

In the initial arrangement of the apparatus only those electrons which were deflected by less than 4.4×10^{-3} radian were used in the analysis. While in quantum theory it is not possible to make accurate calculations to determine the most probable angle of scattering of electrons which have lost energy in a given inelastic collision, this angle can be shown to be of the same order of magnitude as that calculated from classical theory. Thus, in order to obtain the maximum intensity, relative to the background in the lines due to the x-ray levels of the heavier elements, it is necessary to provide a means for directing into the analyzer those electrons which have been scattered through this most probable angle. Figure 13 shows the experimental arrangement for accomplishing this. An asymmetric type of

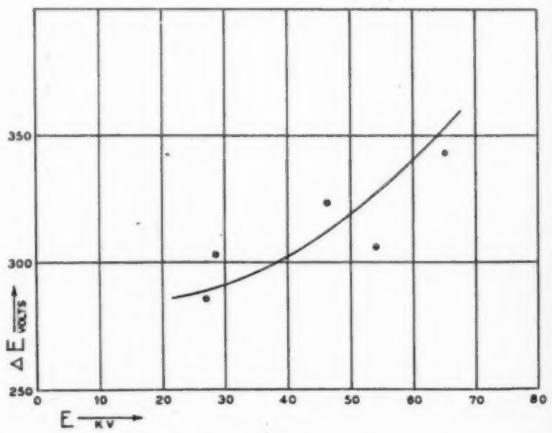

FIG. 12. Curve showing the dependency of ΔE on the velocity of the incident electrons used for the K level of carbon.

pole piece is used so that the probe is formed in the open space of the specimen chamber. Immediately above the specimen is arranged a magnetic deflecting field which deflects the directly transmitted beam onto a fluorescent screen for observation through a low power microscope system. The distance between the fluorescent screen and the axis of the instrument is adjustable. As shown, those rays which are scattered through the selected angle are deflected into the aperture of the third lens.

In addition to using for the analysis that group of electrons in which the intensity of the specifically retarded electrons is a maximum relative to the background, this arrangement has the extra advantage that the image of the specimen can be observed simultaneously with the recording of the velocity distribution. Without it such observations could be carried out only when the analyzer field was turned off. In that case there is no way of determining the effects due to stray fields from the analyzer.

Figure 14 shows the type of velocity distribution obtained with this system. K line of aluminum is quite clearly visible on this plate, yet in earlier work when the deflection system was not used this same line could not be reproduced.[9]

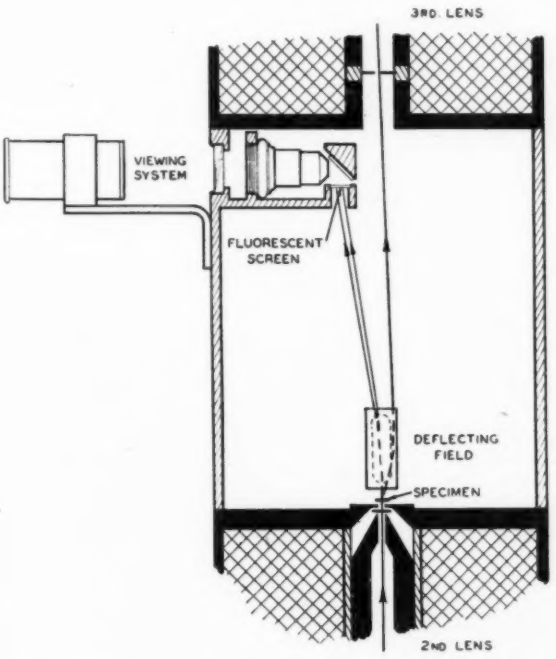

FIG. 13. Diagram showing the arrangement for deflecting electrons scattered through a predetermined angle into the velocity analyzer. This diagram also shows the viewing system used with the instrument in this form.

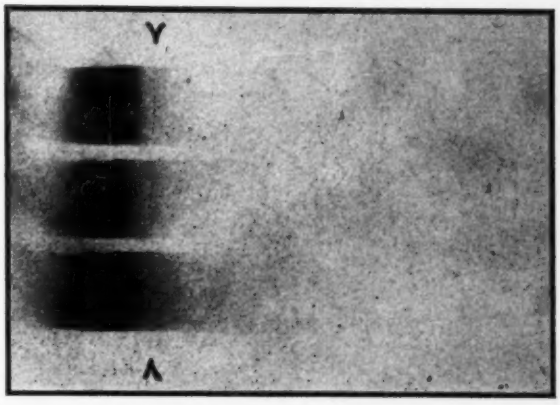

FIG. 14. A photographic reproduction showing the appearance of the peak in the velocity distribution due to the K level of aluminum.

SUMMARY

In the foregoing paragraphs, a new type of electron optical instrument has been described. By the application of an electron probe of extremely fine dimensions it has been possible to obtain, with high resolving power, the velocity distribution in a beam of electrons transmitted by a thin specimen. By further application of the electron probe the region of the specimen transmitting electrons can be made very small and can be accurately located in a specimen.

In the preliminary tests it has been possible to observe and measure the discrete amounts of energy lost by the incident electrons in inelastic collisions with the inner electrons of a number of elements. The discrete energy loss corresponding to the K levels of at least carbon and oxygen have been found to be dependent on the incident electron velocity.

The authors wish to thank Dr. V. K. Zworykin for his interest and suggestions. We wish to thank also Mr. J. M. Morgan for his assistance in converting an early type electron microscope electrical supply for use in the present apparatus.

Torsional Vibration of Multi-Disk Systems

EDWARD FISHER
Cornell University, Ithaca, New York
(Received June 26, 1944)

An asymptotic method is given for computing the lowest frequencies of multi-disk systems having a large number of disks. It is based on the assumption that the frequency to be computed can be represented approximately by a descending series in the disk number and that the form of the leading term of this series can be obtained by inspection of the frequency equation. The method is tried out on three examples, all six-cylinder Diesel engines.

THE first example, Fig. 1, is from Timoshenko.[1] The I's and k's are moments of inertia and torsion constants, respectively. Their values are $I=3920$, $I_1=139{,}800$, $I_2=26{,}400$, $I_3=708$; $k=730\times10^6$, $k_1=402\times10^6$, $k_2=1334\times10^6$, $k_3=2070\times10^6$. To obtain the equation for the natural frequencies in this case—and also in the two following—I used the matrix method of Pipes.[2] With the frequency (vib. per sec.), $f=(1/\pi)(k/I)^{\frac{1}{2}}\sin(\alpha/2)$, and $2(1-\cos\alpha)=a$, this leads to $\sin\alpha\cot 6\alpha=(67.3a-1-197.4a^2+0.820a^3)/(42.58-144.6a+27.62a^2)$. The fourth significant figure in the numbers is not accurate since the calculations throughout this note were done on a ten-inch slide rule.

Setting $6=n$—a "large number"—we write this equation $\sin\alpha\cot n\alpha=(0.3112n^3a-1-0.914n^3a^2+0.820a^3)/(1.183n^2-0.669n^3a+0.767n^2a^2)$, and, in accordance with our basic assumption, seek a solution α, descending in n. Inspection shows a self-consistent one of the form $\alpha=(c_1/n)+(c_2/n^2)+\cdots$. Substituting, and equating like-order terms, we get $c_1=3.804\cot c_1$ for the first approximation and $c_2=[(3.80/c_1)-0.669c_1^3]/(5.65+0.311c_1^2)$ for the second. The equation in c_1 is solved by interpolation in a "trig" table. The smallest root leads to the first approximation for the lowest frequency $f=14.3$; the second approximation then gives $f=14.8$: the correct value is $f=15.3$. Incidentally, the method in this example, instead of failing rapidly for the higher frequencies as one would expect because of the relatively low value of n, persists in giving agreement. With the first approximation these frequencies come out 43.9, 73.7, 100.2, 120.5, 133, as compared with the correct ones, 44.3, 72.4, 98.3, 124, 132.

The second example, Fig. 2, is from Den Hartog.[3] The numerical values are $I=2560$, $I_1=75{,}000$, $I_2=24{,}000$; $k=k_1=675\times10^6$, $k_2=13.5\times10^6$. With the same notation as in example I, and $n=6$ still, the frequency equation is now $\sin\alpha\cot n\alpha=(0.882n^5a^2-2.252n^3a+1)/(1.764n^5a-1.074n^2)$. Inspection shows a self-consistent solution of the form $\alpha=(k+\frac{1}{2})(\pi/n)+(c/n^2)+\cdots$, k any positive integer or zero. And substitution in the equation yields $c=0.406/(k+\frac{1}{2})-1.570(k+\frac{1}{2})$. Here again the agreement persists for higher frequencies: The values of f found are 21.4, 58.2, 92.6, 121.8, 144.3, whereas the correct ones are 21.2, 58.4, 92.8, 122, 145, respectively. This sort of agreement for higher frequencies should be discounted.

In addition, the method fails to point automatically to the lowest frequency. However, if we reduce the frequency equation to the form

$$\sin\alpha\frac{\sin(n+1)\alpha}{\sin n\alpha}=(1.046n^2-0.284n^6a)/(1.046n^2-0.284n^6a+1-0.363n^4a),$$

then the possibility that we have overlooked becomes clear: It is the case where $\sin\alpha$ and

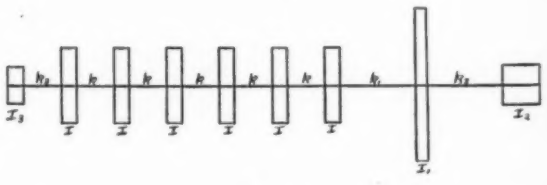

FIG. 1.

[1] Timoshenko, *Vibration Problems in Engineering*, Chapter 3.
[2] L. A. Pipes, J. App. Phys. **13**, 434 (1942).
[3] Den Hartog, *Mechanical Vibrations*, Chapter 5.

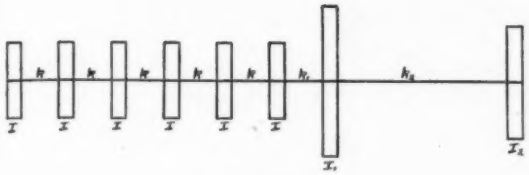

FIG. 2.

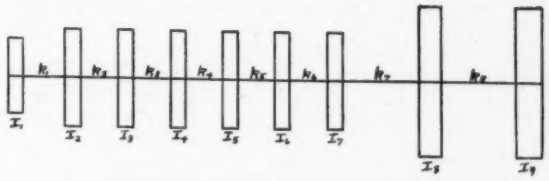

FIG. 3.

$1.046n^2-0.284n^6a$ both approach zero as n grows large. The corresponding self-consistent solution then must have the form $\alpha=(c/n^2)+(c_1/n^6)+\cdots$. The frequency—to the second approximation, as usual—comes out $f=4.36$; the correct value is 4.24.

The third example, Fig. 3, is from Tuplin.[4] The numerical values are $I_1=600$, $I_2=I_3=I_4=I_5=I_6=I_7=4000$, $I_8=60{,}000$, $I_9=30{,}000$; $k_1=1860\times10^6$, $k_2=k_3=k_4=k_5=k_6=928\times10^6$, $k_7=464\times10^6$, $k_8=618\times10^6$. The notation is still the same and $n=6$; but now the frequency equation can be put in either of two forms. If it is written in a form like that of example I, the resulting first-order equation, corresponding to $c_1=3.804\cot c_1$ in example I, is not simple enough to be solved directly from tables. Therefore it is written

$$\sin\alpha\cot n\alpha=(1.343n^2a-1-1.292n^3a^2+1.05na^3)/(0.629n^2-0.813n^3a+1.053n^2a^2),$$

requiring a solution of the form

$$\alpha=(k+\tfrac{1}{2})\frac{\pi}{n}+\frac{c}{n^2}+\cdots,$$

k a positive integer or zero. Then $c=0.506/(k+\frac{1}{2})-6.71(k+\frac{1}{2})$. This gives for the lowest frequency—now in vib. per min.—$f=904$: The correct value is 1030. In an effort to improve the agreement we take the term $1.292n^3a^2$ in the frequency equation and write it $0.2153n^4a^2$ instead. This violates somewhat our expansion procedure but has the advantage of bringing into the approximation an important term that was neglected before. The resulting value of the lowest frequency is now 1070. The higher frequencies computed in this way show no agreement worth mentioning.

On its showing in these examples the method could not stand beside other known methods. Thus Biot[5] has treated the first two of the above examples graphically, obtaining all the frequencies more accurately. However, the method does have three advantages. First, it is not restricted to simple systems: Whenever a frequency equation can be set up containing one number rather larger than the others, it affords a possible means of computing very quickly the lowest frequency at least—or an approximation to it sufficiently close to serve as the basis of a rapidly converging successive-approximation method. Second, it becomes much more accurate for larger values of n—say, a twelve-cylinder rather than a six-cylinder engine. And formulas might then also be derived for the higher frequencies: For example, with the expansion, $\alpha=(k+\frac{1}{2})(\pi/n)+(c/n^2)+\cdots$, we might take $k=0(n)$ rather than $0(1)$. Finally, most important, it can be used when the frequencies are no longer real but, as a result of damping, complex.

[4] Tuplin, *Torsional Vibration*, Chapter 6.

[5] M. A. Biot, J. App. Phys. **11**, 530 (1940).

Studies with the Electron Microscope Diffraction Adapter

ROBERT G. PICARD
RCA Victor Division, Radio Corporation of America, Camden, New Jersey
(Received June 13, 1944)

The RCA diffraction adapter for its electron microscopes uses a weak magnetic lens to focus the diffraction patterns. The accuracy of the results obtained in electron diffraction analysis with such a system is discussed, and it is shown that lattice spacings may be determined with an accuracy of one percent if reasonable precautions are observed in calibration and operation of the instrument. A method is also described for measuring the accelerating voltage of the electrons from data obtained from the diffraction pattern. Electron diffraction patterns are shown of a number of thin film materials which are commonly used as specimen supports in electron diffraction analyses and electron microscopy. The effects of aging and beam exposure on the patterns produced by these films are determined.

INTRODUCTION

IN a previous issue of this journal there appeared a paper[1] describing an adapter which, when installed in an RCA type B electron microscope, permitted the instrument to function either as an electron microscope or an electron diffraction camera. The exceedingly well-regulated high voltage supply of this electron microscope produces a very nearly monochromatic beam of electrons which is ideally suited for diffraction studies. It is the purpose of this paper to describe some results obtained with this unit, and to report the results of a study of the effect of a weak magnetic focusing lens on the accuracy of diffraction data obtained with such a camera.

ACTION OF THE LENS

Sharp lines in an electron diffraction pattern may be obtained either by using a very small aperture placed immediately above the specimen or by focusing the diffracted electrons onto the photographic plate by means of a lens. The action of the lens permits the use of a larger beam cross section and thus integrates the reflections from a larger area of specimen. This effect is clearly illustrated in Fig. 1, which shows two patterns of the same sample of MgO, one made using a 0.015″ aperture and focused with a weak magnetic lens, and the other made using a 0.003″ collimating aperture with the lens current turned off. In the first picture the rings are continuous, while in the second they can be seen to be made up of dots. This may be attributed to the fact that for the latter picture only 4 percent as many crystals contributed to the pattern as did in the first picture. Use of the small aperture with the lens gives no appreciable increase in line sharpness over the combination of larger aperture and lens.

[1] Hillier, Baker, and Zworykin, J. App. Phys. **13**, 571–577 (1942).

CALIBRATION

Calibration of the diffraction camera is accomplished by making use of a sharply focused ring pattern of a material having well-known atomic interplanar spacings (from x-ray diffraction data). The basic equation for diffraction, $n\lambda = 2d_{hkl} \sin\theta$, reduces to

$$Dd_{hkl}/n = 2KL\lambda \qquad (1)$$

for the small angles used in this instrument, where D is the measured diameter of a given ring; d_{hkl} is the interplanar spacing; n is the order of the reflection; λ, the deBroglie wave-length of the electrons; L, the specimen to photographic plate distance; and K, an instrumental constant having the value unity for zero lens current and a value somewhat less than unity (between 0.90 and 0.91 for the EMD diffraction adapter) when the lens is focused. K is related to the index of refraction of the magnetic field for electrons and KL is the effective specimen-to-plate distance.

For a fixed accelerating voltage (constant λ) and fixed specimen to plate distance L, Eq. (1) may be written

$$Dd_{hkl}/n = K', \text{ a constant.} \qquad (2)$$

The graph of D *vs.* d_{hkl} on logarithmic paper is a straight line of slope -1 and intercept K'; hence, calibration of the instrument for a given accelerating voltage may be accomplished by measuring the diameter D of a single ring of known spacing d_{hkl}, plotting this point on logarithmic paper using D as abscissa and d_{hkl}/n as ordinate, and drawing a straight line of slope -1 through this point. Of course, several ring diameters should be measured to serve as a check on the calibration, but it has been found that the distortion produced by the lens is so slight for the range of θ employed that the deviation from the straight line of points corresponding to large ring diameters is a small fraction of one percent.[2]

The choice of specimen to use for calibration is a matter to which some consideration must be given. Several hundred crystalline materials have accurately known lattice spacings determined by x-ray diffraction methods. Those which can be obtained in the form of fine powders or very thin films can be used as calibration standards for studies by transmitted electrons. The powders may also be used on reflection type holders, as may any solid material which has had its surface so treated that a diffraction pattern is obtained. Thin films of gold formed by thinning gold leaf or by evaporation of the metal onto a substrate and subsequent stripping from the base material are commonly used as diffraction standards. Magnesium oxide and zinc oxide smokes are also very satisfactory.

Certain spurious effects must be checked for any specimen used as a standard. Evaporated films in particular must be prepared so that the particle size is not so small that lattice distortion results and, hence, d_{hkl} values different from those obtained from bulk materials by x-ray methods will result. Many specimens which can be deposited on a substrate for either transmission or reflection studies take up a preferred orientation on the surface and thus exhibit relative intensities quite different from those determined by x-ray methods. Finally, the electronically transparent substrate materials used to support specimens for transmission studies contribute patterns of their own which must be identified as arising from the substrate and not from the specimen.

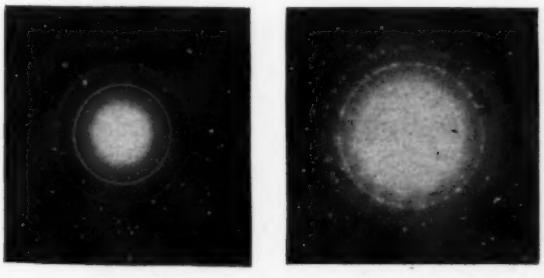

(a) (b)

FIG. 1. Magnesium oxide. (a) Made with 0.015″ aperture and focused with a weak magnetic lens. (b) Made with 0.003″ aperture and no lens.

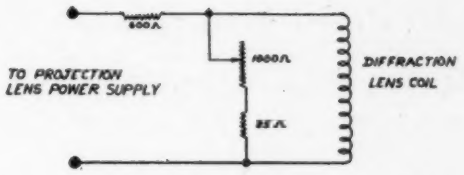

FIG. 2. Control circuit for diffraction focusing lens.

It is advisable to calibrate the instrument using a specimen having known interplanar spacings and then to make a pattern of another known material and check its d_{hkl} values obtained from the calibration curve against well-established x-ray data.

MEASUREMENT OF ACCELERATING VOLTAGE

The diffraction pattern also serves as a simple, accurate method of measuring the voltage used to accelerate the electrons. If the pattern of a material of known lattice spacings is photographed using no current in the focusing lens—a small aperture must be placed on the source side of the specimen to insure sharp lines—the value of K in Eq. (1) is unity, and this equation can be solved for λ. The corresponding voltage is obtained from the de Broglie relation.

$$\lambda = \left(\frac{150}{V}\right)^{\frac{1}{2}} (1 - 0.5 \times 10^{-6} V) \text{A}, \qquad (2)$$

where V is in volts. The term in parentheses is a relativity correction amounting to $\frac{1}{2}$ percent per 10 kilovolts, and hence must be considered for high voltage electrons. The power supplies of the RCA type B electron microscopes generate po-

[2] Hillier, Baker, and Zworykin, J. App. Phys. **13**, 576 (1942).

tentials from 30 kv to 60 kv; so when these instruments are used as electron diffraction cameras by installation of the diffraction adapter, the pattern may be used to measure accurately the accelerating voltage. All of the new RCA type EMU electron microscopes are capable of using a diffraction unit nearly identical with the adapter for the type B instruments, and the above procedure may be used to check the accelerating voltage in these instruments also.

If the wave-length λ and corresponding voltage V are determined for several lines of a "no-lens" pattern, the mean value of V should be accurate to within 1 percent, an accuracy difficult to obtain by any other method for this range of voltages.

LENS CHARACTERISTICS

The weak magnetic lens used to focus the diffraction pattern in the RCA instruments obtains its power from the projection lens power supply. In both the type EMU and the diffraction adapter for the type EMB microscope full current regulation is maintained in the diffraction lens for any chosen value of lens current. The circuit of the diffraction unit is shown in Fig. 2.

The current required to focus the pattern is a function of the stiffness of the electron beam which is determined by the accelerating voltage. For a weak magnetic lens

$$1/f = CI^2/V = C'I^2\lambda^2, \tag{3}$$

where C and C' are constants. This equation does not take into account the relativistic increase in mass of the electron at high velocities. If this is considered, the focal length of the lens is increased by an amount which can be calculated from the equation

$$f_{\text{rel}} = f(1 + V \times 10^{-6}), \tag{4}$$

where V is in volts.

If u and v represent, respectively, object and image distances measured from the lens, the lens equation becomes

$$\frac{1}{u} + \frac{1}{v} = \frac{1}{f} = C\frac{I^2}{V} = C'I^2\lambda^2. \tag{5}$$

In the diffraction unit u and v are fixed, so that

$$I\lambda = \text{constant}, \tag{6}$$

and

$$I^2/V = \text{constant}. \tag{7}$$

The graph of Eq. (6) is an equilateral hyperbola, a portion of which is shown in Fig. 3. In Fig. 4 is shown the graph of Eq. (7) plotted using the average value of C' determined from experimental data. The experimentally determined points are shown at 30, 40, 50, and 60 kv. The focusing current was adjusted to the nearest scale division, and the deviation of the 30- and 40-kv values from the calculated curve can be explained by the fact that the current increments per scale division in the focal range for 30 and 40 kv are considerably larger than those for the range corresponding to 50 and 60 kv. This effect is due to the taper of the current control rheostat and the fact that lens current is controlled by a parallel connected resistance.

Examination of Fig. 4 also shows that in the range from 30 to 60 kilovolts little accuracy is lost by assuming a linear relationship between focusing current and accelerating voltage.

Focus for a given accelerating voltage is found photographically by making a series of pictures of a pattern for slightly different values of lens current. Once the correct current is determined, it need not be rechecked for several weeks.

However, with the passage of time both the output of the projector power supply and the accelerating voltage will change slightly because of aging of the standardizing batteries and other circuit components. These changes will produce

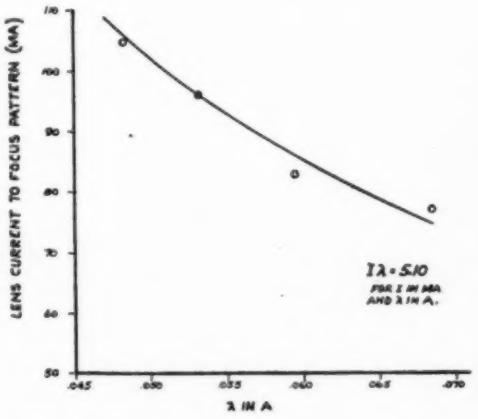

FIG. 3. Theoretical variation of diffraction lens focusing current with electron wave-length. Circles are experimentally determined values.

slightly out of focus patterns unless the lens current is readjusted. For this reason, it is important to know the error introduced in the determination of d_{hkl} if the pattern is slightly out of focus, either because the current required for focus has not been rechecked for too long a period or because of inaccuracy on the part of the operator.

In Table I are listed data which show the error introduced in d_{hkl} if the diffraction lens is defocused by one division of the current control. Figure 5 shows the same data with additional values to cover a wider current variation plotted in terms of percent variation in lens current from the current which produces a sharp pattern. The sharply focused pictures are assumed to have zero error and the corresponding d_{hkl} values are obtained from x-ray data.

A study of these data shows that for a 60-kv accelerating potential the error in d_{hkl} produced by defocusing the lens a whole division above or below focus position is less than 1 percent. Similarly, at 50 kv the error is less than 1.5 percent; at 40 kv, about 2 percent; and at 30 kv, about 3.5 percent. As the focusing current can be set much more closely than 1 scale division, the error can easily be made less than these values. Figure 5 illustrates this fact.

PATTERNS OF ELECTRONICALLY TRANSPARENT THIN FILMS

Specimens for which diffraction patterns are to be obtained by transmitted electrons are generally mounted on thin, structureless, electronically transparent films. Such films diffract electrons, and their diffraction patterns appear with that of the material being studied. In order to determine what spurious effects may be expected because of the presence of the supporting film, patterns were obtained from some of the films most commonly used in this work and in electron microscopy.

The choice of film materials to be studied was made on the basis of the experience of electron microscopists with these materials. Nitrocellulose and Formvar are widely used and readily soluble in a variety of solvents. A number of combinations of materials were tried in order to determine the effect of the solvent on the diffraction pattern.

Probably the simplest method of preparing suitable supporting films is to allow a drop of solution to spread over water and then let the solvent evaporate. Thinner films can be made in this manner than by any other, and, as thick films contribute more diffuse scattering than thin ones to the diffraction pattern, it is desirable to

TABLE I. Percent error in d_{hkl} caused by defocusing lens by one scale division of current control rheostat. Measurements made on a diffraction pattern of MgO.

Dial setting	Lens current I in ma	Voltage in kv	$\frac{I-I_f}{I_f}\times 100$	% error d_{100}	% error d_{110}	% error d_{120}	% error d_{112}
10	109	60	+ 3.8	+0.48	+0.67	+0.85	+0.58
11*	105	60	0	0	0	0	0
12	101	60	− 3.8	−0.95	−0.34	−0.85	−0.93
12	101	50	+ 5.5	+0.48	+1.01	+1.3	+0.81
13*	95.7	50	0	0	0	0	0
14	90.6	50	− 5.3	−1.4	−1.01	−1.1	−1.16
14	90.6	40	+ 9.3	+1.9	+2.4	+2.1	+1.7
15*	83.0	40	0	0	0	0	0
16	77.0	40	− 7.2	−1.9	−2.0	−1.9	−2.1
15	83.0	30	+ 7.8	+2.9	+3.0	+3.1	+2.7
16*	77.0	30	0	0	0	0	0
17	68.4	30	−11.2	−3.8	−3.4	−3.4	−3.5

* These values correspond to sharp focus.

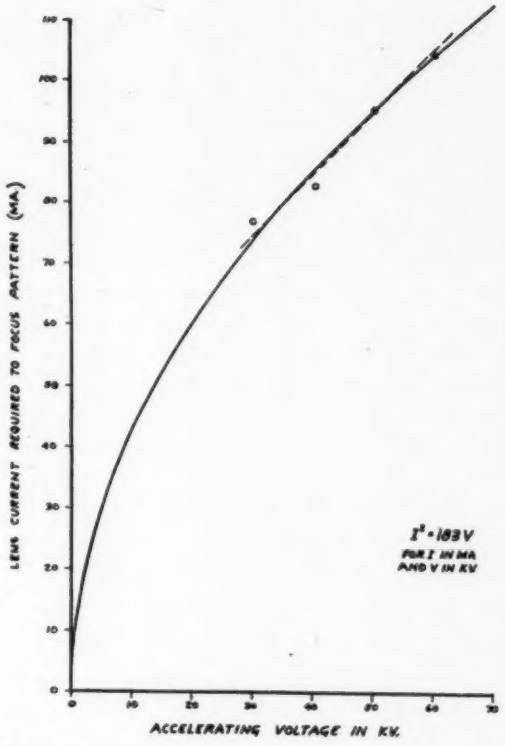

FIG. 4. Theoretical variation of diffraction lens focusing current with electron accelerating voltage. Circles are experimentally determined values. Dotted line is a straight line.

use as thin films as possible. For this reason only films that could be formed on water were studied.

The following combinations of materials were used:

(1) ½ percent and 2 percent solutions of Formvar 15-95 in ethylene dichloride;
(2) 2 percent solution of Parlodion in amyl acetate;
(3) J26AR nitrocellulose solution thinned with amyl acetate to 2 percent nitrocellulose by weight;[3]
(4) J26AR nitrocellulose solution thinned with dioxan to 2 percent nitrocellulose by weight.

Formvar dissolved in dioxan is also a satisfactory film-forming solution for use in electron microscopy. However, it will not form a film on water but must be stripped from a polished surface. As such films will be somewhat thicker than the water formed films (thus contributing more background to the diffraction patterns), their pattern was not obtained.

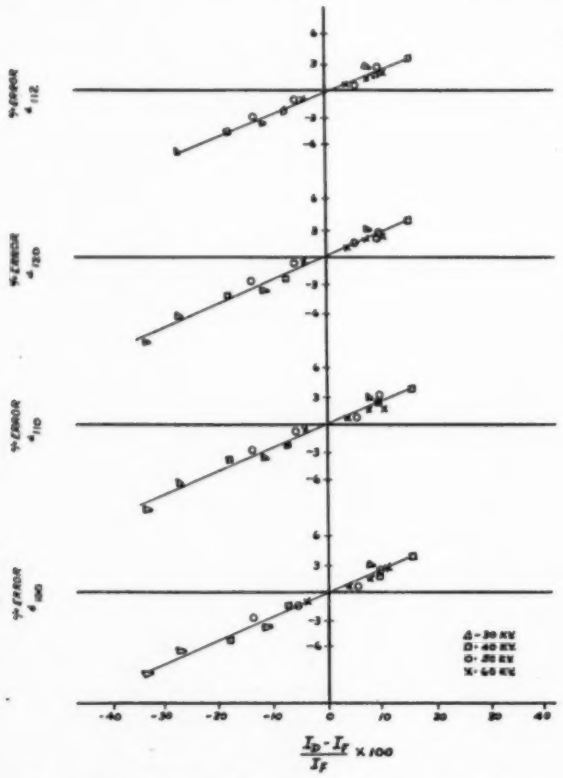

FIG. 5. Percent error in d_{hkl} as a function of percent error in diffraction lens focusing current. Measurements made from a magnesium oxide pattern.

[3] J26AR is a commercially available solution of nitrocellulose in toluene and butyl acetate. When thinned with amyl acetate, it forms excellent films. It may also be thinned with dioxan, but the films formed are not as satisfactory.

In addition, a thin film of silica prepared by the method of Heidenreich and Peck[4] by evaporation on to polystyrene was studied. This material has important possibilities as a substrate for electron diffraction studies and electron microscopy, as it can safely be raised to temperatures at which Formvar and nitrocellulose films would be destroyed.

The procedure consisted in making a number of specimens of each film and obtaining the transmission patterns of some of them at once. All were then carefully preserved free from dust for a period of about six weeks. Those that had been previously exposed to the beam were again photographed, as were some that had not been subjected to electron bombardment. Thus, the effect of aging both before and after being exposed to the beam could be determined. A few specimens were given a prolonged and intense electron bombardment to see if this would affect their structure.

Diffraction patterns of Formvar films from an ethylene dichloride solution all consist of three diffuse rings. Thick films have, in addition, a number of sharp rings (Fig. 6). Thinner films show evidence of sharp rings also, but less clearly defined (Fig. 7a). Very thin films show only diffuse rings. After six weeks' aging the film whose pattern is shown in Fig. 7a showed a number of dotted rings (Fig. 7b) which agree quite well with the positions of the rings originally present and are evidence of further crystallization.

Patterns of Parlodion from amyl acetate solution also show three diffuse rings (Fig. 8). No evidence of crystallization of these films was found after aging or prolonged exposure to the electron beam. The thickness of the film did not affect the diffraction pattern as long as the film was thin enough to produce a pattern at all.

Diffraction patterns of films of J26AR thinned with amyl acetate again show three diffuse rings (Fig. 9a) having the same diameters and widths as those produced by Parlodion films. A pattern

[4] R. D. Heidenreich and V. G. Peck, Phys. Rev. **62**, 292 (1942).

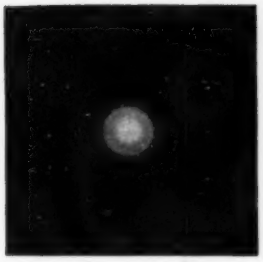

FIG. 6. Thick film of Formvar.

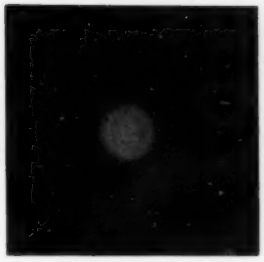

(a)

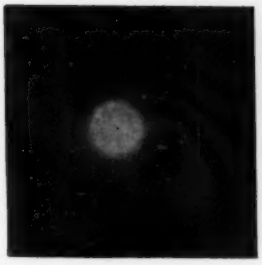

(b)

FIG. 7. Formvar. (a) Fresh film. (b) Same film after six weeks aging.

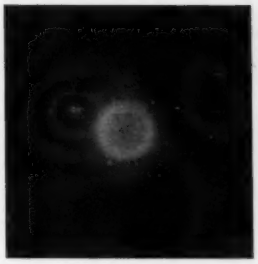

FIG. 8. Parlodion from amyl acetate solution.

made six weeks later from this same film shows evidence of crystallization by the presence of rings of dots (Fig. 9b). Other aged films not previously exposed to the beam and freshly made thick films of this material had patterns consisting of the diffuse rings only.

Figures 10a and 10b are diffraction patterns of the same specimen of magnesium oxide smoke deposited on J26AR. That shown in Fig. 10b appeared after several hours' exposure to the electron beam, and is an excellent example of an effect that may be encountered due to crystallization of the supporting film. The two dotted rings correspond to those illustrated in Fig. 9b.

TABLE II. Summary of diffraction patterns produced by electronically transparent thin films of organic materials. The diffuse rings correspond to a range of d_{hkl} values which is estimated roughly, as the edges of the rings are very poorly defined.

Material	Diffuse rings d in A	Sharp rings d in A	Dotted rings d in A	Remarks
FORMVAR from ethylene dichloride solution	5.4–3.7 2.3–2.0 1.4–1.1	4.3 4.2 4.0 3.7 2.5	4.1 3.7 2.5 2.2	The dotted rings appeared only in patterns from old films. Very thin films gave only diffuse rings.
PARLODION from amyl acetate solution	5.1–3.2 2.2–1.9 1.3–1.1			Only diffuse rings observed from fresh, old, thin, or thick films.
J26AR from amyl acetate solution	5.1–3.2 2.2–1.8 1.3–1.1		4.1 3.7 2.5 2.2 2.1	The dotted rings appeared only in patterns from films exposed to the electron beam for at least an hour.
J26AR from dioxan solution	5.4–3.2 2.1–1.7 1.2–1.0 4.9* 3.3* 2.5* 1.7* 1.2*			The figures with asterisks were diffuse arcs appearing in pairs along a single diameter of the pattern.

Patterns of films of J26AR thinned with dioxan again show three diffuse rings of the same diameters as those produced by films from the amyl acetate solution. In addition, five pairs of arcs are present (Fig. 11) which are evidence of orientation in the film.

In Table II the diffraction properties of the above films are summarized. In general, it may be said that these film materials will always give a pattern of three diffuse rings corresponding to average d_{hkl} values of about 4.5, 2.1, and 1.2 angstrom units. Other investigators also have found this pattern to be present for other organic materials (cellulose acetate, ethyl cellulose, celluloid) dissolved in a variety of solvents including ether, alcohol and ether, and acetone.[5–7]

Electronically transparent fresh films of silica formed by evaporation onto polystyrene also produce a diffraction pattern (Fig. 12). After long exposure to the electron beam, these films produce patterns which show a few faint lines corresponding to the cristobalite structure, thus showing that some devitrification is taking place.

It should be emphasized that considerable care must be exercised in preparing films. A number of papers[8,9] have appeared giving evidence that very thin layers of fatty substances will nearly always coat anything left in a laboratory. Oil vapors from pumps and machinery or grease from the fingers are generally the source of this material. Such thin surface layers will contribute

[5] J. J. Trillat and H. Motz, Trans. Faraday Soc. **31**, Part 9a, 1127–8 (1935).
[6] A. Dauvillier, Comptes rendus **191**, 708–9 (1930).
[7] Finch, Quarrell, and Wilman, Trans. Faraday Soc. **31**, Part 9a, 1057 (1935).
[8] G. P. Thomson and W. Cochrane, *Theory and Practice of Electron Diffraction* (Macmillan and Company, Ltd., London, 1939), first edition, pp. 150–151.
[9] See reference 5, pp. 1127–35.

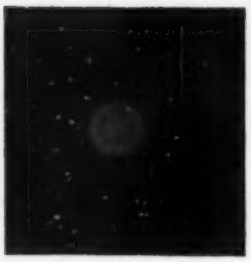

(a)

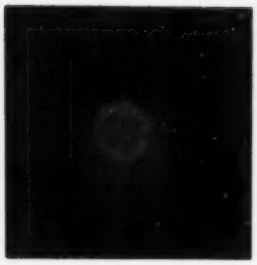

(b)

FIG. 9. J26AR nitrocellulose solution thinned with amyl acetate. (a) Fresh film. (b) Film aged six weeks.

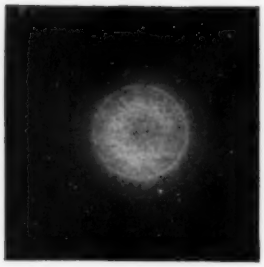

(a)

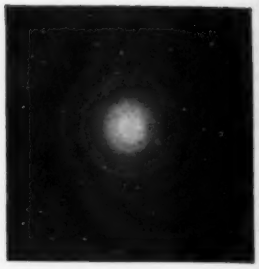

(b)

FIG. 10. Magnesium oxide on J26AR film. (a) Fresh specimen. (b) After long exposure to the electron beam.

patterns in electron diffraction work, so prepared supporting films should not be left for future use without taking special precautions, and surfaces to be studied by reflection should be washed with a solvent before use whenever possible.

SUMMARY

The foregoing discussion presents some characteristics of magnetically focused diffraction cameras with particular reference to the RCA electron diffraction adapter for its electron microscopes. The accuracy of lattice spacings calculated from patterns obtained with the instrument is shown to be better than 1 percent if suitable precautions are taken in choosing a calibration specimen and operating the instrument. It is also pointed out that a diffraction pattern made with the lens power turned off can be used to measure the electron accelerating voltage with high accuracy.

The results of a brief study of the electron diffraction patterns of thin films of a number of organic materials show that such films all produce patterns of their own which are in agreement with those obtained by other investigators working with similar materials. Most of these films crystallize to some extent with age and exposure to high voltage electrons; therefore, when these films are used as the support for substances being studied by electron diffraction, it is necessary to identify that portion of the pattern due to the film in order to avoid confusion and the possibility of attributing these lines to an impurity in the specimen.

In the microphotometric determination of relative intensities of lines of diffraction patterns produced by specimens mounted on electronically transparent substrates, it is also necessary to consider the non-uniform background caused by the diffraction pattern of the substrate, in order to subtract it from the pattern being measured.

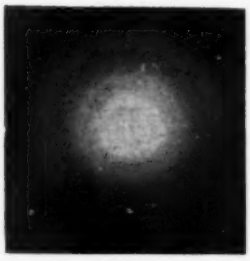

FIG. 11. J26AR nitrocellulose solution thinned with dioxan.

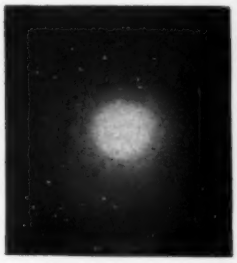

FIG. 12. Silica.